

**UNIGIS**

## Master Thesis

submitted within the UNIGIS MSc programme  
Interfaculty Department of Geoinformatics - Z\_GIS  
University of Salzburg

# Adaptive behaviour in active transportation The influence of traffic lights on bicycle traffic in the city centre of Salzburg/Austria

by

**Dipl.-Ing. (FH) Peter Rauscher**  
GIS\_104575

A thesis submitted in partial fulfilment of the requirements of  
the degree of  
Master of Science (Geographical Information Science & Systems) – MSc (GISc)

Advisor:

Prof. Dr. Gudrun Wallentin

Vancouver, 27/02/2019

## **Acknowledgements**

I would like to thank my thesis supervisor Prof. Dr. Gudrun Wallentin for her support and her valuable feedback to my numerous questions, Dr. Martin Loidl for his helpful suggestions, Dana Kaziyeva for providing me with insights from her experience with the GAMA platform, and my tutor Anna Karnassioti for being the helping hand that I always could count on during my studies.

I especially would like to thank my wife Beatriz for carrying most of the burden that this Master programme and the thesis put on our private life.

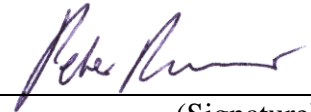
Thanks also to my friend Rubber Duck for always listening to my ideas.

## Science Pledge

By my signature below, I certify that my thesis is entirely the result of my own work. I have cited all sources I have used in my thesis and I have always indicated their origin.

Vancouver, 27/02/2019

(Place, Date)

A handwritten signature in blue ink, appearing to read 'Pete ...', written over a horizontal line.

(Signature)

## Abstract

The constant increase in urban populations and the negative effects from motor vehicle traffic that come with this growth can be felt every day. Communities are struggling with road congestion and environmental challenges like noise and air pollution. Bicycles are older than motorcars and they are experiencing a revival in recent years, due to their suitability for clean and space-preserving short-distance transportation. With this increased attention and the ever-evolving computer technology at hand, there are many bicycle-related topics worth exploring with computer models, especially around safety, planning, and environmental concerns. Agent-based modeling (ABM), an increasingly popular technique that can be applied in a spatial context, uses representations of objects and living organisms (agents) which can be equipped with attributes, behaviours and the ability to make decisions. The models can then simulate situations of interest and the resulting data and observations of how these situations develop allow to draw conclusions for the future.

The presented thesis uses ABM to model bicycle traffic in the city centre of Salzburg/Austria in order to observe the effects of traffic lights on the spatio-temporal distribution of this bicycle traffic as a result of the adaptive behaviour of the cyclists. For this, the cyclists are monitored at various locations over time. The model uses a simplified version of the road network of Salzburg, and the cyclist agents travel on these roads by following pre-calculated shortest-distance trajectories. The traffic lights are controlled by pre-set phase timing from an external file. When the cyclist agents encounter red traffic lights or other cyclists during their trip, they react by observing the right of ways. Since this has an effect on their trip timing, it changes the spatio-temporal distribution of the bicycle traffic. The emerging patterns observed during these changes clearly reflect the influence of the traffic lights. Due to the generalisations in the model, the numbers of the cyclists (aggregated with the mean over 100 simulations and presented in charts comparing three different phase timing scenarios) are useful for an impression of the overall character of the traffic situations, they don't reflect real counting numbers though. However, the time delays experienced by the cyclist agents exhibit an unexpected accuracy in the results, and they prove that adaptive cyclist behaviours can be captured in a meaningful way at such a scale with the help of ABM models.

## Contents

Abstract .....	I
Contents .....	II
List of Figures .....	IV
List of Tables .....	VI
Abbreviations .....	VII
1. Introduction .....	1
1.1. Motivation .....	1
1.2. Literature review .....	3
1.3. Aims and Objectives .....	5
2. Methods .....	8
2.1. Study area and application context .....	8
2.2. Transportation modeling approaches .....	8
2.3. Cyclist behaviour at traffic lights .....	9
2.3.1. Traffic light detection based on spatial query .....	9
2.3.1.1. Detection ranges .....	9
2.3.1.2. Distance measuring .....	11
2.3.1.3. Additional concerns .....	11
2.3.2. Traffic light detection based on list comparison .....	12
2.3.2.1. Stop list functionality .....	13
2.3.2.2. 'Sandbox' model with stop list .....	13
2.3.2.3. Stop list structure .....	15
2.3.2.4. Stop list substitute .....	16
2.3.2.5. Stop list generation .....	16
2.3.2.6. Stop visualisation .....	19
2.3.3. Other behavioural aspects .....	19
2.4. Preparing input datasets .....	22
2.4.1. Provided datasets .....	22
2.4.2. Extent of the study area .....	23
2.4.2.1. Clipping of the point and polygon datasets .....	23
2.4.2.2. Clipping of the road network dataset .....	24
2.4.3. Adding intersection nodes .....	25
2.4.4. Assigning traffic light status to intersection nodes via attributes .....	25
2.4.5. Adding reversed roads in the model code .....	27
2.4.6. Combining roads and nodes in stop list spreadsheet .....	27
2.4.7. Traffic light scenarios .....	28
2.4.7.1. Scenario 0 .....	28
2.4.7.2. Scenario 1 .....	29
2.4.7.3. Scenario 2 .....	30
2.4.7.4. Scenario comparison .....	31
2.5. Traffic flow factors .....	32
2.6. Counting stations in the study area .....	35
2.6.1. Heat map and additional counting stations .....	35

2.7.	Simulations .....	36
2.7.1.	Number of executed simulations.....	36
2.8.	Data export and processing.....	38
2.9.	ODD protocol .....	39
2.9.1.	Purpose .....	39
2.9.2.	Entities, state variables, and scales.....	39
2.9.3.	Process overview and scheduling.....	43
2.9.4.	Design concepts.....	45
2.9.5.	Initialization .....	47
2.9.6.	Input data.....	49
2.9.7.	Submodels .....	49
3.	Results.....	51
4.	Discussion .....	67
4.1.	Chart interpretation - general.....	67
4.1.1.	Potential chart series inaccuracies.....	67
4.1.1.1.	Start cycles .....	67
4.1.1.2.	End cycles .....	67
4.1.2.	Differences in chart series .....	68
4.1.3.	Emerging patterns .....	69
4.1.4.	Categorisation of charts.....	72
4.1.5.	Observed errors in the results.....	76
4.2.	Chart interpretation - individual .....	77
4.2.1.	Counting stations CS 0 to CS 2.....	77
4.2.1.1.	CS 2 ('Elisabethkai').....	77
4.2.1.2.	CS 0 ('Rudolfskai').....	79
4.2.1.3.	CS 1 ('Giselakai') .....	81
4.2.2.	Counting stations CS 3 to CS 6.....	82
4.2.2.1.	CS 3 ('Mozartsteg').....	82
4.2.2.2.	CS 4 ('Staatsbrücke') .....	84
4.2.2.3.	CS 5 ('Makartsteg').....	85
4.2.2.4.	CS 6 ('Müllnersteg') .....	88
4.3.	Discussion summary .....	90
4.3.1.	Model detail level.....	90
4.3.2.	Model category.....	91
4.3.3.	Processing effort.....	91
4.3.4.	Confirmation of traffic light influence .....	92
4.3.5.	Positioning of counting stations .....	95
4.3.6.	Transferability to other locations .....	96
4.3.7.	Model as a reference .....	96
5.	Conclusion.....	97
6.	References .....	98
6.1.	Data sources.....	100
6.2.	Link to model file and associated data files .....	100

## List of Figures

Fig. 2-1: Cyclists with detection cones travelling towards traffic lights.....	10
Fig. 2-2: Agents on road 4 and road 5 detecting two traffic lights with their cones.....	10
Fig. 2-3: Traffic light point locations with circular detection buffers.....	11
Fig. 2-4: 'Sandbox' model with additional traffic light points.....	14
Fig. 2-5: Stop list content example.....	15
Fig. 2-6: Intersection example.....	15
Fig. 2-7: Spreadsheet example with stop markers (to be exported into a CSV file).....	16
Fig. 2-8: Transfer list example with sub-transfer lists per cycle (full road agent names).....	17
Fig. 2-9: Transfer list example with sub transfer lists per cycle (road feature IDs only) .....	17
Fig. 2-10: Pseudo-code flowchart for stop list creation and substitution.....	18
Fig. 2-11: Transfer lists per cycle being assigned to stop list index [0].....	19
Fig. 2-12: Intersection example with red stop arrows and stopped cyclists.....	19
Fig. 2-13: Extent of study area (orange square, 1600 m x 1600 m).....	24
Fig. 2-14: Traffic light points at 'Dr.-Franz-Rehrl-Platz' (Orthophoto: Geoland.at 2019).....	25
Fig. 2-15: Traffic light point at 'Max-Ott-Platz' (Orthophoto: Geoland.at 2019) .....	26
Fig. 2-16: Overview of study area, traffic light scenario 0 (no traffic lights).....	28
Fig. 2-17: Overview of study area, traffic light scenario 1, cycle 1 (stop roads in red).....	29
Fig. 2-18: Overview of study area, traffic light scenario 2, cycle 1 (stop roads in red).....	30
Fig. 2-19: Intersection with stopped cyclists, scenario 1 (left) and scenario 2 (right).....	31
Fig. 2-20: Study area with distribution of employed residents .....	32
Fig. 2-21: Study area with distribution of universities .....	33
Fig. 2-22: Overview of major traffic flow areas (one simulation with scenario 0).....	35
Fig. 2-23: Scenario 1 represented by five series, each showing the mean of 20 simulations ..	36
Fig. 2-24: Scenario 2 represented by five series, each showing the mean of 20 simulations ..	37
Fig. 2-25: Scenarios 1 and 2, each showing the mean of 100 simulations.....	37
Fig. 2-26: Cyclist counting data organisation schema .....	38
Fig. 2-27: Counting data aggregated per scenario (example for 20 simulation cycles).....	38
Fig. 2-28: Submodel processing the traffic light phase timing matrix.....	50
Fig. 3-1: Study area with numbered counting stations (Orthophoto: Geoland.at 2018) .....	52
Fig. 3-2: Distribution of cyclists at CS 0 (Rudolfskai), inbound .....	53
Fig. 3-3: Distribution of cyclists at CS 0 (Rudolfskai), outbound .....	54
Fig. 3-4: Distribution of cyclists at CS 1 (Giselakai), inbound.....	55
Fig. 3-5: Distribution of cyclists at CS 1 (Giselakai), outbound.....	56
Fig. 3-6: Distribution of cyclists at CS 2 (Elisabethkai), inbound .....	57
Fig. 3-7: Distribution of cyclists at CS 2 (Elisabethkai), outbound .....	58
Fig. 3-8: Distribution of cyclists at CS 3 (Mozartsteg), inbound.....	59
Fig. 3-9: Distribution of cyclists at CS 3 (Mozartsteg), outbound.....	60
Fig. 3-10: Distribution of cyclists at CS 4 (Staatsbrücke), inbound .....	61
Fig. 3-11: Distribution of cyclists at CS 4 (Staatsbrücke), outbound .....	62
Fig. 3-12: Distribution of cyclists at CS 5 (Makartsteg), inbound.....	63
Fig. 3-13: Distribution of cyclists at CS 5 (Makartsteg), outbound.....	64
Fig. 3-14: Distribution of cyclists at CS 6 (Müllnersteg), inbound.....	65

Fig. 3-15: Distribution of cyclists at CS 6 (Müllnersteg), outbound.....	66
Fig. 4-1: Differences in chart series, example chart.....	68
Fig. 4-2: CS 0 (Rudolfskai), inbound / outbound.....	70
Fig. 4-3: CS 1 (Giselakai), inbound / outbound .....	70
Fig. 4-4: CS 2 (Elisabethkai), inbound / outbound .....	70
Fig. 4-5: CS 3 (Mozartsteg), inbound / outbound .....	71
Fig. 4-6: CS 4 (Staatsbrücke), inbound / outbound.....	71
Fig. 4-7: CS 5 (Makartsteg), inbound / outbound .....	71
Fig. 4-8: CS 6 (Müllnersteg), inbound / outbound.....	72
Fig. 4-9: Distinctive phase shift .....	73
Fig. 4-10: CS 3 (Mozartsteg), outbound .....	73
Fig. 4-11: Non-distinctive phase shift.....	74
Fig. 4-12: CS 6 (Müllnersteg), outbound .....	74
Fig. 4-13: CS 5 (Makartsteg), outbound .....	75
Fig. 4-14: CS 2 (Elisabethkai), inbound / outbound .....	78
Fig. 4-15: Study area with distribution of employed residents .....	78
Fig. 4-16: Study area with distribution of universities.....	79
Fig. 4-17: CS 0 (Rudolfskai), inbound / outbound.....	80
Fig. 4-18: CS 0 (Rudolfskai), with nearby traffic lights (Orthophoto: Geoland.at 2018).....	80
Fig. 4-19: CS 1 (Giselakai), inbound / outbound .....	82
Fig. 4-20: CS 1 (Giselakai), with nearby traffic lights (Orthophoto: Geoland.at 2018) .....	82
Fig. 4-21: CS 3 (Mozartsteg), inbound / outbound .....	83
Fig. 4-22: CS 3 (Mozartsteg), with nearby traffic lights (Orthophoto: Geoland.at 2018) .....	84
Fig. 4-23: CS 4 (Staatsbrücke), inbound / outbound.....	85
Fig. 4-24: CS 4 (Staatsbrücke), with nearby traffic lights (Orthophoto: Geoland.at 2018).....	85
Fig. 4-25: CS 5 (Makartsteg), inbound / outbound .....	86
Fig. 4-26: CS 5 (Makartsteg), with nearby traffic lights (Orthophoto: Geoland.at 2018) .....	88
Fig. 4-27: CS 6 (Müllnersteg), inbound / outbound.....	89
Fig. 4-28: CS 6 (Müllnersteg), with nearby traffic lights (Orthophoto: Geoland.at 2018).....	89
Fig. 4-29: Distribution of cyclists at CS 5 (Makartsteg), outbound.....	92
Fig. 4-30: Distribution of cyclists at CS 2 (Elisabethkai), inbound .....	93
Fig. 4-31: Distribution of cyclists at CS 3 (Mozartsteg), outbound.....	93



**List of Tables**

Table 2-1: Variables provided by the 'advanced_driving' skill .....	20
Table 2-1: Variables provided by the 'advanced_driving' skill (continued) .....	21
Table 2-2: Overview of datasets.....	22
Table 2-3: Overview of entities, variables, attributes, and parameters .....	39
Table 2-3: Overview of entities, variables, attributes, and parameters (continued).....	40
Table 2-3: Overview of entities, variables, attributes, and parameters (continued).....	41
Table 2-3: Overview of entities, variables, attributes, and parameters (continued).....	42
Table 2-4: Overview of entities and variables at initialisation.....	47
Table 2-4: Overview of entities and variables at initialisation (continued) .....	48
Table 2-4: Overview of entities and variables at initialisation (continued) .....	49
Table 3-1: Counting station numbers and names .....	52
Table 4-1: Overview of chart series pattern differences .....	69
Table 4-2: Overview of charts with no apparent effect of traffic lights.....	72
Table 4-3: Overview of monitored counting station road segments with their lengths .....	94

**Abbreviations**

ABM	Agent-based modeling
BM	Bicycle model
CS	Counting station
CSV	Comma-separated values
E	East
EPSG	European Petroleum Survey Group
GAMA	GIS Agent-based Modeling Architecture
GAML	GAMA Modeling Language
GIS	Geographic Information System
MS	Microsoft
N	North
NE	Northeast
NW	Northwest
S	South
SBM	Salzburg Bicycle model
SC / Sc	Scenario
SE	Southeast
SW	Southwest
UTM	Universal Transverse Mercator
W	West
WGS 84	World Geodetic System 1984

## 1. Introduction

### 1.1. Motivation

Around the globe, urban regions are suffering from the consequences of motor vehicle traffic. The population that is immediately participating in it is impacted through congestion, accidents, and noise (Dora and Phillips 2000), but other consequences like air pollution also affect everybody else (HEI Panel on the Health Effects of Traffic-Related Air Pollution 2010). As underlined by the recent discussion about particulate matter and driving bans in some urban centres in Germany and other European countries, air pollution doesn't disappear at the end of the rush hour.

In addition to the environmental impact of traffic on these urban areas (especially for those with limited ability to expand), the constant increase in urban population (The World Bank 2018) often results in an increase in their population density – an effect that can be well observed in places like the Metro Vancouver/Canada region. Although buildings can sometimes be replaced with higher buildings (containing even smaller dwellings) to house more people, this growth often also challenges the transportation systems of these regions, the more since they are usually publicly funded.

The topic of this thesis relates to factors affecting the attractiveness of the bicycle as a component of such transportation systems and is, as a consequence, also relevant to fields such as traffic planning, bicycle traffic safety, urban planning, and environmental concerns for communities.

As a short-distance alternative to cars and a counter-measure to congestion and pollution, bicycles are gaining popularity, and many urban regions increasingly focus on them for relief from their traffic problems. Bicycles have a smaller footprint per passenger than most motorised vehicles, they don't rely on fossil fuels and emit harmful substances, and they even help combating wide-spread lack of exercise. However, in order to integrate well with other transportation modes, bicycle traffic also has to be planned.

In this planning process, stakeholders often review the demand in existing situations, for instance with automated traffic counting stations or even video observation, surveys among the current user population, or comparisons with other regions. However, these methods always require a traffic situation to be already established before it can be studied. Aside from surveys of potential participants in prospective traffic scenarios, computer simulations can be used to study such scenarios before shovels hit the ground. They are based on computer models and

can help to understand the dependencies between various aspects of traffic and their potential outcomes.

Agent-based modeling (ABM) is a computer modeling technique where entities (so-called 'agents') can be equipped with their own characteristics (attributes), behaviours, and decision-making capabilities (Macal and North 2014). Although they often embody animals or people, they can also represent other objects. These agents can be programmatically controlled (for instance with conditions and loops) to act or react in a certain way every time the program code is executed. Every iteration (cycle) of the program execution represents a unit in time and is usually intended to happen repeatedly until a certain condition is met (e.g. one day passed, a group of animals reproduced 100 times, a food source is depleted). The combination of the time component with the spatial capabilities of GIS-enabled ABM platforms allows to investigate spatio-temporal aspects of a modeled situation, for instance whether patterns emerge from seemingly random movements or other actions.

Agent-based modelling is considered to be a promising approach to computerised traffic modelling (Bazzan and Klügl 2014), including bicycle traffic. Wallentin and Loidl (2015) confirmed this through their research and the 'Salzburg Bicycle model' (Wallentin 2016). In ABM traffic models, the agents (e.g. cyclists) move from source locations to target locations (e.g. building agents). They usually move along lines (edges) in a road network (represented by road agents), based on parameters defined in the model code. One aspect requiring further research in bicycle traffic modeling, as identified in Wallentin and Loidl's (2015) result discussion, is adaptive behaviour of these agents.

There are many influences on cyclists that can affect their behaviour and require them to adapt. Besides factors such as weather, bicycle path surface conditions, or path widths, traffic lights seem to be a major concern for urban cyclists. Cyclists are often criticised for breaking traffic rules, and the disregard for traffic lights is one of the commonly cited violations. One of the reasons for such behaviour is time savings. As the 'Salzburg Bicycle model' offers two route settings (the shortest or the safest route), it leaves out the third of the three most important routing decision criteria amongst 'non-leisure' cyclists: time (Loidl and Zigel 2010). It should be noted that these aspects are not mutually exclusive and can affect each other (traffic lights can also make bike rides safer, but this may come at a time cost).

The thesis topic is thus motivated by this combination of agent-based modelling, traffic lights, and the concern for bicycle travel times. The time impact can be observed at any individual traffic light - but how does this play out on a larger scale?

The presented work is an attempt to implement traffic lights in an agent-based spatial simulation model in such a way that variations of traffic situations and the effects of these variations on the spatio-temporal distribution of bicycle traffic can be explored (with the help of model parameters). The underlying question was: "Does the application of traffic lights in a setting like the inner city of Salzburg lead to emerging patterns in the spatio-temporal distribution of bicycle traffic that can be identified and visualised with a simulation created in an agent-based model?" The intention is to raise stakeholder awareness for this modeling technique as a support tool for their decision-making processes in fields concerning bicycle transportation, and to further the research in this subject matter.

## 1.2. Literature review

The available literature was reviewed with a twofold focus:

- What is known about different cyclist types and how can this be applied to a bicycle traffic simulation model with regard to cyclist behaviour at traffic lights?

The intention here was to find out whether there are typical behaviours that could potentially be applied in form of numeric values or probabilities as parameters in a model.

- What is known with regard to bicycle traffic modeling with agent-based modeling techniques, on the local scale of a city centre?

With the first automated traffic lights emerging in the early 20th century and the long history of the bicycle as a transportation medium in many parts of the world, it is not surprising that these and related topics triggered many studies. In their efforts to characterise the cyclist population beyond demographics like gender or age groups, many of these studies make use of cyclist type classifications. To mention two prominent examples, Geller (2006) categorised the population of transportation cyclists in Portland/USA into four groups ('The Strong and the Fearless', 'The Enthused and the Confident', 'The Interested but Concerned', and the 'No Way No How' group of non-cyclists), based on his experience. His classification was often cited and - although some limitations were identified over the years - is still considered relevant. In order to address the limitations in his and other studies, Damant-Sirois *et al.* (2014) created a multidimensional cyclist typology by incorporating 35 variables (related to topics such as personal motivation or social and infrastructural cycling environments) into seven different factors, from which they finally also derived four different cyclist types ('Dedicated cyclists',

'Path-using cyclists', 'Fair weather utilitarians', and 'Leisure cyclists'). However, these studies are mainly concerned with the reasons why people use or don't use bicycles, but this question has little relevance for this thesis. Consequentially, the focus shifted to studies related to traffic lights in the context of bicycle traffic.

The most obvious and easiest detectable reaction to traffic lights is whether a cyclist stops or doesn't stop at a red light. This narrowed the field of literature further down to studies specifically concerned with red-light infringements by cyclists. The most suitable classifications found for the cyclists in the planned bicycle traffic model with regard to traffic light-violating behaviours were the type adjectives 'law-obeying', 'risk-taking', and 'opportunistic' used by Pai and Jou (2014) and Wu *et al.* (2012) in their studies. The primary focus with regard to the model was not to find out why the cyclists would qualify for these categories, but what percentage of cyclists in these groups would typically violate red traffic lights. However, with regard to numeric study results that could be applied as parameters in the model, even with such narrow topics as red light infringements in bicycle traffic, the results of different studies are often not directly comparable. In their study regarding traffic light violations by cyclists in the city centre of Dublin/Ireland, Richardson and Caulfield (2015) provide an extensive overview of similar, globally conducted studies. They found that there is no typical percentage of cyclists violating red lights, as they ranged from under 10% to almost 90% in these studies. Their conclusion underlines that these numbers very much depend on the researched situation, e.g. with regard to the applied methods, but also the types of intersections and other infrastructure, the types of bicycles involved, the laws in effect in the study area, and even cultural differences - a notion that is echoed frequently in other studies. However, the planned simulation model was not going to differentiate between these circumstances, and the consideration of these percentages as parameters in the model was of a lesser priority.

Some of the aforementioned factors are also a matter of the functional level at which a modeled system is represented. Morvan (2012) differentiates between micro-, meso-, and macroscopic levels at which traffic models (as a category of flow modeling) can be modeled. According to his classification, a model at the scale of an urban area with a complex road network and traffic interactions at the vehicle level would fall under the micro- or mesoscopic level definition. He also points out that these levels can be combined into multi-level systems (not to be confused with multi-scale systems). A popular traffic simulation package designed to work at the micro- or mesoscopic level is SUMO (Alvarez Lopez *et al.* 2018). However, based on a review of the available information about it, it cannot be considered as an agent-based modeling platform (as per the definition in Macal and North's (2014) introductory tutorial

on agent-based modeling and simulation) because the entities (e.g. vehicles) modeled in SUMO lack autonomy. Soares *et al.* (2014), for instance, combined SUMO with the multi-agent system development framework JADE for their research into artificial transportation systems. Furthermore, with the topic of this thesis in mind, SUMO does not provide a bicycle modeling structure, and the SUMO team therefore suggests to adapt a car or a pedestrian modeling structure for this purpose (SUMO 2017). As determined by multiple other studies over the past decade, there is an abundance of agent-based modeling platforms available. The more specific the list of requirements for the application is though (e.g. microscopic modeling level, agent-based simulation, bicycle traffic-specific, GIS-capable, time-sensitive, considering traffic lights, etc.), the smaller is the number of examples that can be found in the literature. Ziemke *et al.* (2017) used the open-source ABM framework MATSim in their study regarding the modeling of bicycle traffic in Berlin/Germany. However, their focus was rather on road types and surface conditions, not on traffic lights. Accordingly, they incorporated the time component in the speed calculations for the various modeled road types. MATSim uses the interesting concept of 'scoring' (a technique that optimises the routing based on a score that a 'dry run' of the cyclists' itineraries produces), but one might wonder how traffic light delays could be captured in these scores. Wallentin's (2016) aforementioned 'Salzburg Bicycle model' was developed in the multi-agent programmable modeling environment NetLogo (Wilensky 1999), a tool that Kaziyeva *et al.* (2018) later reviewed and compared with MATSim and the modeling and simulation development environment GAMA (Grignard *et al.* 2013) in the context of bicycle flow modeling. Although they consider NetLogo in their conclusions to be a reasonable option for the development of less demanding models, they recommend the GAMA platform for the kind of spatial transportation modeling as planned in this thesis.

### ***1.3. Aims and Objectives***

The aim of this thesis was to explore how and to what degree traffic lights affect the spatio-temporal distribution of bicycle traffic by studying the effect of adaptive cyclist behaviour by means of an agent-based computer model and on the basis of the 'Salzburg Bicycle model' (SBM) by Wallentin (2016) and the 'Bicycle model' (BM), a further developed version by Kaziyeva *et al.* (2019). The aim was not to make recommendations to decision makers on how to consider cyclists in their traffic plans, but rather to show that there is potential in agent-based modelling as a tool to obtain meaningful results for specific topics (such as the effect of traffic lights on bicycle traffic) on a localised scale.

The intention of traffic control with traffic lights is to grant the right of way on a road network to the participants in that traffic in such a way that conflicts between the participants over the use of specific spaces (e.g. intersections) are avoided. This forces some participants to stop, while others are allowed to proceed and to use these spaces. After a certain amount of time (usually in consideration of the demand), the right of way is granted to other participants in order to establish a balanced use of the spaces and to avoid unreasonable interruptions of the overall traffic flow. From the point of view of the participants, this means that their right of way might change at any given time (depending on their location at that time and the state of the traffic lights at that location). The participants are required to notice this change and to react accordingly by either stopping or continuing their trip. Since there are often multiple participants involved in the traffic, the actions of one participant might affect another participant's situation. For instance, if one participant has to stop at a traffic light, the space that it occupies is not available anymore for the following participant (since they also have the obligation to avoid space conflicts among themselves). On the other hand, if a participant clears such a space by continuing its trip when the traffic light turns green, the following participant is also required to continue its trip (hence temporarily occupying the space and then clearing it again right away for the next participant). All this means that the participants need to constantly monitor their situation, detect potential changes to it, decide on the required actions (as per the rules of participation in traffic), and to react accordingly - they need to adapt to changes in their environment.

The primary aspect in this investigation into this adaptive behaviour was the immediate effect of the traffic lights on the 'outgoing' side of intersections, i.e. the change in the traffic distribution 'behind' the traffic light, caused by holding up the participants or by suddenly 'releasing' them. Obviously, in a closed network this cannot be completely decoupled from cascading effects on the 'incoming' side, but the main interest was in demonstrating how much longer it takes for the traffic to occupy a certain space due to the fact that traffic lights were in its way.

The most promising way to record and visualise such changes in the spatio-temporal distribution seemed to be a monitoring system with space as a fixed parameter and time as a variable parameter, i.e. the observation of the traffic volume at specific locations during the simulations. In a similar way, the SBM and the BM were already using point locations representing fixed counting stations in the City of Salzburg to compare simulation results with real-world counting data. The hypothesis was that the delays which the traffic lights cause in the bicycle traffic flow would manifest themselves in discernible patterns when plotted in charts



for fixed locations with the number of cyclists (dependent variable) over time (independent variable). The maximum recognisable effect was anticipated to occur with red/green phases of equal duration (i.e. not considering the difference in demand from the roads that lead to the intersections) in one scenario, and with additional inverted sequences (for direct comparison and affirmation) in another scenario. The expected outcome of the comparison of these traffic light scenarios were patterns of similar character, but shifted over time. In order to distinguish these flow patterns from those not caused by the traffic lights, a reference scenario without traffic lights had to be established as well. The main objectives in order to achieve the above with a model were:

- Review the 'Salzburg Bicycle model' (SBM) and the 'Bicycle model' (BM) incl. associated datasets.
- Define the area of interest (within the city centre of Salzburg/Austria).
- Research suitable modelling techniques to represent traffic lights and cyclist behavioural patterns (i.e. agent reaction to traffic lights).
- Create and test a 'sandbox' model.
- Determine to what degree the traffic lights in the area of interest are relevant to bicycle traffic.
- Determine how these traffic lights can be controlled.
- Prepare input datasets for a prototype model (including datasets from the SBM / BM).
- Create and test a prototype model.
- Define the boundary for the study area as applicable. This will be influenced by the findings from the steps above, for instance with regard to feasibility, abundance of counting stations, expected demand on the computing environment, etc.
- Prepare input datasets (including datasets from the SBM / BM).
- Revise the model structure as needed.
- Create and test the model.
- Run the model, document and interpret the results.

## 2. Methods

The following chapter combines the methods applied throughout this thesis, background information, and descriptions of software functionality. However, it is not strictly divided along these lines. The sections are rather written to provide relevant information when it is needed and at the level of detail that is necessary to follow the course of action.

### 2.1. Study area and application context

The chosen area for the research is the City of Salzburg/Austria. It is based on the 'Salzburg Bicycle model' (SBM) by Wallentin (2016) and the 'Bicycle model' (BM) by Kaziyeva *et al.* (2019). These models cover the region of Salzburg or, in a spatially reduced simulation option, the city limit of Salzburg. The model for this thesis works with an even further reduced spatial extent of approx. 1.6 km x 1.6 km (which is centred around the southern end of the Salzburg Mirabell Gardens and rotated for approx. 3.8°). The BM was developed in GAMA (Grignard *et al.* 2013). In order to leverage some of the know-how already gained during its development, and to follow the recommendation by Kaziyeva *et al.* (2018), this thesis continues on this path of model development with GAMA.

In the SBM and the BM, agent-based modeling techniques were used to simulate the spatio-temporal distribution of bicycle traffic under consideration of the cyclist population in the region of Salzburg, spatial distribution of source and target locations, trip purpose, and trip parameters such as start/end time windows and speed. The simulated distribution of the bicycle traffic was then compared to counting data from a number of real bicycle counting stations. Although the models account for many trip-related aspects, they do not consider cyclist behaviours such as interaction between the agents and their environment, or between the agents themselves.

### 2.2. Transportation modeling approaches

Another commonality of these models is that the agents move along a graph which is built from a network of edges - the edges represent roads and their connected ends represent intersections. The GAMA Modeling Language (GAML) provides multiple skills (sets of pre-programmed properties and abilities) which enable the movement of agents along such a network of edges (gama-platform 2018):

- The 'moving' skill, as used in the model by Kaziyeva *et al.* (2019), defines the minimal set of behaviours for this kind of movement.
- The 'driving' skill extends this functionality by considering other agents in the network (for instance through the definition of obstacle species).
- The 'advanced\_driving' skill further extends these skills, as it provides more driving-specific functionalities through the definition of additional properties, but also enables the control of agents based on behavioural probabilities.

Corresponding to the order of these three skills, there is also an increase in the potential for the implementation of certain driver agent behaviours in the model.

### ***2.3. Cyclist behaviour at traffic lights***

There are many factors that can influence the behaviour of a cyclist - before, after, or (more importantly in the context of a traffic model) during the trip. These factors could, for instance, be infrastructure-related (e.g. whether there are dedicated cycle paths available) or environment-related (e.g. whether these cycle paths are exposed to strong winds). In agent-based modelling, any behaviour of agents or their interaction with their surroundings has to be programmed into their type (species) definition. For instance, to avoid collisions on a road network in a traffic model, agents have to be able to detect whether a specific space is already occupied by another agent. In the case of the effect of traffic lights on the agents, they first have to be equipped with the ability to detect the status of a traffic light (in a simplified version: red/green), and subsequently with instructions how to behave once they detect such a signal.

#### **2.3.1. Traffic light detection based on spatial query**

##### ***2.3.1.1. Detection ranges***

Initially, the intention was to provide every cyclist agent with a cone-shaped detection range which it would push ahead of itself in the direction of travel along the network edges, similar to NetLogo's (Wilensky 1999) 'in-cone' reporter function. A spatial query would then determine when a traffic light is located within the cone. The agents in Fig. 2-1 are travelling towards an intersection with a traffic light point on every road. The agent on road 3 would detect a green light and be allowed to proceed, while all others would detect red lights and have to slow down and stop. In this ideal situation, every agent would only detect the traffic light on the road which it is travelling on.

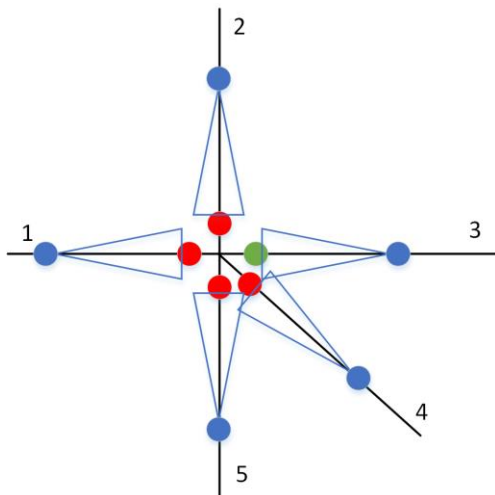


Fig. 2-1: Cyclists with detection cones travelling towards traffic lights.

Fig. 2-2 shows a situation where the cones of the agents on road 4 and road 5 would detect two traffic lights, leading to an ambiguous result. This illustrates that the cones in this 'active' detection method would have to be dimensioned in such a way that they only detect the intended traffic light in any given situation on the road network. Considering the many different angles at which roads intersect, and potentially very short or strongly curved road segments in the road network, this would likely not be feasible with one universal combination of cone angle and length.

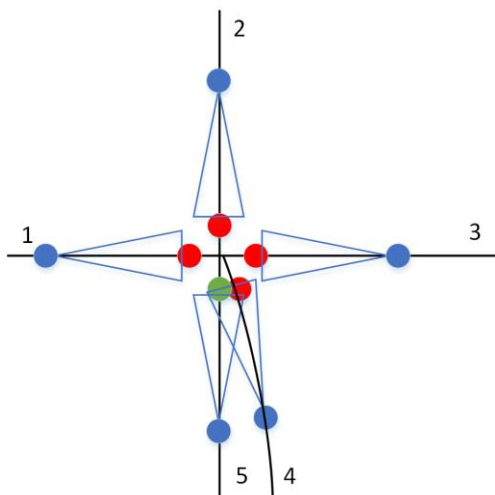


Fig. 2-2: Agents on road 4 and road 5 detecting two traffic lights with their cones.

It appeared as if a reversed ('passive') detection method could eliminate some of these concerns. In the variation in Fig. 2-3, the traffic light points would be buffered. The buffers

would be used to detect the approaching agents, which would then trigger the control of their movements towards the traffic lights. An agent entering a green buffer zone (road 3) could proceed, while an agent entering a red buffer zone (all other roads) would have to slow down and come to a stop at the traffic light.

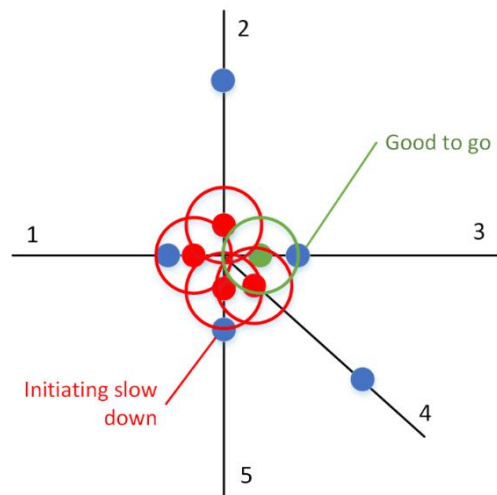


Fig. 2-3: Traffic light point locations with circular detection buffers.

The implementation of either of the two concepts would require extensive preparation work (e.g. adding a traffic light point feature for every incoming road at traffic light-equipped intersections, buffering these points, and linking them to the buffers) and fine-tuning (e.g. finding the right cone or buffer dimensions) - with uncertain success.

### 2.3.1.2. Distance measuring

The testing of the spatial relationship could be simplified by limiting permissible interaction to traffic light points and cycling agents on the same road. In this case, the Euclidean distance between the agent's location and the traffic light point location (measured and added up along the segments of the road graph) could be monitored and trigger the stopping process as soon as it falls below a certain threshold.

### 2.3.1.3. Additional concerns

However, a concern regarding all three concepts was that the locations of the agents at the end of each simulation step depend on their previous movements, as they are determined by the agents' speed and the accumulated distances which they travelled since the start of their trip. Depending on these variables, an agent's next step could result in a 'jump' over the traffic light

without detection (in cases where the agent would be close enough and the detection range too small).

Furthermore, it would have to be ensured that an agent that leaves the intersection and passes a traffic light that is intended to control oncoming traffic won't trigger another detection. This could be achieved by limiting the traffic light's 'active' range to be oriented away from the intersection, but it would require to determine every agent's current bearing and to compare it with the traffic light's sensitive direction.

Although especially the detection method with the cone would resemble closely how a cyclist detects a traffic light in reality, the overall approach to implement the detection functionality in the model through this kind of spatial relationship between the traffic lights and the cyclist agents seemed problematic. Therefore, a different potential solution within the GAMA platform was explored: The 'advanced\_driving' skill.

### 2.3.2. Traffic light detection based on list comparison

Note: The following section describes the theoretical requirements and options of the GAMA platform to create the intended model functionality, as well as the decisions and actions that had to be taken accordingly in order to prepare and provide the appropriate datasets for the model. This content is interrelated; the two aspects are therefore not strictly separated.

The GAMA platform provides a 'driving' plugin that is intended for transportation-related simulations (Taillandier 2014). It requires a road network, and nodes to be placed at the end vertices of the road polylines. The roads (which can be comprised of multiple road segments) and the nodes can be loaded into the model as ESRI shapefiles (ESRI 1998). The plugin works with a combination of three GAML skills (one of which is the aforementioned 'advanced\_driving' skill):

- The 'skill\_road' skill:
  - This skill registers the roads under consideration of the road direction.
  - The roads can be equipped with multiple lanes and can be assigned a speed limit (for instance via number attributes in the shapefile, as in the model for this thesis).

- The 'skill\_road\_node' skill:
  - This skill determines which roads lead towards a node and which ones lead away from it. These roads are stored in a 'roads\_in' list and a 'roads\_out' list.
  - The skill also provides a 'stop' list, which can contain roads from the 'roads\_in' list. If an agent travels towards a node on a road in the stop list, it will be forced to stop at the node.
- The 'advanced\_driving' skill:
  - This skill contains the 'drive' action which moves the agent along a pre-calculated trajectory to its target location node.
  - This movement is influenced by a number of variables which concern the description of the agent itself and the surrounding environment, but also the agent's behaviour.

To take advantage of these three skills, the agents' movements have to be based on a 'driving graph'. The 'driving' plugin provides a special operator to generate this driving graph. Since this operator uses the roads and nodes species as arguments, the road network and the nodes first have to be loaded from the shapefiles, and their respective species have to be declared (gama-platform 2016a).

#### *2.3.2.1. Stop list functionality*

The stop list functionality provided by the 'skill\_road\_node' skill appeared to be a suitable alternative method for traffic light detection. It has the advantage that a successful detection does not depend on the geometries of the involved agents and their spatial relationship, but solely on whether a road agent is included in the stop list or not. The cyclist agents that are equipped with the 'advanced\_driving' skill recognize when they travel on roads that are included in this list. They will then stop at the nodes which the listed roads lead to. If the roads are removed from the stop list during the next simulation cycle, the agents will continue to move according to their trajectories. Hence, the stop list can be regarded as a panel of (traffic) light switches whose positions are reconsidered for every cycle.

#### *2.3.2.2. 'Sandbox' model with stop list*

The GAMA platform team provides multiple tutorial models, some of them offering driving-specific solutions (e.g. gama-platform 2016b). A 'sandbox' model was set up with components (code segments and datasets) from some of these tutorial models. The chosen datasets contained

a road network shapefile with a very limited spatial extent, and matching nodes at the end vertices of its edges in a separate shapefile. However, the tutorial function generating the stop list for the control of the traffic lights was set up in such a way that the roads at an intersection were all either set to stop or to go at the same time. In addition, it was determined randomly during the model initialization which intersections would be in which state. In order to limit the red phase to only specific individual roads at the intersections, this stop list was substituted with a hardcoded version for some testing. Furthermore, a shapefile with a point feature class showing an additional traffic light point on the right side at every road end was added to indicate the road's stop list status (Fig. 2-4). The graphical appearance of agents in GAMA is controlled with 'aspects' (methods which also allow the use of conditions). In this case, the aspect instructions for the traffic light point features were written in such a way that the points appeared in red when the corresponding roads were in the stop list and green when they weren't.

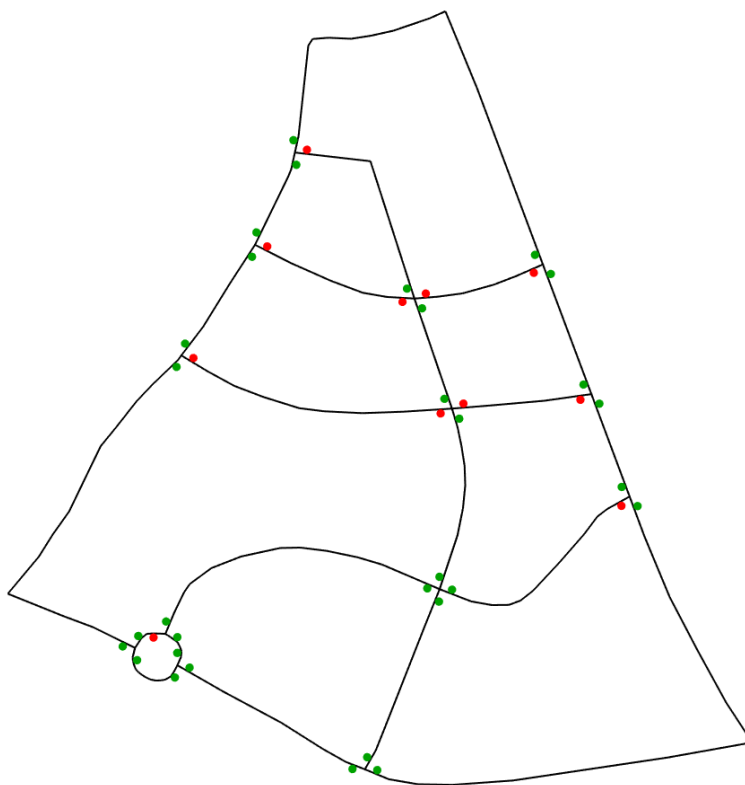


Fig. 2-4: 'Sandbox' model with additional traffic light points

In order to avoid hardcoding the stop list in the final model code, options to import a pre-generated stop list with phase timing from an external file were investigated. The remaining subsections focus on the stop list format and how it was used for this purpose, while section 2.3.3 ('Other behavioural aspects') elaborates on additional behavioural aspects.



### 2.3.2.3. Stop list structure

According to Taillandier's (2014) paper about traffic simulation with the GAMA platform, the stop list has the format of a list of lists and can contain information about different types of stop signals. However, it remained unclear what these types are and how they would have to be stored in the stop list. From the available information and from observation of test simulations with the sandbox model, it can be assumed though that the sub list with index [0] in the stop list represents traffic lights. It contains the road agents with their species name and a feature ID, for instance:

```
[ road (2396) , road (125) , road (147) , road (1788) ]
```

Fig. 2-5: Stop list content example

This format allows for the assignment of individual roads as stop roads. Consequently, the list has to contain all roads that are supposed to have the same traffic light state during the current simulation cycle (i.e. individual traffic lights which are to be controlled together for different directions at an intersection). Since the list only represents traffic lights in stop mode (i.e. red), this implies that traffic lights which are not represented by a road in this list are green, or that the road doesn't have a traffic light and the underlying traffic rules (as further described in the 'Probabilities' section in Table 2-1) are applied. The example stop list in Fig. 2-5 could therefore represent an intersection as shown in Fig. 2-6:

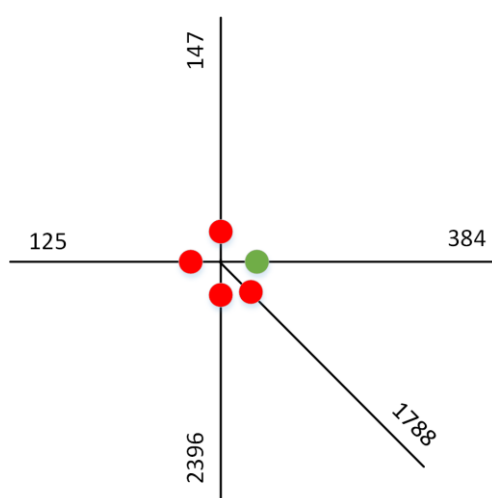


Fig. 2-6: Intersection example

#### 2.3.2.4. Stop list substitute

It seemed as if the initial stop list was always automatically created by the tutorial function and could only afterwards be substituted with a self-generated list in a matching format. With the stop list being applied during every simulation cycle, there would never be any change in traffic light phases with a static list. In order to be able to control the change of red/green phases during the simulations based on own rules, the list was therefore extended in such a way that it contains the intended roads for every simulation cycle. However, there are also multiple other processing steps involved in the generation of this substitute list. To avoid confusion, the interim stages are referred to as 'transfer list' in the following.

#### 2.3.2.5. Stop list generation

This transfer list is created by the GAML model code from a comma-separated values (CSV) file which is exported from a MS Excel<sup>®</sup> spreadsheet. The spreadsheet contains one column per road that is leading to a traffic light-controlled intersection (taken from the 'roads\_in' list) and one row for every simulation cycle. Every road that should appear in the final stop list for a specific cycle is marked with an 'x'. As an example, the roads '926', '1651', and '2004' (leading towards intersection node '16') in Fig. 2-7 are set to appear in the stop list for the first ten cycles in the simulation.

	A	B	C	D	E	F	G	H	I	J	K	L	M
1	x_nodes	16					166		459			565	
2	roads_in	926	1651	1931	2004	2082	882	1998	931	1709	1904	635	1403
3	1	x	x		x		x	x		x			
4	2	x	x		x		x	x		x			
5	3	x	x		x		x	x		x			
6	4	x	x		x		x	x		x			
7	5	x	x		x		x	x		x			
8	6	x	x		x		x	x		x			
9	7	x	x		x		x	x		x			
10	8	x	x		x		x	x		x			

Fig. 2-7: Spreadsheet example with stop markers (to be exported into a CSV file)

The GAMA driving plugin expects a list of road agents - a list imported from a CSV file is handled as one long character string instead. Therefore, the GAML code reads the exported CSV file into a matrix (a two-dimensional array structure). It then loops through every row of this matrix. Within every row, it loops through all columns. Whenever it detects an 'x'

(character), it reads the corresponding road name (i.e. the characters representing the feature ID of the road) from the second header row and appends it to the sub-transfer list for this cycle. The cycle lists are themselves appended to the transfer list.

The example in Fig. 2-8 shows the first few cycles in such a transfer list as it would appear with the full road agent names. Every individual sub list represents one row in the matrix (one cycle) and is enclosed in '[' ]' brackets. The first three sub lists in this example only contain three roads, but it could be many more. These sub lists are combined in another list (hence enclosed by additional '[' ]' brackets) for the whole simulation.

```
[ [road(2396), road(125), road(147)], [road(1788), road(920), road(3136)],
  \_____ CYCLE 1 _____/ \_____ CYCLE 2 _____/

[road(2396), road(125), road(147)], [road(1788), road(920), ... ]
  \_____ CYCLE 3 _____/ \_____ CYCLE ... ____/
```

Fig. 2-8: Transfer list example with sub-transfer lists per cycle (full road agent names)

As noted above, the CSV file used in the model only carries the feature IDs for the roads, hence the same example would look as in Fig. 2-9.

```
[ [2396, 125, 147], [1788, 920, 3136], [2396, 125, 147], [1788, 920, ... ]
  \__ CYCLE 1 __/ \__ CYCLE 2 __/ \__ CYCLE 3 __/ \__ CYCLE ... __/
```

Fig. 2-9: Transfer list example with sub transfer lists per cycle (road feature IDs only)

Besides reducing the matrix size by avoiding the redundant character string 'road' in the CSV file, these number strings can be easily cast into integer values. The same applies when finally substituting the stop list with the transfer list: The integer values can be cast into the 'road' type during the substitution, the new stop list will then contain the required road agents. The flowchart in Fig. 2-10 shows the stop list creation and substitution process in pseudo-code.

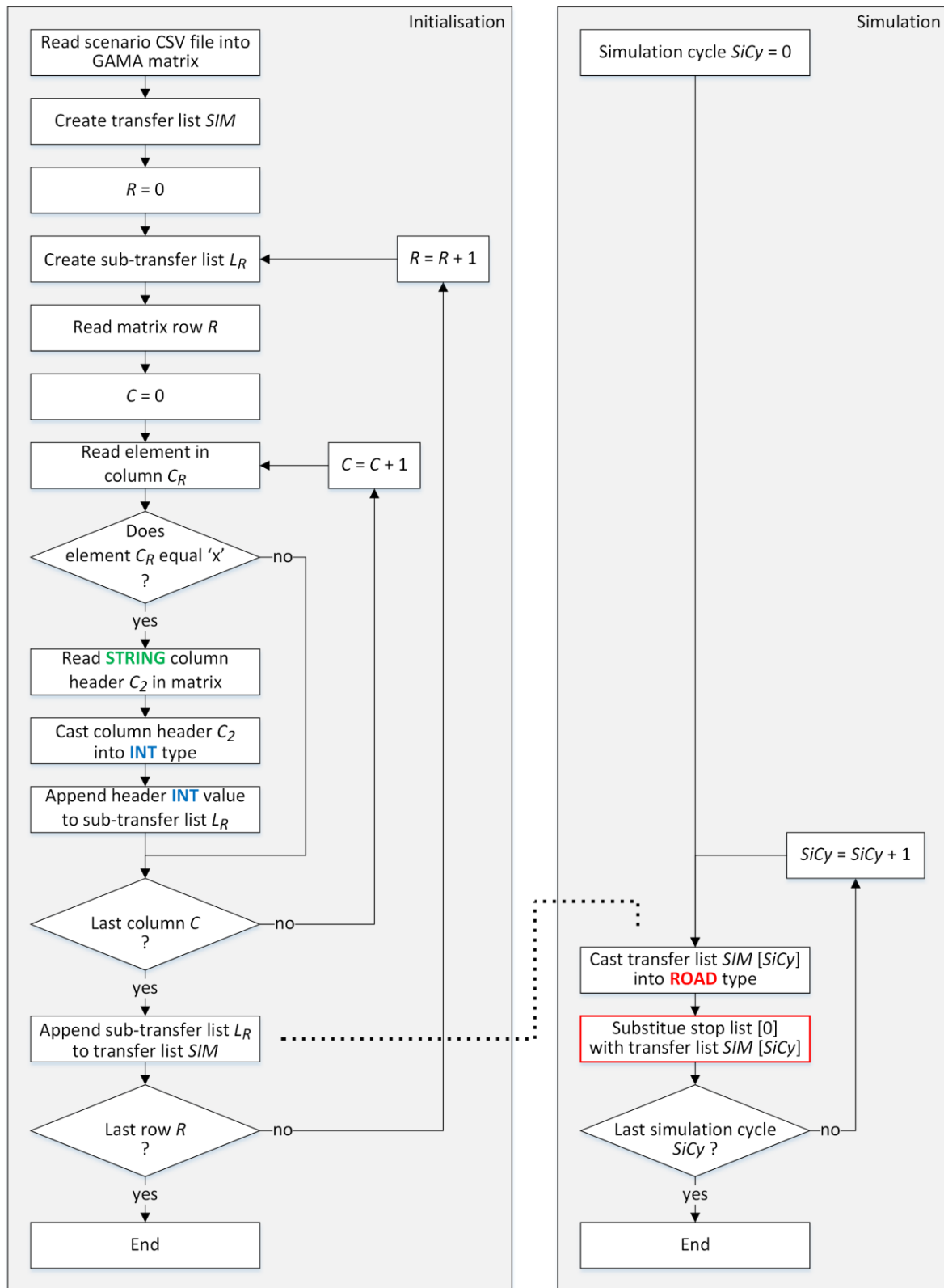


Fig. 2-10: Pseudo-code flowchart for stop list creation and substitution

The simulation cycle-specific transfer list always replaces index [0] of the stop list (the index for traffic lights). Fig. 2-11 shows an example of this substitution (with the values from the example in Fig. 2-8). In this example, the traffic light phases would switch with every cycle.

```

Stop[0] <- [road(2396), road(125), road(147)]      for cycle 1
Stop[0] <- [road(1788), road(920), road(3136)]    for cycle 2
Stop[0] <- [road(2396), road(125), road(147)]    for cycle 3
Stop[0] <- [road(1788), road(920), ...]          for cycle ...
...

```

Fig. 2-11: Transfer lists per cycle being assigned to stop list index [0]

### 2.3.2.6. Stop visualisation

In order to be able to visualise which roads are in the stop list (without having to add an additional traffic light point for every road leading to a traffic light intersection as in the sandbox model), the aforementioned ability to format agents within aspects is used to display the stop roads themselves as red arrows that point to the intersection. This is based on the same transfer list described in the previous section, only here it is used to generate red arrow graphs with GAML's 'as\_edge\_graph' function. Fig. 2-12 shows an intersection with stopped cyclists next to two stop roads. In this situation, cyclists on the other three roads would be allowed to proceed.

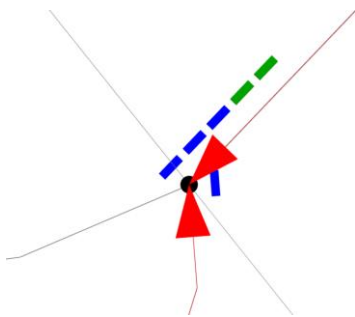


Fig. 2-12: Intersection example with red stop arrows and stopped cyclists

Although this visualisation method results in an additional computational effort, it greatly helped during the model troubleshooting and benefits the viewer during the simulation.

### 2.3.3. Other behavioural aspects

The previous section already described the 'skill\_road\_node' skill's stop list and its functionality as the foundation for the chosen traffic light detection method. However, the 'advanced\_driving' skill provides additional functionality in form of variables (Table 2-1) that affect the agents' behaviour directly or indirectly. Although these variables are not cyclist-specific, they can be set to cyclist-typical values. Please note that they cannot be renamed, as they act as an interface with the driving plugin. In addition to the variables in Table 2-1, the 'advanced\_driving' skill provides various read-only variables that can be used to control the program flow in the model.

Table 2-1: Variables provided by the 'advanced\_driving' skill

<b>Physical variables</b>	<b>Description</b>
vehicle_length	Since the agents don't share the same space, the vehicle length indirectly determines the distance to other agents in front of them. For the cyclist agents in this model, the vehicle length was assumed to be 1.5 m.
max_acceleration	The application example in Taillandier's (2014) paper provides a numeric value, but no unit. It is therefore not entirely clear what this variable represents. However, it is assumed that the effect of acceleration on the overall simulation results is minimal. The variable was therefore set to be similar to the example (randomly selected between 0.5 and 1.0).
max_speed	Unlike the 'maxspeed' variable (provided by the 'skill_road' skill) which sets the speed limit for roads, this variable defines the maximum vehicle speed (Taillandier 2014). As with the max_acceleration variable, the application example provides a numeric value, but no unit. Based on the standard units (meter, second) in GAMA simulations, it is assumed that the unit for this speed would be m/s. However, since the speed in the model was already limited to 20 km/h by the 'MAXSPEED' attribute in the road network shapefile (see 2.4.1, 'Provided datasets'), no additional maximum speed was defined here.
right_side_driving	This variable determines on which side of the road the agents drive. In this model, this variable is set to 'true' (for right-side driving).
<b>Coefficients</b>	<b>Description</b>
speed_coeff	According to Taillandier's (2014) paper, this coefficient "defines if the driver will try to drive above or below the speed limits." However, since it is a numeric factor, it will also determine which speed the driver is attempting to reach. In the application example, this coefficient was set to be a random value between 0.8 and 1.2. This range was also applied for this model. With a maximum speed of 20 km/h (as defined in the corresponding attribute in the road network shapefile), this defines a range of 16 km/h – 24 km/h for the speed that the driver might attempt to reach.
security_distance_coeff	This coefficient is used in the calculation of the security distance between two drivers as a function of the real speed: $\text{security distance} = \text{security\_distance\_coeff} * \text{real\_speed}$ For this model, the value range was chosen as in the application example (randomly set between 1 and 3).

Table 2-1: Variables provided by the 'advanced\_driving' skill (continued)

Probabilities	Description
proba_lane_change_up / proba_lane_change_down	The 'driving' plugin allows for roads to have multiple lanes. These probabilities can be used to influence a driver agent's decision to change the lane. The roads in the dataset for this model are set to only have one lane, therefore these probabilities don't have any effect. However, this functionality could potentially be useful in future bicycle traffic research for the specification of bicycle infrastructure.
proba_use_linked_road	As described earlier, roads are considered as directed and therefore have to be reversed and linked to the original road in order to create a two-way road. This probability affects a driver agent's decision to use such a linked road. However, it couldn't be determined from the available information about the 'advanced_driving' skill (Taillandier 2014) whether this use of a linked road refers to a passing manoeuvre (moving in the same direction) or to a change in direction (essentially making a U-turn). In order to prevent both, this probability was set to 0 in this model. However, in a more sophisticated bicycle traffic model, this probability could be a helpful parameter.
proba_respect_priorities	This probability variable refers to the right of way rules at intersections that are not controlled by any other traffic signal. It appeared from observation that this simulates the 'right before left' rule (for right-side driving) as it is applied in countries such as Germany. In order to avoid violations during the simulations with this model, the value was set to 1.0.
proba_respect_stops	Contrary to the previous variable, the probability to respect stops refers to intersections that are controlled by traffic signals (Taillandier 2014). As mentioned in section 2.3.2.3 ('Stop list structure'), this can refer to different types of traffic signals and the values are therefore also stored in a list structure. Corresponding to the chosen stop list index for traffic lights for this thesis, the list for this probability was set to contain only one value (index [0]) of the list. This value was set to 1.0 in order to create reference simulations without traffic light violations. However, further research could potentially use this probability to simulate red light infringements.
proba_block_node	This probability variable would allow driver agents to block intersection nodes. Although it is set to 0 in this model, it could occasionally be observed during simulation tests that cyclist agents blocked others when a traffic light line-up extended beyond a neighbouring intersection. It is therefore unclear how the effect caused by a different value for this probability would differ.

## 2.4. Preparing input datasets

With the spreadsheet structure and the methods to extract and process the stop list information from the CSV file in place, the sandbox model datasets were to be replaced with the datasets for the study area.

### 2.4.1. Provided datasets

Except for those created during the work on this thesis, the model uses datasets provided by the team of the Interfaculty Department of Geoinformatics (Z\_GIS) at the University of Salzburg, as received from the original sources. Table 2-2 provides an overview of these datasets.

Table 2-2: Overview of datasets

Dataset	Type	Format	Purpose	Source
counting_stations <sup>1</sup>	Point	Shapefile	Counting station locations	[1]
homes <sup>2</sup>	Polygon	Shapefile	Residents distribution	[2]
lichtsignalanlagen <sup>1</sup>	Point	Geodatabase	Traffic light locations	[3]
network <sup>2</sup>	Line	Shapefile	Road network	[4, 5]
universities <sup>1</sup>	Point	Shapefile	University locations	[6, 7]
work_places <sup>1</sup>	Polygon	Shapefile	Work places distribution	[8]
boundary	Polygon	Shapefile	Study area boundary	[9]
nodes	Point	Shapefile	Intersection nodes	[9]
scenario_00	Alphanumeric	CSV-file	Traffic light phase timing	[9]
scenario_01	Alphanumeric	CSV-file	Traffic light phase timing	[9]
scenario_02	Alphanumeric	CSV-file	Traffic light phase timing	[9]

These datasets were adapted to the requirements of this thesis with regard to:

- Spatial extent (as indicated in Table 2-2 and described in the following sections)
- Attributes in the 'network' dataset (road network shapefile)
  - MAXSPEED: The cyclist speed in the model was limited by setting the maximum speed on the roads to 20 km/h, analogous to the average cyclist speed in the SBM (Wallentin and Loidl 2015)
  - LANES: The number of lanes per road was limited to one lane

<sup>1</sup> The dataset was clipped to the study area boundary during the adaptation for the model

<sup>2</sup> The dataset was clipped during the adaptation for the model, but exceeds the study area boundary



- **ONEWAY:** The one-way property attributes were combined in one attribute for all possible one-way states

All spatial datasets use the WGS 84 / UTM zone 33N coordinate system (EPSG:32633).

#### 2.4.2. Extent of the study area

The extent of the study area as described in section 2.1 ('Study area and application context') was chosen to satisfy the following requirements:

- It should be much smaller than the 'city' extent in the original 'Salzburg Bicycle model' (Wallentin 2016), since the computational effort for simulation calculations with the 'advanced\_driving' skill was expected to be too big otherwise.
- It should cover the city centre of Salzburg. Since no clear definition of this area was found, a position close to the historic city centre was chosen.
- It should be oriented along the 100 m x 100 m and 250 m x 250 m population grids as in the provided datasets and the size should match a multiple of the grid cell sizes.
- It should still include at least three of the counting stations from the original 'Salzburg Bicycle model'.
- It should not be too big, since a high number of traffic light locations was expected to cause extensive preparation and evaluation work.
- It should not be too small, as it was expected that this could lead to non-representative results in the spatio-temporal distribution of the bicycle traffic.

Fig. 2-13 shows the resulting study area, with the orange square representing the minimum boundary. The study area is not strictly limited to this boundary though, due to the following circumstances:

##### 2.4.2.1. Clipping of the point and polygon datasets

The intention was to not have data gaps within the study area. However, since there was no congruent delimitation boundary shared by all involved datasets, the 100 m x 100 m polygon grid cells were chosen as the common base unit. These polygons (Fig. 2-13, green) represent the distribution of work places which some of the cyclists are travelling towards. The original dataset was then clipped along this grid to the size of 1600 m x 1600 m, based on the criteria mentioned in the section above - this is the area as indicated by the orange square.

The university point locations which the other group of cyclists is travelling to in the simulations were also clipped to this square boundary, the remaining university locations all fall within the boundary.

The distribution of homes is represented by the 250 m x 250 m polygon grid cells (Fig. 2-13, blue). The cyclists in the simulations start their trip from random locations within these polygons. The polygons protrude over the square boundary to ensure complete data coverage of the study area. They were not clipped to the 100 m x 100 m grid size since this would have altered the spatial distribution.



Fig. 2-13: Extent of study area (orange square, 1600 m x 1600 m)

#### 2.4.2.2. Clipping of the road network dataset

It appeared that the driving graph could only be calculated from a closed and connected road network. In order not to alter the original dataset too much, the roads that crossed the square boundary (up to the point where they connected with another road to a closed loop) were kept in place, instead of clipping them along the square boundary and reconnecting their ends. This

ensured that the cyclist agents could make unrestricted use of the road segments within the boundary, but it also resulted in some long road loops outside of it (especially in the 'Kapuzinerberg' area E of the centre).

#### 2.4.3. Adding intersection nodes

As the available datasets didn't contain a nodes feature class, they were created in the GIS software QGIS (QGIS Development Team 2018) from the edges in the road network shapefile. After eliminating duplicate nodes, an attribute field was added to designate which intersections should be considered to be controlled by traffic lights.

#### 2.4.4. Assigning traffic light status to intersection nodes via attributes

A preview of the traffic light dataset at the beginning of the thesis work had revealed that their point locations didn't coincide with the polyline network in the road shapefile, as shown in the example of 'Dr.-Franz-Rehrl-Platz' in Fig. 2-14 (lower traffic light point).



Fig. 2-14: Traffic light points at 'Dr.-Franz-Rehrl-Platz' (Orthophoto: Geoland.at 2019)

In some instances, it was also not clear from the information in the traffic light geodatabase file which roads at an intersection are in fact controlled by the light – even after comparison with underlying aerial imagery (Fig. 2-14 and Fig. 2-15).

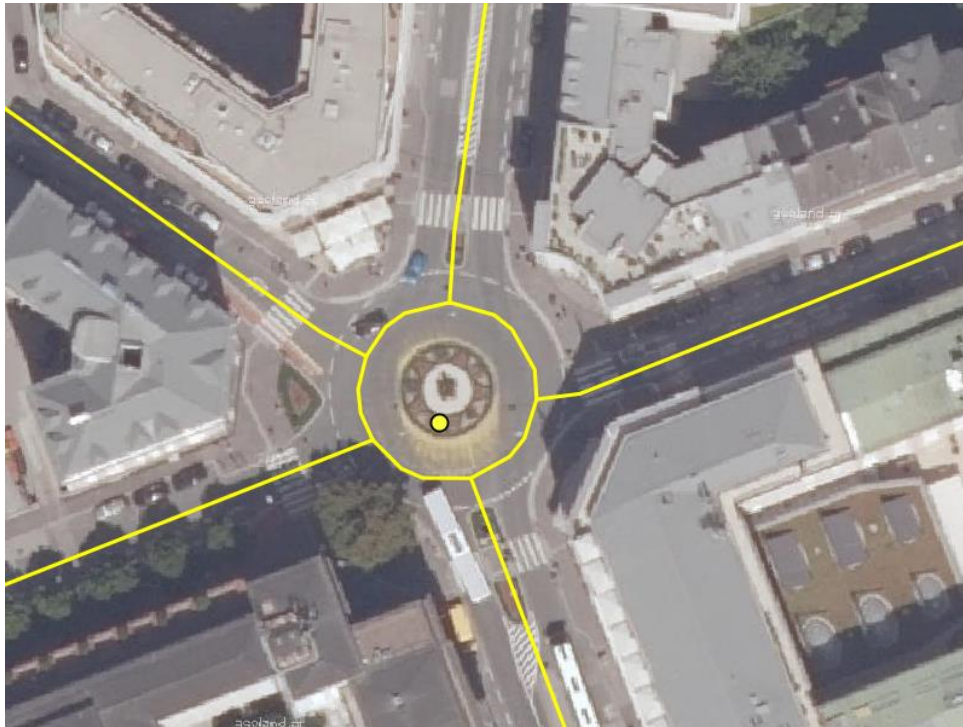


Fig. 2-15: Traffic light point at 'Max-Ott-Platz' (Orthophoto: Geoland.at 2019)

On a few occasions, ground level imagery had to be searched on the internet to verify traffic light locations. Since Google Street View<sup>®</sup> is not available in Salzburg, there is unfortunately only a small number of publicly accessible sources. However, even this did not always clarify the situation. For instance, after reviewing a panoramic ground level photograph (Schmiedbauer 2016) of the roundabout at 'Max-Ott-Platz' (Fig. 2-15), it is questionable whether there is a traffic light at all at this location.

Of the 43 traffic light point locations within the study area, six had to be disregarded due to unclear situations on the ground. The remaining 37 traffic light point locations were then reviewed in order to find the nodes on the road network that best represent each traffic light. These nodes were then marked with a corresponding 'traffic\_signals' value in their 'TYPE' attribute field, which is used by the 'skill\_road\_node' skill in the model to determine which nodes to consider for the 'roads\_in' list.

#### 2.4.5. Adding reversed roads in the model code

The driving graph operator assumes road directions as they are defined for the polyline geometries in the shapefile, i.e. by default every road is considered to be a one-way road. If the direction of the polyline does not correspond to the one-way property of the represented road in the real world, it will have to be reversed (either already in the input dataset, or through the model code). Similarly, a second (reversed) road has to be added to the road network before building the graph in order to represent a two-way road.

To avoid modification of the road geometries in the original input dataset (beyond adding a value to the corresponding attribute in the original shapefile in order to be able to distinguish between the road directions in the model code), the addition and reversing of the roads (to create linked roads) was set up to be done in the model code. This approach proved to have one disadvantage: When agents are generated from a shapefile in GAMA, they carry the feature ID in their name that was assigned to them when they were created and then written into a shapefile in the external application. Due to its ease of operation compared to the object browsing options in GAMA, the GIS software QGIS was also used for object identification and troubleshooting during the development phase. However, agents created in GAMA after the shapefile objects were processed cannot be known to the GIS software (unless they are exported and loaded back into the GIS software), i.e. only a subset of the roads could be identified in QGIS. This led to a cumbersome process in the setup of the traffic light scenarios (section 2.4.7).

#### 2.4.6. Combining roads and nodes in stop list spreadsheet

As mentioned in section 2.3.2.5 ('Stop list generation'), the spreadsheet had to contain all roads that lead towards an intersection and are equipped with a traffic light. Due to the described process of creating the additional reversed roads, the sequential assignment of their feature IDs didn't allow for meaningful combinations of IDs in such a way that one would be able to tell which roads would lead to a specific intersection node. The combinations rather had to be extracted and written out by a GAML function. They then had to be manually transcribed and grouped in the spreadsheet in such a way that the phase timing markers could be placed on a per intersection basis, and even then the roads had to be identified individually in order to switch the appropriate traffic lights at the same time at every intersection. Unfortunately this also means that any change in the road network or the nodes feature class would require a reorganisation of the spreadsheet based on a new extraction of feature ID combinations.

### 2.4.7. Traffic light scenarios

After determining the combinations of the intersection nodes and the roads from the 'roads\_in' list in the spreadsheet, three traffic light scenarios were set up for the study area datasets.

#### 2.4.7.1. Scenario 0

This scenario is set up to not contain any road agents in the stop list (i.e. no traffic light functionality). The traffic is only controlled by the underlying traffic rules as they are applied through the 'advanced\_driving' skill (see section 'Probabilities' in Table 2-1).



Fig. 2-16: Overview of study area, traffic light scenario 0 (no traffic lights)

#### 2.4.7.2. Scenario 1

The traffic light intersections in this scenario are set up in such a way that all those roads are included in the stop list that are oriented approx. parallel to the Salzach river (Fig. 2-17), i.e. mainly in approx. N-S direction (with some variation towards NW-SE or NE-SW). This phase lasts for 60 seconds, then the roads are removed from the stop list and their counterparts with main direction perpendicular to the Salzach river (i.e. mainly in approx. E-W direction, with some variation towards NE-SW or NW-SE) are included. This corresponds to Fig. 2-18 in the next section (2.4.7.3 'Scenario 2'). After another 60 seconds (and alternating every 60 seconds thereafter), the roads are switched back. This phase switching pattern continues for a total duration of 720 seconds.



Fig. 2-17: Overview of study area, traffic light scenario 1, cycle 1 (stop roads in red)

### 2.4.7.3. Scenario 2

This scenario (Fig. 2-18) is a reversed version of scenario 1, i.e. the simulation starts with stop roads in E-W direction and switches to the N-S direction after 60 seconds, and so on.



Fig. 2-18: Overview of study area, traffic light scenario 2, cycle 1 (stop roads in red)



#### 2.4.7.4. Scenario comparison

The intention with this scenario setup was to create three directly comparable situations. Scenario 0 serves as a reference scenario, i.e. any difference between this scenario and the scenarios 1 and 2 with regard to the cyclist distribution can be attributed to the existence of traffic lights. The only difference between the two scenarios 1 and 2 is the 60-second cycle shift between them, i.e. by comparing the cyclist distribution over time in charts, it can be observed to what degree this 60-second delay manifests itself in the emerging patterns. Fig. 2-19 shows an intersection with stopped cyclists during the same simulation cycle, on the left side with the applied scenario 1, on the right side with the applied scenario 2.

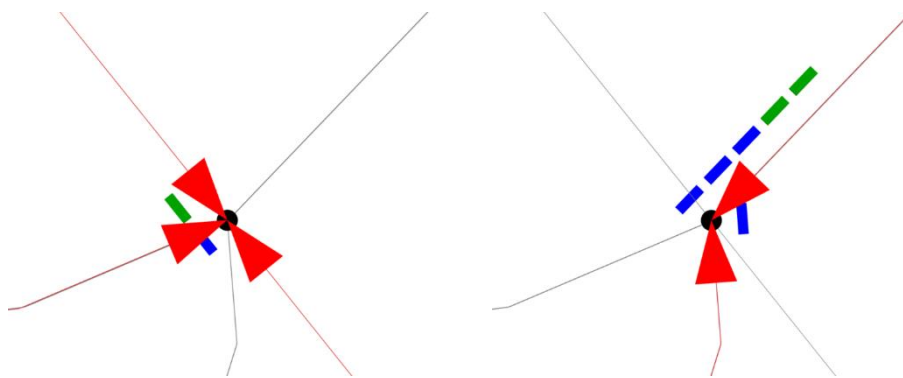


Fig. 2-19: Intersection with stopped cyclists, scenario 1 (left) and scenario 2 (right)

The time period of 60 seconds was chosen as an estimate of a reasonably realistic average traffic light phase duration. In reality, the specific phase timing for every traffic light is determined by many factors (Bonneson *et al.* 2009) - unfortunately these factors could not be considered in the scope of this thesis.

It should be noted that a closer examination of Fig. 2-17 and Fig. 2-18 might reveal that not every intersection with red arrows in one map has counterparts in the other map. This is due to the fact that not every road is indeed leading toward the common intersection nodes - in some cases the remaining roads might be one-way streets (leading only away from the nodes).

## 2.5. Traffic flow factors

The cyclist agents in the model represent the following two types:

- Employed cyclists
- Student cyclists

This distinction was made in order to base the simulations on different trip characters with regard to their source and target location type and distribution (as described below), while still being able to identify the cause for the emerging patterns as discussed in section 4.2 ('Chart interpretation - individual').

Fig. 2-20 shows the distribution of employed residents in the study area (red 250 m x 250 m squares), with a high density in the northern part. This means that this is where the majority of employed cyclists start their trip.

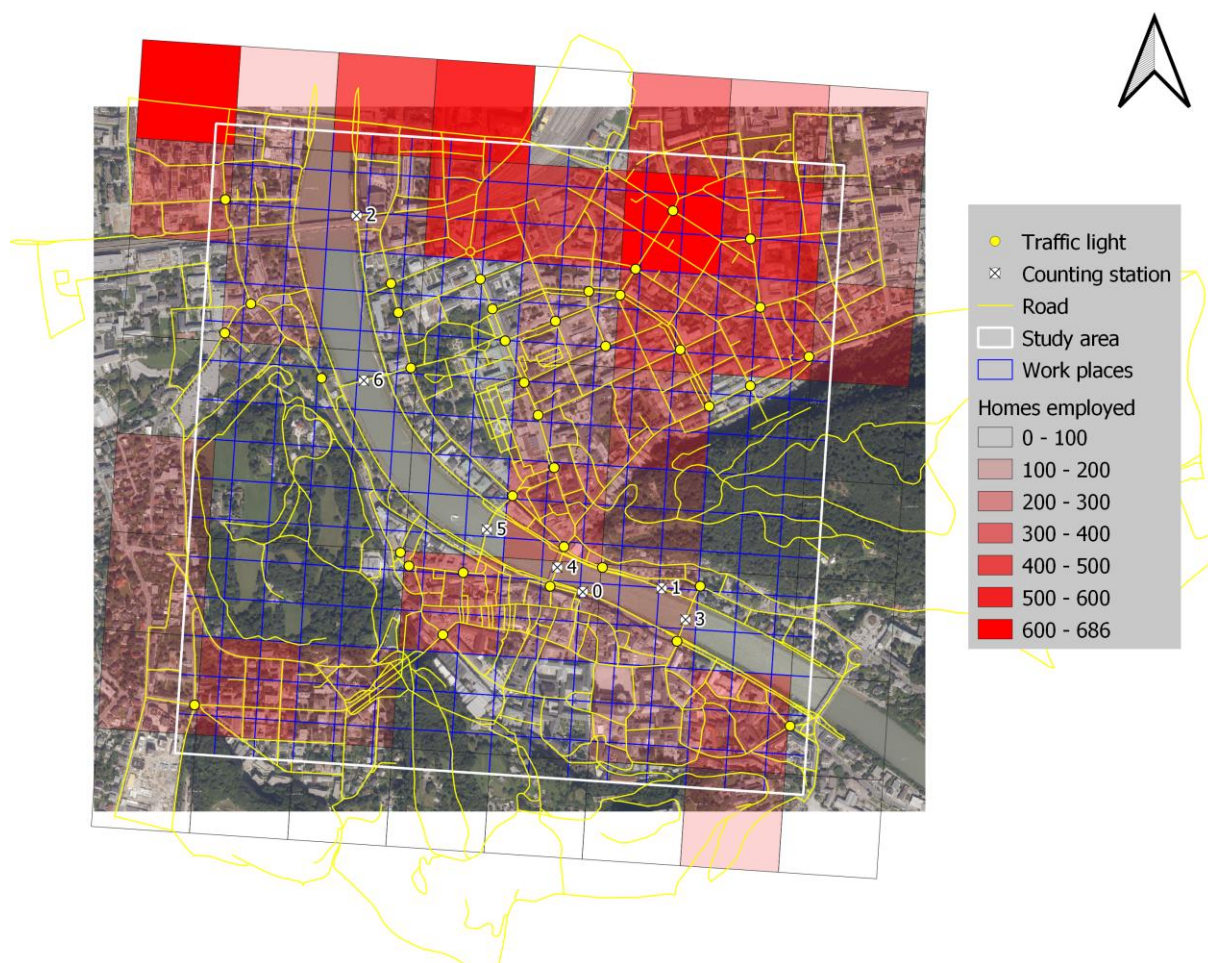


Fig. 2-20: Study area with distribution of employed residents

The distribution of student residents in Fig. 2-21 also concentrates in the northern part of the study area, although the areas with higher density reach a bit further S.

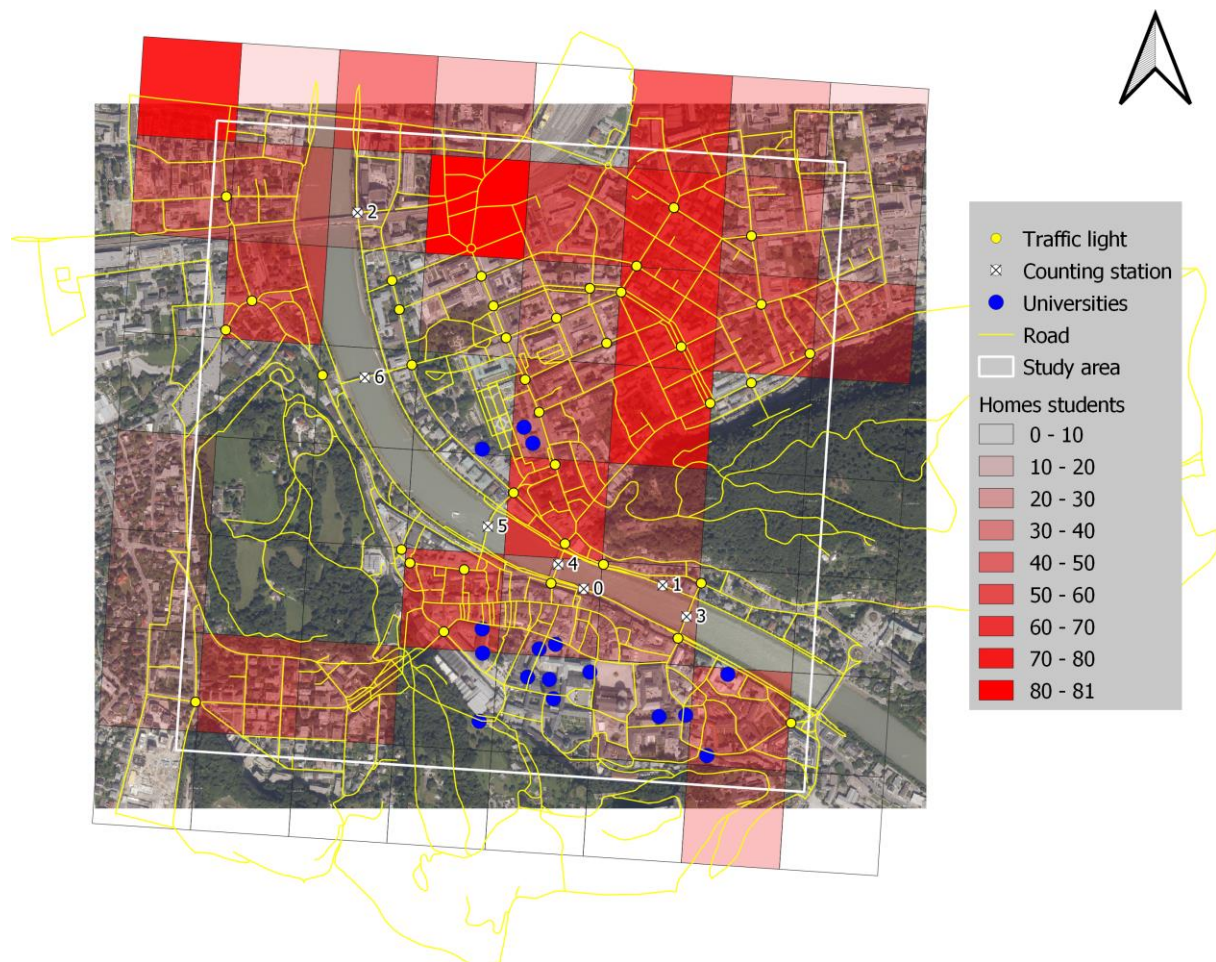


Fig. 2-21: Study area with distribution of universities

The traffic flow generated by the cycling population in the model is the result of simulations based on the following rules and with the following limitations:

- The cyclists are instructed to start their trip at a random location within their 250 m x 250 m residence grid cell, and to travel to a randomly selected target location.
  - In the case of employed cyclists ('workers'), this target location is chosen randomly from within one of the 256 blue 100 m x 100 m work place grid cells enclosed by the white study area boundary in Fig. 2-20.
  - If the cyclist agents represent 'students', they travel towards one of the blue university point locations (Fig. 2-21).
- While the density in the 250 m x 250 m population grid cells determines the number of cyclist who start their trip there, the density of work places within the 100 m x 100 m

grid cells (Fig. 2-20) and student enrollment numbers at the university point locations (Fig. 2-21) are not considered. I.e., due to the regular distribution of the 100 m x 100 m grid cells, workers might travel to any location within the study area boundary. Since the university point locations are distributed irregularly within the study area, these locations will see more student cyclist traffic than others.

- All cyclists start their trip at the same time. Although this would be unrealistic in a city, this schedule was deliberately chosen in order to increase the expressiveness of the results through higher cyclist numbers, and to be able to limit the required simulation duration to a minimum (determined to be 720 seconds in consideration of the established scenarios) while still allowing the majority of cyclists to complete their trip.
- The cyclist agents using the 'advanced\_driving' skill travel for as long as they are not stopped by traffic lights or other agents blocking the road, until they reach their final target location. During these movements along the road segments, they constantly monitor their distance and speed to their next target location and decide whether they can keep moving (Taillandier 2014).
- Cyclist agents using the 'advanced\_driving' skill can only travel to the node on the road network that is closest to their destination, they cannot complete the trip directly to the actual destination location. Since they would block the following traffic by stopping at their last target node, they have to be removed once they reach this node. A common practise in situations like this is to let these agents 'die' (i.e. to remove them from the agent population). However, attempts to do so caused an error in the plugin, which could not be troubleshooted due to insufficient information about the error. Therefore, these agents are moved to a different location off the road network by overwriting their location coordinates. This can be observed as flashing points during simulations with activated map view ('City display').
- The number of cyclists that are created for the simulation is derived from the total number of employed and student residents, as described above. However, due to the computational effort, the model is set up to execute the simulations with a default number of cyclists of 10% of these residents. This amounts to 1140 cyclists, of which approx. 88% are 'workers' and 12% are 'students'.
- The various deviations from Wallentin's (2016) and Kaziyeva *et al.*'s (2019) models in the implementation of the model for this thesis prohibit the direct comparison with these models, as well as with the real counting data from the three original counting stations.

## 2.6. Counting stations in the study area

Note: The counting stations in the following sections are identified by a number and/or by their location name. In order to be able to differentiate between traffic directions, the counting station roads leading towards the centre of the study area (approx. at the southern end of the Mirabell Gardens) are indicated as 'inbound', the ones leading away from the centre as 'outbound'.

### 2.6.1. Heat map and additional counting stations

In preliminary test simulation results for the three original counting stations 'Rudolfskai' (CS 0), 'Giselakai' (CS 1), and 'Elisabethkai' (CS 2), only the outbound station CS 1 exhibited patterns that would suggest an influence of traffic lights on the traffic flow. Therefore a heat map (Fig. 2-22) was generated to provide an overview over major traffic flow areas in the model during a simulation based on scenario 0 (no traffic light influence). The map shows the mean (> 1.0) of the number of cyclists calculated for each of the 2129 roads in the study area. Due to the computation effort, this map was created from one simulation only. It can be gathered from the map that there is some traffic flow across the Salzach river. Therefore four virtual counting stations (CS 3: 'Mozartsteg', CS 4: 'Staatsbrücke', CS 5: 'Makartsteg', and CS 6: 'Müllnersteg') were added on the closest bridges to the centre of the study area (Fig. 2-22).



Fig. 2-22: Overview of major traffic flow areas (one simulation with scenario 0)

## 2.7. Simulations

### 2.7.1. Number of executed simulations

The simulations for the three scenarios were executed and aggregated in small batches in order to determine how many simulations might be required overall to produce meaningful results. Fig. 2-23 shows five series for scenario 1 at the Mozartsteg station (outbound), Fig. 2-24 shows five series for scenario 2 at the same station. Each of the series were created by calculating the mean of 20 simulations. Although there are some outliers in the levels of the taller peaks, the overall character of the simulations can be well observed. Based on these results, 100 simulations were deemed to be sufficient for the purpose of visualising the traffic light influence. The chart in Fig. 2-25, as an example for all the charts presented later in section 3 ('Results'), was thus created by calculating the mean over 100 simulations.

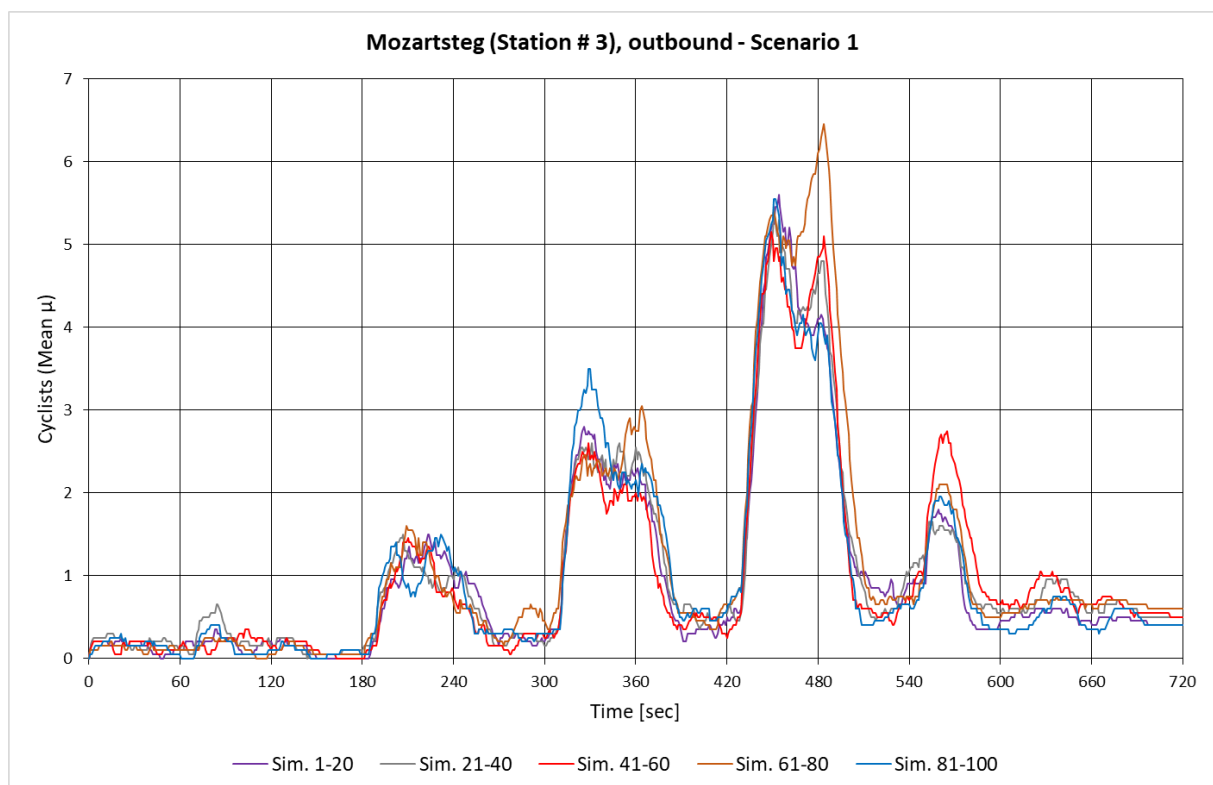


Fig. 2-23: Scenario 1 represented by five series, each showing the mean of 20 simulations

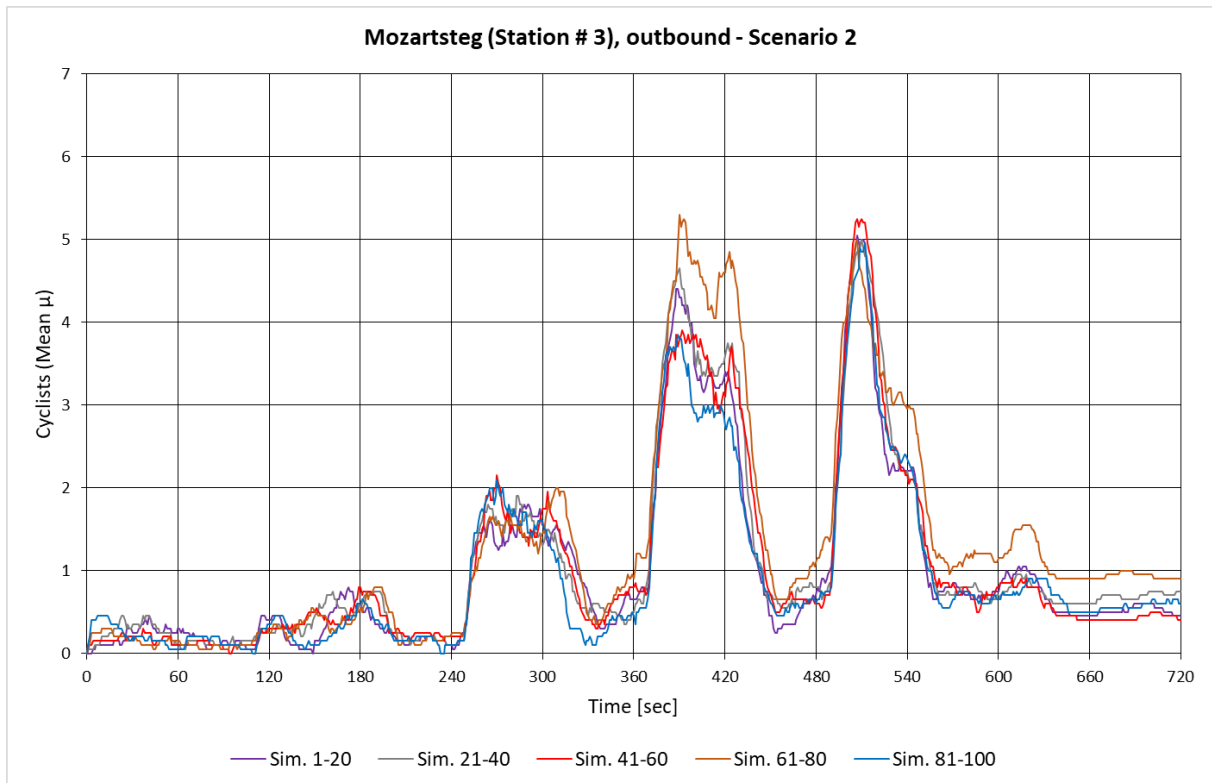


Fig. 2-24: Scenario 2 represented by five series, each showing the mean of 20 simulations

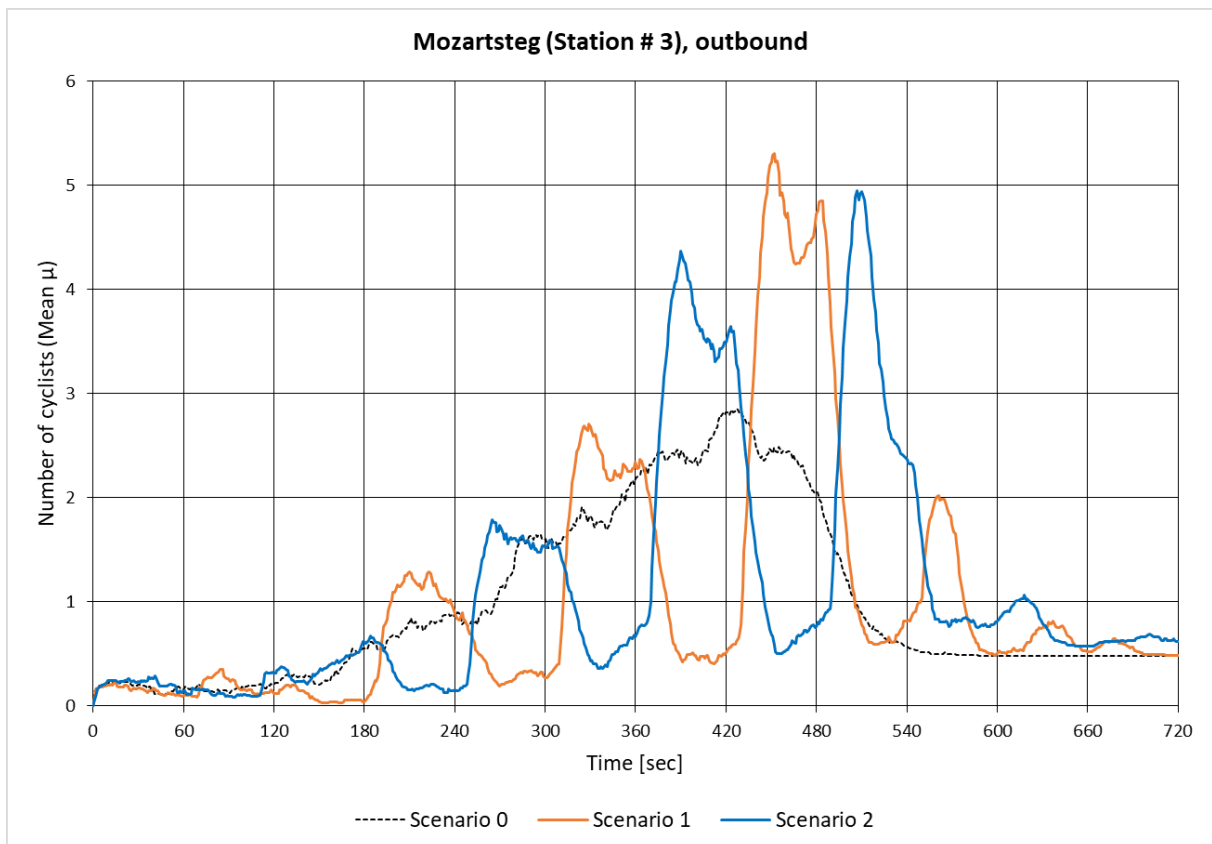


Fig. 2-25: Scenarios 1 and 2, each showing the mean of 100 simulations

## 2.8. Data export and processing

The cyclist counts for the 720 simulation cycles were exported into a separate CSV file for each of the 14 counting station roads (seven original roads and their linked counterparts in the opposite direction), for each of the 100 simulations, and for all three scenarios (Fig. 2-26).

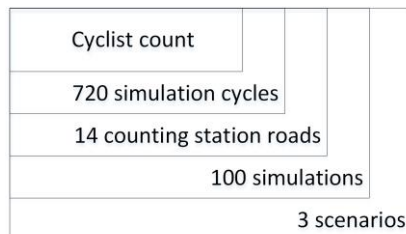


Fig. 2-26: Cyclist counting data organisation schema

After removing duplicate data, these individual CSV files were converted into the native MS Excel<sup>®</sup> format to facilitate linking of the data (Fig. 2-27, left). A spreadsheet in a separate MS Excel<sup>®</sup> file with links to the individual files was set up for every counting station road (Fig. 2-27, centre) and for every traffic light scenario. The mean values from these 14 resulting files per scenario (Fig. 2-27, right) were then used as source data for the charts series, with three scenarios displayed per chart.

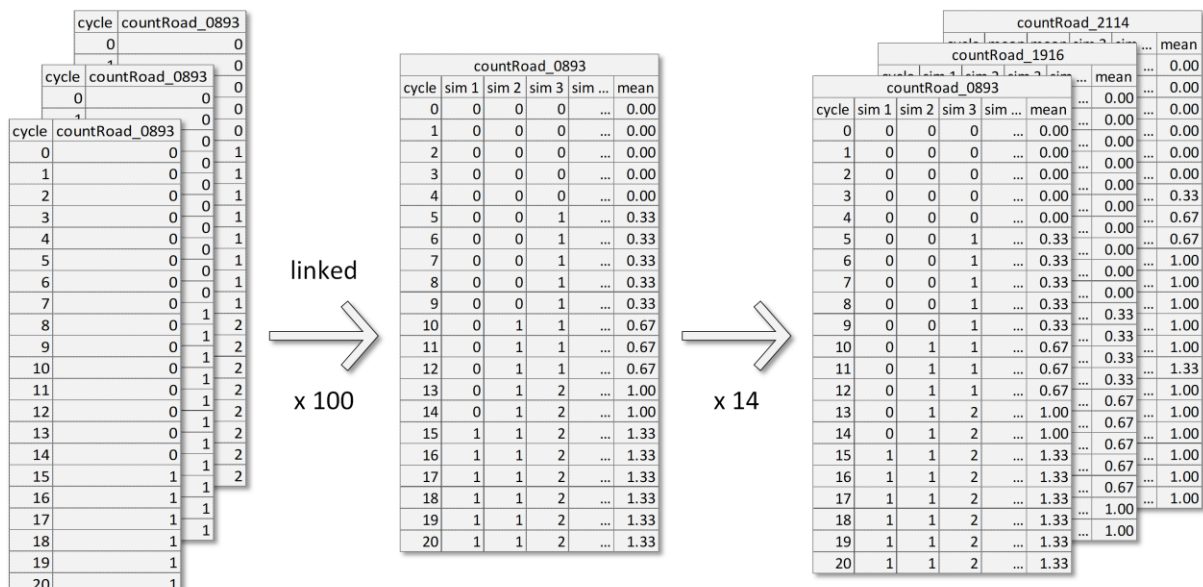


Fig. 2-27: Counting data aggregated per scenario (example for 20 simulation cycles)



## 2.9. ODD protocol

This section describes the thesis model ('SBM\_PR\_MSC.gaml', version 2019/02/27) with the intention to provide information that is sufficient to understand it and to reproduce the simulations that were generated with it. The model description follows the ODD (Overview, Design concepts, Details) protocol (Grimm *et al.* 2006) in its reviewed and updated version (Grimm *et al.* 2010).

### 2.9.1. Purpose

The purpose of the model is the visualisation of the effect of traffic lights on the spatio-temporal distribution of bicycle traffic in the city centre of Salzburg/Austria. The hypothesis is that the delays which cyclists experience at red traffic lights lead to shifts in the traffic volume at fixed cyclist counting stations, and that these shifts are prominent enough to be noticeable while observing different traffic light phase scenarios.

### 2.9.2. Entities, state variables, and scales

Please note that the following table (Table 2-3) only lists variables that were created for use within the model, or provided and actively used by the GAMA modeling platform. Other such variables whose default values were not explicitly changed or used to control the model execution are not listed. Some of the variable names contained in these lists are stated literally, as required by the model functions.

Table 2-3: Overview of entities, variables, attributes, and parameters

Entities (type / species)	State variables / attributes	Initial value / description
World (agent / global)	cycle <sup>1</sup>	0
	shape <sup>1,8</sup>	"network_clipped.shp" (polyline)
Model (agent / model)	name <sup>1,8</sup>	"SBM_PR_MSC"
Experiment (experiment plan)	name <sup>1,8</sup>	"Bicycle traffic simulation"
	percentage <sup>8</sup>	10, parameter (sets percentage of cyclist agent population for simulation)

Table 2-3: Overview of entities, variables, attributes, and parameters (continued)

<b>Entities (type / species)</b>	<b>State variables / attributes</b>	<b>Initial value / description</b>
Roads (agent / road)	all_agents <sup>1,3</sup>	calculated by skill
	name <sup>1,2</sup>	species + feature ID
	shape <sup>1</sup>	"network_clipped.shp" (polyline)
	lanes <sup>1,7</sup>	'LANES' attribute
	linked_road <sup>1,8</sup>	reversed shape
	maxspeed <sup>1,7</sup>	'MAXSPEED' attribute
	oneway <sup>8</sup>	'ONEWAY' attribute
	roadGeom <sup>8</sup>	shape
	roadNetwork <sup>8</sup>	graph, calculated from 'road' and 'xNodes'
	generalSpeedMap <sup>8</sup>	weights, calculated from 'shape.perimeter' and 'maxspeed'
	countingStationRoad <sup>8</sup>	List of counting station roads (beginning with "[road(893), ...]")
color <sup>1,8</sup>	road color	
Nodes (agent / xNodes) (agent / xNodesRedGraph)	name <sup>1,2</sup>	species + feature ID
	roads_in <sup>1,4</sup>	calculated by skill
	shape <sup>1</sup>	"nodes_clipped.shp" (point)
	is_traffic_signal <sup>6,8</sup>	'TYPE' attribute
	stop <sup>1,3,8</sup>	calculated from 'roads_in'
	redGraph <sup>8</sup>	arrow graph, calculated from 'roads_in'
	redArrow <sup>8</sup>	arrow graph edge
	color <sup>1,8</sup>	arrow color
	width <sup>1,8</sup>	arrow width
	end_arrow <sup>1,8</sup>	arrow tip size
	stopListCycle <sup>8</sup>	[ ], stop transfer list for current cycle (from 'allRowsList')
color <sup>1,8</sup>	fill color	
Homes (agent / homes)	shape <sup>1</sup>	"homes_clipped.shp" (polygon)
	employPop <sup>8</sup>	'f_employed' + 'm_employed' attributes
	employSample <sup>8</sup>	'percentage' (parameter) of 'employPop'
	studentPop <sup>8</sup>	'students' attribute
	studentSample <sup>8</sup>	'percentage' (parameter) of 'studentPop'
	color <sup>1,8</sup>	fill color
	border <sup>1,8</sup>	border color
width <sup>1,8</sup>	border width	
Work places (agent / workPlaces)	shape <sup>1</sup>	"work_places_clipped.shp" (polygon)
	color <sup>1,8</sup>	fill color
	border <sup>1,8</sup>	border color
	width <sup>1,8</sup>	border width

Table 2-3: Overview of entities, variables, attributes, and parameters (continued)

<b>Entities (type / species)</b>	<b>State variables / attributes</b>	<b>Initial value / description</b>
Universities (agent / universities)	shape <sup>1</sup>	"universities_clipped.shp" (point)
	color <sup>1,8</sup>	fill color
	border <sup>1,8</sup>	border color
Cyclists (agent / cyclist)	current_lane <sup>1,5</sup>	calculated by skill
	current_road <sup>1,5</sup>	calculated by skill
	final_target <sup>1,5</sup>	calculated by skill
	heading <sup>1,5</sup>	calculated by skill
	shape <sup>1</sup>	point
	colorCyclist <sup>8</sup>	"blue" (cyclistType = 'worker') "green" (cyclistType = 'student') (overwritten at end of trip)
	current_path <sup>1,5</sup>	calculated from graph (roadNetwork) and target (xNodes)
	cyclistType <sup>8</sup>	"worker" or "student"
	location <sup>1,8</sup>	randomly selected from 'homes' (overwritten at end of trip)
	loc <sup>8</sup>	location point offset for visibility
	val <sup>8</sup>	location point offset distance
	max_acceleration <sup>1,8</sup>	randomly set between 0.5 and 1.0
	placeToGo <sup>8</sup>	randomly selected from 'workPlaces' or randomly selected from 'universities'
	proba_block_node <sup>1,8</sup>	0
	proba_lane_change_down <sup>1,8</sup>	0
	proba_lane_change_up <sup>1,8</sup>	0
	proba_respect_priorities <sup>1,8</sup>	1.0
	proba_respect_stops <sup>1,8</sup>	[1.0]
	proba_use_linked_road <sup>1,8</sup>	0
	right_side_driving <sup>1,8</sup>	true
security_distance_coeff <sup>1,8</sup>	randomly set between 1.0 and 3.0	
speed_coeff <sup>1,8</sup>	randomly set between 0.8 and 1.2	
suspended <sup>8</sup>	0 (changes to 1 at end of trip)	
vehicle_length <sup>1,8</sup>	1.5 m	

Table 2-3: Overview of entities, variables, attributes, and parameters (continued)

Entities (type / species)	State variables / attributes	Initial value / description
Boundary (agent / boundary)	shape <sup>1</sup>	"boundary_clipping.shp" (polygon) (for visualisation only)
Counting stations (agent / countingStation)	name <sup>1,2</sup>	species + feature ID
	shape <sup>1</sup>	"counting_stations_clipped_combined.shp" (point)
	countRoad_0893 <sup>8</sup>	calculated from 'all_agents'
	countRoad_1037 <sup>8</sup>	calculated from 'all_agents'
	countRoad_1051 <sup>8</sup>	calculated from 'all_agents'
	countRoad_1078 <sup>8</sup>	calculated from 'all_agents'
	countRoad_1110 <sup>8</sup>	calculated from 'all_agents'
	countRoad_1116 <sup>8</sup>	calculated from 'all_agents'
	countRoad_1121 <sup>8</sup>	calculated from 'all_agents'
	countRoad_1916 <sup>8</sup>	calculated from 'all_agents'
	countRoad_2045 <sup>8</sup>	calculated from 'all_agents'
	countRoad_2058 <sup>8</sup>	calculated from 'all_agents'
	countRoad_2084 <sup>8</sup>	calculated from 'all_agents'
	countRoad_2114 <sup>8</sup>	calculated from 'all_agents'
	countRoad_2119 <sup>8</sup>	calculated from 'all_agents'
	countRoad_2124 <sup>8</sup>	calculated from 'all_agents'
	color <sup>1,8</sup>	fill color
	border <sup>1,8</sup>	border color
Simulation iteration	iteration <sup>8</sup>	"0000", numbering for output files
Phase timing scenario	scenario <sup>8</sup>	"01", numbering for input and output files
	TL_matrix <sup>8</sup>	"scenario_01.csv", phase timing matrix input file
Stop transfer list	stopList <sup>8</sup>	[ ], stop transfer list for all cycles (from 'allRowsList')
	cycleRepeat <sup>8</sup>	0, dimensioning counter
	rowNumber <sup>8</sup>	2, matrix row number
	singleRowList <sup>8</sup>	[ ], stop transfer list for one matrix row
	allRowsList <sup>8</sup>	[ ], list of stop transfer lists for all matrix rows
	columnNumber <sup>8</sup>	1, matrix column number
	singleRowInt <sup>8</sup>	matrix column header
	singleRowIntList <sup>8</sup>	[ ], list of matrix column headers

<sup>1</sup> built-in attribute / variable

<sup>2</sup> numeric component corresponds to feature ID as provided in shapefile

<sup>3</sup> defined by 'skill\_road' skill

<sup>4</sup> defined by 'skill\_road\_node' skill

<sup>5</sup> defined by 'advanced\_driving' skill

<sup>6</sup> defined in shapefile

<sup>7</sup> defined in shapefile, required by 'advanced\_driving' skill

<sup>8</sup> defined in model

The temporal resolution of the model is one second (represented by one iteration cycle). The simulation stops after a period of 12 minutes (720 cycles). The model does not include raster image data; therefore, spatial resolution is not applicable. However, the population data is derived from two polygon grids (with associated population attributes) with 100 m x 100 m and 250 m x 250 m squares. The spatial extent of the core model area has a size of 1600 m x 1600 m and is oriented along the axis of the population polygons (approx. 3.8°). The coordinate system of the spatial datasets is UTM zone 33N based on the WGS 84 datum (EPSG:32633).

### 2.9.3. Process overview and scheduling

During the **initialisation** phase, the following processes are executed (in listed order):

- Set input filenames (spatial datasets and CSV file)
- Set output file names (CSV files)
- Define world extent
- Load CSV file (traffic light phase timing) into matrix
- Initialise variables
- Set cycle counter for stop list dimensioning
- Create stop transfer list from matrix (see submodels)
- Create species from shapefiles:
  - Boundary
  - Homes
  - Work places
  - Universities
  - Intersection nodes
- Create initial stop list from traffic light intersections
- Create child species from shapefile:
  - Intersection nodes
- Create species from shapefile:
  - Roads (original and reversed linked roads)
- Set weights for roads
- Create driving graph from roads and nodes

- Create species from shapefile:
  - Counting stations
- Assign counting station roads
- Create species
  - Cyclists (workers)
  - Cyclists (students)
- Create output displays
  - One chart display (seven charts)
  - One map view display

The **simulation** processes are executed as discrete steps (in listed order), with every step (model cycle) representing one second:

Note: (A) indicates asynchronous updates, (S) indicates synchronous updates.

- Count cyclist agents on counting station roads (A)
- Write cyclist agent count per road into CSV file (A)
- Assign stop transfer list index for current cycle to stop list (see submodels)
- Calculate cyclist agents' routes to final targets, if unset (A)
- Move cyclist agents to next locations, if applicable (see submodels) (A)
- Remove cyclist agents, if final targets reached (A)
- Create road network graph for stop arrows
- Create stop arrows from graph edges where applicable (A)
- Display cyclist agent counts in chart display (S)
- Display cyclist agents at new locations in map view display (S)
- Display stop arrows (S)
- Increase cycle count
- Stop simulation, if applicable

#### 2.9.4. Design concepts

- Basic principles

The model simulates bicycle traffic in the city centre of Salzburg/Austria under the influence of traffic lights which are controlled by phase timing scenarios loaded from CSV files. The resulting spatio-temporal distribution of this traffic is captured by counting station roads whose data are saved in CSV files for further processing. The assumption is that traffic lights affect the spatial distribution of the traffic by influencing its timing. The hypothesis is that this effect can be visualised by capturing the results from the underlying processes when modeled in an agent-based modeling environment. The model focuses on the immediate reactions of cyclist agents to traffic lights and to their environment (i.e. other cyclist agents).

- Emergence

The results that the model is aiming for are emerging patterns from the influence of traffic lights on the spatio-temporal distribution of bicycle traffic. However, these emerging patterns are difficult to detect by means of the charts displayed within the modeling platform. The comparison with the map view display during simulations is helpful, but the restriction of only being able to view one traffic light scenario during one simulation at a time still applies. The most meaningful results can be obtained when superimposing the counting data from all three traffic light scenarios ("00" without the influence of traffic lights, and "01" and "02" with the influence of traffic lights in a 60-second alternating phase timing pattern). In the presented thesis, these data were aggregated in the mean of the number of cyclists per simulation cycle over 100 simulations. This comparison not only reveals the main (and most anticipated) emerging patterns that show oscillations with a clear 60-second base rhythm when plotting the number of cyclists at the counting station locations over time - reviewing these chart results in the spatial context in the map view display during a simulation reveals relationships that reach beyond the immediate vicinity of individual traffic light intersections or counting stations.

- Adaptation

The primary adaptive behaviour which the cyclist agents are set to apply is the reaction to the states of traffic lights along their planned paths from their trip starting points to their final destinations. They are instructed to obey red traffic lights, and the expectation is that this adaptive behaviour (leading to time delays) will be reflected in results as described

above. However, besides their reaction to these stop signals, the cyclist agents are also instructed to consider their environment (specifically their fellow cyclist agents) by observing basic underlying right of way rules in locations without traffic lights, and by respecting single occupancy of space (i.e. avoiding collisions).

- Prediction

The cyclist agents apply prediction insofar as they determine before every step whether the target location for the step is available to them based on their current movement parameters. For instance, if the location they intend to move to is occupied by another cyclist agent (e.g. because of a line-up at a red traffic light in front of them), they do not make this move (respecting single occupancy of space). This functionality is provided by the 'advanced\_driving' skill in the GAMA platform (Taillandier 2014).

- Sensing

The counting stations were initially set up to sense which roads are closest to them. However, due to the linking of reversed roads (adding congruent geometries) this functionality sometimes returns erroneous results. The counting station roads were therefore hardcoded. Nevertheless, these roads themselves sense which agents are travelling on them. The cyclist agents 'sense' stop signals by comparing the roads in their trajectory with the roads in the stop list. They also sense if a desired space in their direction of travel is occupied.

- Interaction

The modeled interactions are uni-directional, with the cyclist agents reacting to intersection nodes (acting as traffic lights) and reacting to occupied spaces (in this model version solely occupied by other cyclist agents, but potentially also by other obstacle species).

- Stochasticity

The stochastic components of the model are limited to the trip source and target locations for both, the 'workers' cyclist agents and the 'students' cyclist agents, and to some probabilities affecting the behavioural aspects of the cyclist agents' movements. The two main reasons for this are that the model is based on the 'Salzburg bicycle model' (Wallentin 2016) and the 'Bicycle model' (Kaziyeva *et al.* 2019), which both contain stochastically modeled processes, and that the results are more meaningful if they are obtained based on



(in this context more realistic) stochastic processes, rather than repeated ('rehearsed') processes.

- Collectives

The cyclist agents are divided into two groups ('workers' and 'students'). However, this distinction only has an effect on the spatial distribution of their (still stochastically selected) trip destination locations.

- Observation

The data for observation are collected from the roads that the counting stations are located closest to. Since they are represented by one original road (from the spatial dataset) and an additional reversed linked road (created by the model code), there are 14 observed roads for the seven counting stations. They can be observed in two ways: in the chart display within the modeling platform (updated for every elapsed simulation cycle), and by means of processing the data contained in the exported CSV files (see section 'Emergence'). Although the data for the chart display and the map view display are generated from the same simulations, they are not identifiable as easily in the map view, since it would require the observer to count the agents 'manually'.

### 2.9.5. Initialization

After the initialisation of the model (and before the execution of the first simulation cycle) the following entities are loaded:

Table 2-4: Overview of entities and variables at initialisation

Entities	Quantity	Variables	Initial state
Roads (road)	2129	all_agents	[ ]
		lanes	1
		linked_road	varies
		location	varies
		maxspeed	5.55 m/s
		name	varies ('road...')
		oneway	varies (-1, 0, 1)
		roadGeom	varies (polyline (...))
		shape	varies (polyline (...))
		source_node	varies (xNodes...)
target_node	varies (xNodes...)		

Table 2-4: Overview of entities and variables at initialisation (continued)

Entities	Quantity	Variables	Initial state
Nodes (xNodes)	2985	is_traffic_signal	varies (true, false)
		location	varies
		name	varies ('xNodes...')
		roads_in	varies ([road(...),road(...)])
		roads_out	varies ([road(...),road(...)])
		shape	varies ({...} as geometry)
		stop	varies ([road(...),road(...)])
Nodes (xNodesRedGraph)	1	is_traffic_signal	false
		location	varies
		name	'xNodesRedGraph0'
		roads_in	[ ]
		roads_out	[ ]
		shape	varies ({...} as geometry)
		stop	[ ]
Cyclists (cyclist)	1001 'workers' 139 'students'	colorCyclist	varies ( 'workers' = blue, 'students' = green)
		cyclistType	varies ( 'workers', 'students')
		destination	varies
		heading	varies
		location	varies
		max_acceleration	varies
		max_speed	
		name	varies ('cyclist...')
		proba_block_node	0.0
		proba_lane_change_down	0.0
		proba_lane_change_up	0.0
		proba_respect_priorities	1.0
		proba_respect_stops	[1.0]
		proba_use_linked_road	0.0
		right_side_driving	true
		security_distance_coeff	varies
		shape	varies ({...} as geometry)
		speed_coeff	varies
suspended	0		
vehicle_length	1.5		

Table 2-4: Overview of entities and variables at initialisation (continued)

Entities	Quantity	Variables	Initial state
Homes (homes)	64	location	varies
		name	varies ('homes...')
		shape	varies (polygon (...))
Work places (workPlaces)	256	location	varies
		name	varies ('workPlaces...')
		shape	varies (polygon (...))
Universities (universities)	16	location	varies
		name	varies ('universities...')
		shape	varies ({...} as geometry)
Counting stations (countingStations)	7	location	varies
		name	varies ('countingStation...')
		shape	varies ({...} as geometry)
Boundary (boundary)	1	location	<i>x, y, z coordinates</i>
		name	'boundary0'
		shape	polygon ( <i>coordinates</i> )

### 2.9.6. Input data

The model uses three external comma-separated values (CSV) input files which contain the traffic light phase timing for the three modeled scenarios. However, only one of the files is used at a time in a simulation (at the current state of the model, they have to be 'manually' switched in the code before initialising the model). Furthermore, although each file holds data representing multiple traffic light phase states, the file is loaded and processed only during the initialisation, i.e. no further input files are loaded during the simulations.

### 2.9.7. Submodels

The model code reads the CSV file with the traffic light phase timing data into a matrix. It then processes the data in the matrix to create a stop transfer list which holds the stop lists for all 720 simulation cycles. This transfer list is used during the simulation to update the stop list during every cycle. Fig. 2-28 illustrates this submodel in a pseudo-code flowchart.

The cyclist agents' movements are controlled by GAMA's 'advanced\_driving' skill, in conjunction with the 'skill\_road' and 'skill\_road\_node' skills. The functionalities of these skills are explained extensively in Taillandier's (2014) paper about traffic simulation with the GAMA platform.

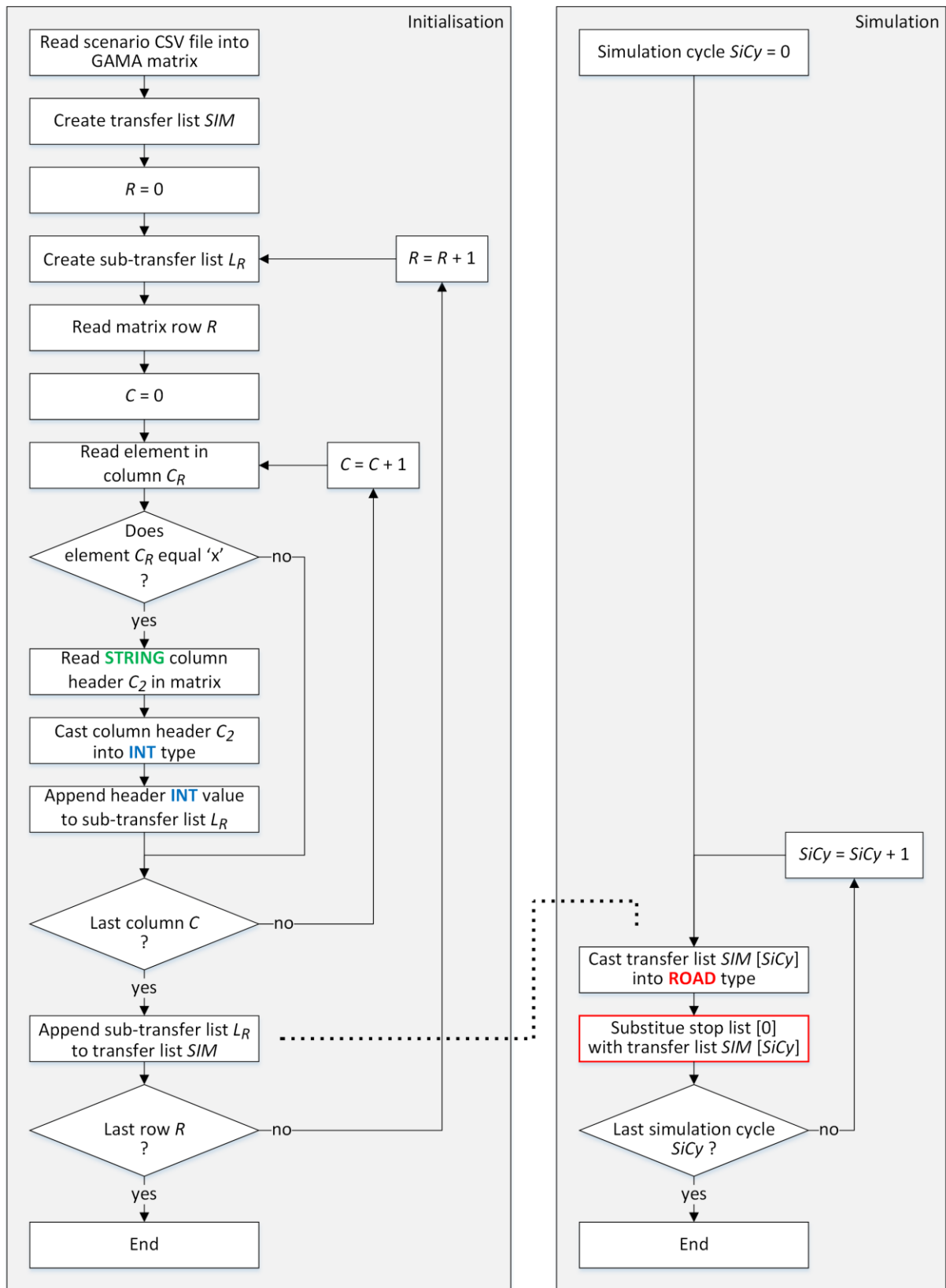


Fig. 2-28: Submodel processing the traffic light phase timing matrix

### 3. Results

In this section, the generated data is presented in charts with the means  $\mu$  of the number of cyclists displayed over time. These means were calculated from 100 simulations per phase timing scenario, each simulation covering a time period of 12 minutes (= 720 seconds, represented by 720 cycles). For every cycle during these simulations, the current count of cyclist agents on the seven counting station roads was written out into CSV files (one file per road, direction, and scenario). These files were then linked into a MS Excel<sup>®</sup> worksheet per counting station (CS) and direction (inbound/outbound), in which the means were calculated for every cycle. The time axis of each chart shows 60-second intervals (60 cycles). This corresponds to the phase timing shift between the scenarios 1 and 2. All charts show three series (scenarios 1, 2, and 3) for comparison. The charts are ordered by counting station number (see Fig. 3-1 and Table 3-1 for reference) and are intended to provide an overview of the results - they will be discussed in detail in section 4 ('Discussion'). There are two groups of counting stations (as indicated in Table 3-1): The stations CS 0, CS 1, and CS 2 were part of the models of Wallentin's (2016) and Kaziyeva *et al.* (2019). The stations CS 3, CS 4, CS 5, and CS 6 were added to this model as described in section 2.6.1 ('Heat map and additional counting stations'). Please also note that references to cyclist numbers in the charts in this section refer to the calculated means.



Fig. 3-1: Study area with numbered counting stations (Orthophoto: Geoland.at 2018)

Table 3-1: Counting station numbers and names

Counting station number	Counting station name
CS 0	Rudolfskai <sup>3</sup>
CS 1	Giselakai <sup>3</sup>
CS 2	Elisabethkai <sup>3</sup>
CS 3	Mozartsteg <sup>4</sup>
CS 4	Staatsbrücke <sup>4</sup>
CS 5	Makartsteg <sup>4</sup>
CS 6	Müllnersteg <sup>4</sup>

<sup>3</sup> Original counting station (physical, City of Salzburg)

<sup>4</sup> Additional counting station (virtual, model only)

The three series in Fig. 3-2 appear very similar. After an initial cyclist number maximum between 60 and 120 seconds into the simulations, the curves drop over the next 60 to 120 seconds and then remain almost constantly low.

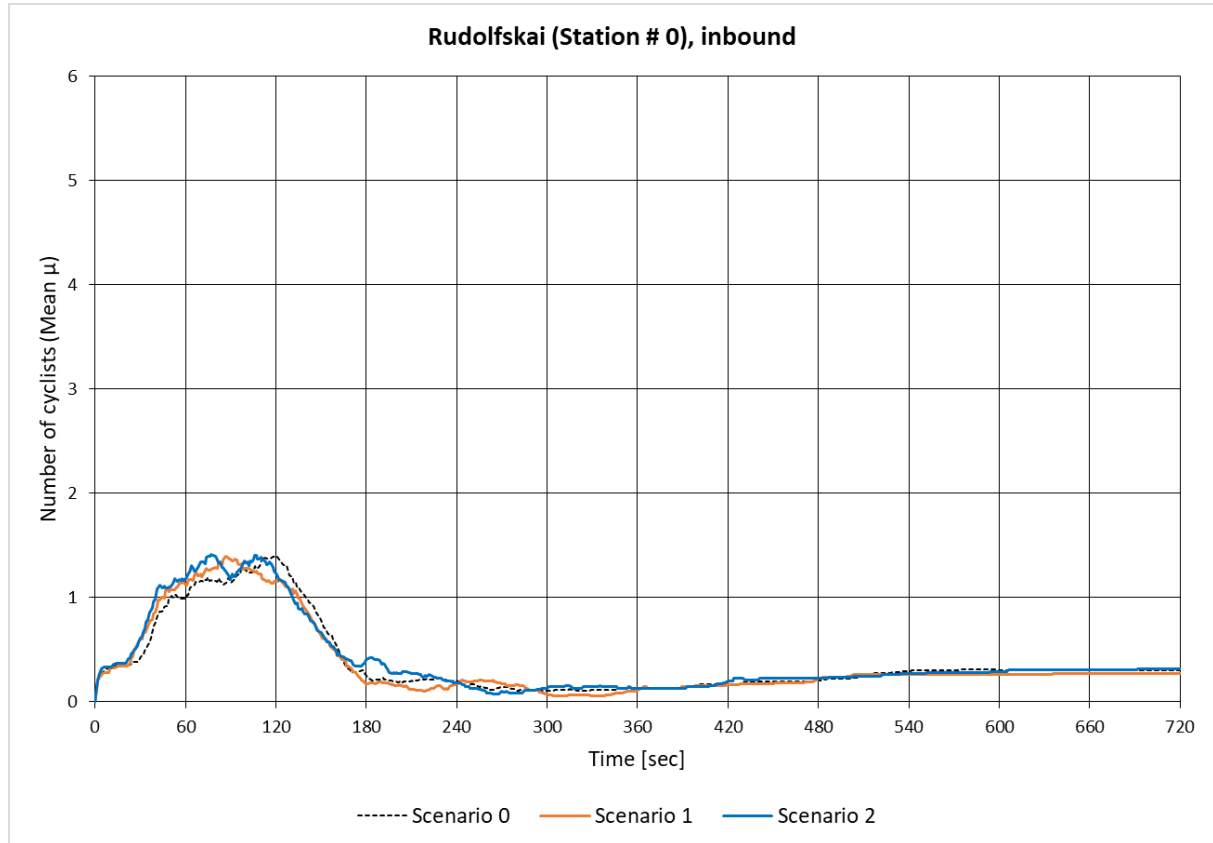


Fig. 3-2: Distribution of cyclists at CS 0 (Rudolfskai), inbound

The opposite direction at the 'Rudolfskai' counting station (Fig. 3-3) shows more activity. There is still a noticeable (but less pronounced) increase during the same time as in Fig. 3-2, but the main activity peaks between 420 and 480 seconds.

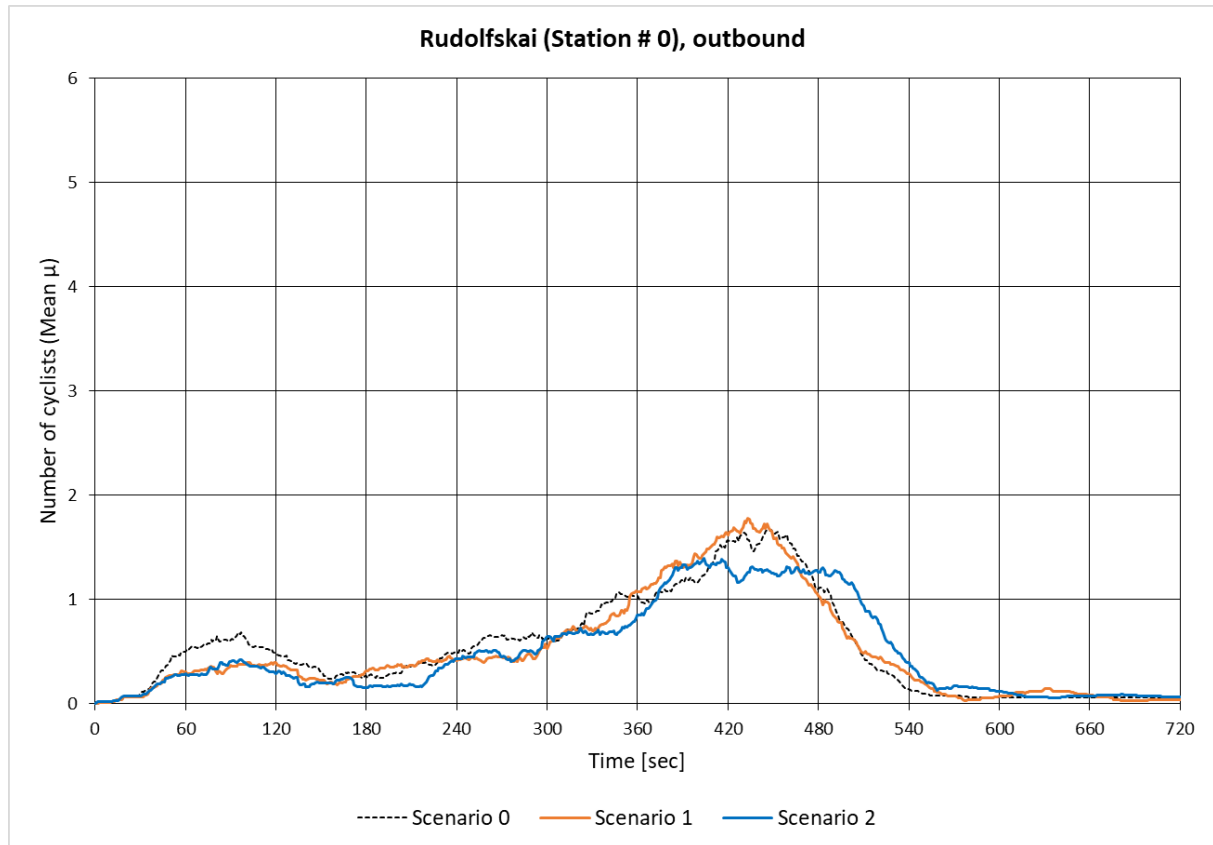


Fig. 3-3: Distribution of cyclists at CS 0 (Rudolfskai), outbound



The pattern of the three series at the inbound 'Giselakai' counting station (Fig. 3-4) is 'unusual' insofar that the activity at all other stations increases at some point during the simulations and then declines again before their end, while the agents in this chart seem to get active in the second half of the simulations and then maintain this activity all the way towards the end.

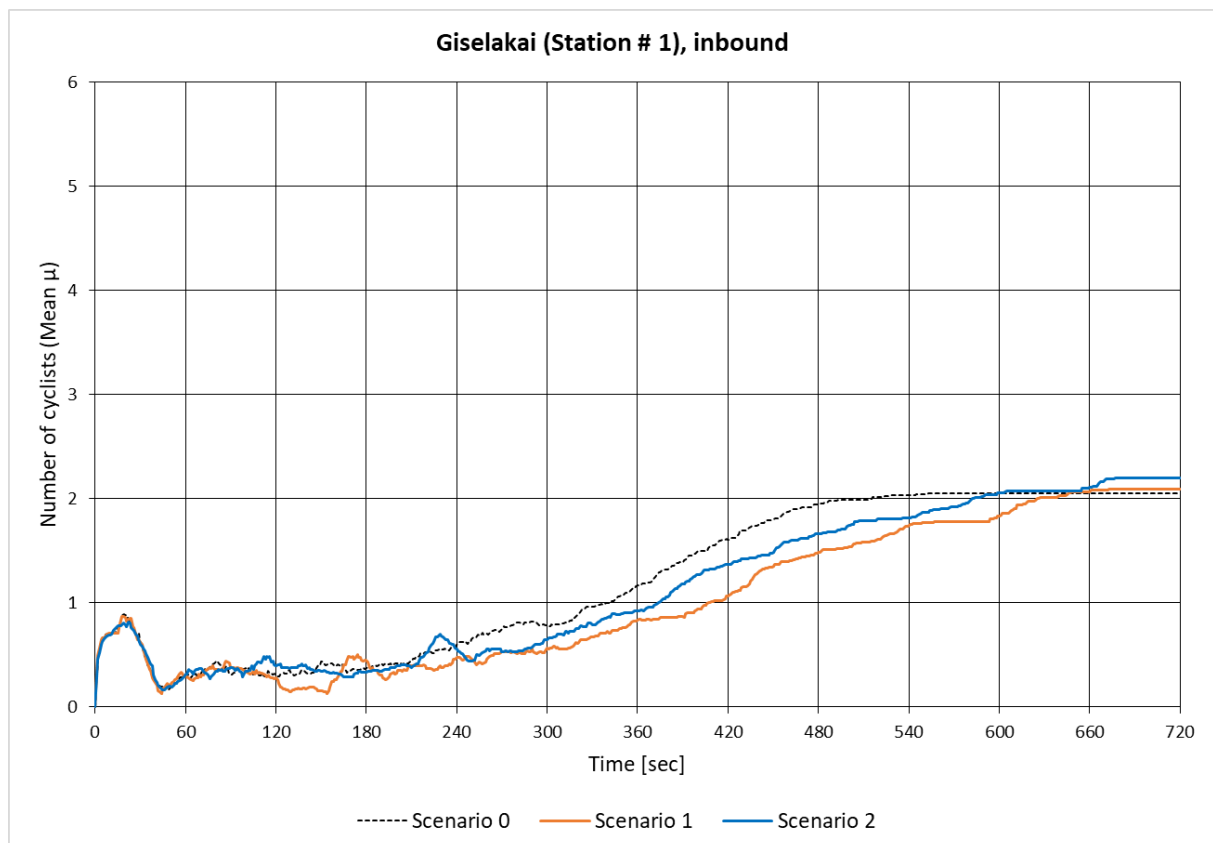


Fig. 3-4: Distribution of cyclists at CS 1 (Giselakai), inbound

The activity in Fig. 3-5 appears somewhat symmetrical around the midpoint of the simulations at 360 seconds, at least with regard to the elapsed time at the peaks within the individual scenarios. Furthermore, although they vary in shape, there is a noticeable shift of approx. 60 seconds between the peaks of the scenarios 1 and 2 around the 360-second centre mark.

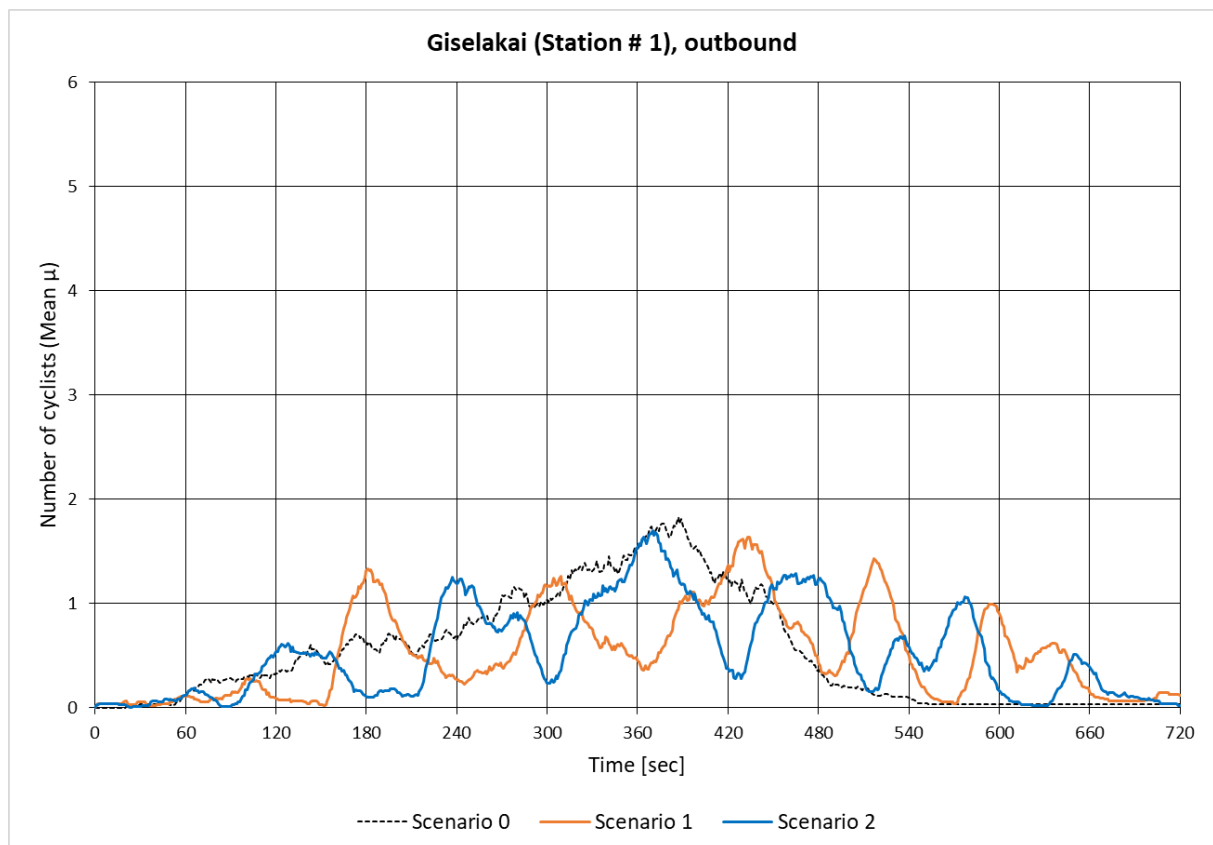


Fig. 3-5: Distribution of cyclists at CS 1 (Giselakai), outbound

The 'Elisabethkai' counting station exhibits a very unique pattern in the inbound direction (Fig. 3-6). It has two distinct peaks - the first one showing the steepest increase (around the 60-second mark) over such a big range of cyclist numbers among all charts. Another remarkable characteristic is the strong similarity between the curves of the three scenarios.

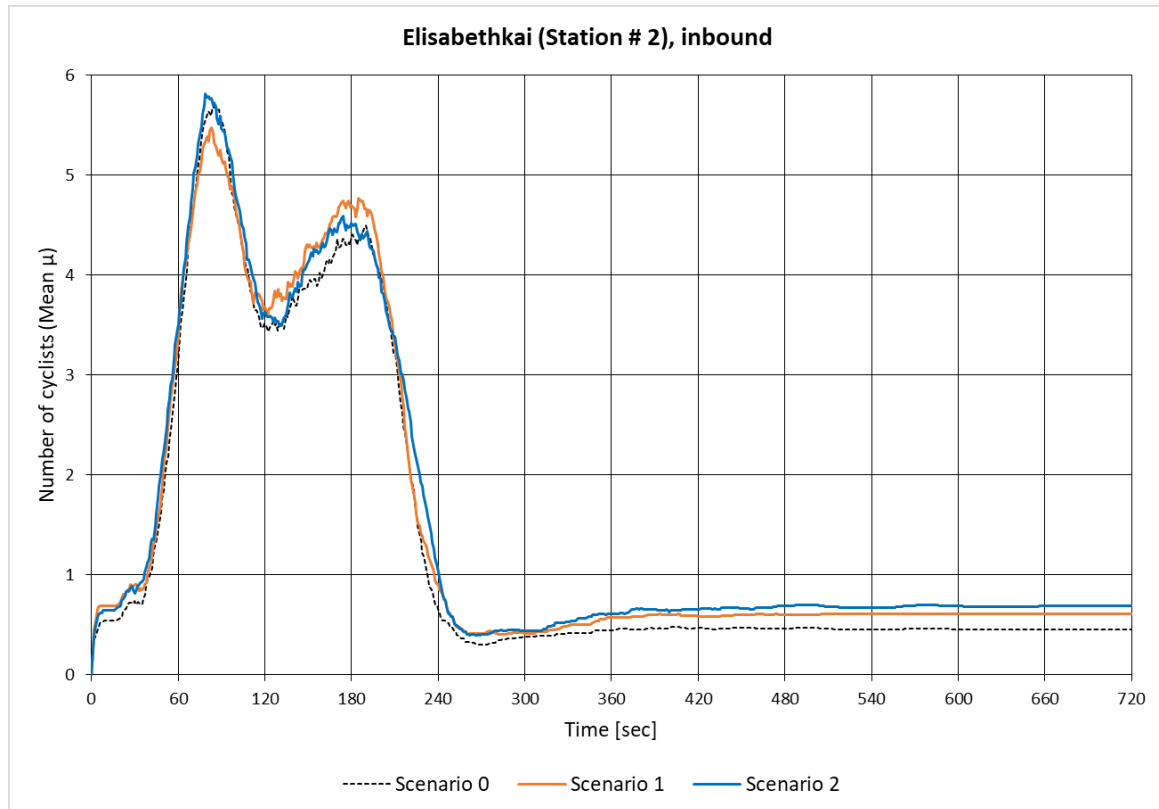


Fig. 3-6: Distribution of cyclists at CS 2 (Elisabethkai), inbound

The chart for the outbound direction of the 'Elisabethkai' counting station (Fig. 3-7) seems to show the opposite of the inbound direction. Although the main activity also happens in the time period between 0 and 270 seconds, the overall level here is minimal – it is the lowest number of cyclists of all the charts.

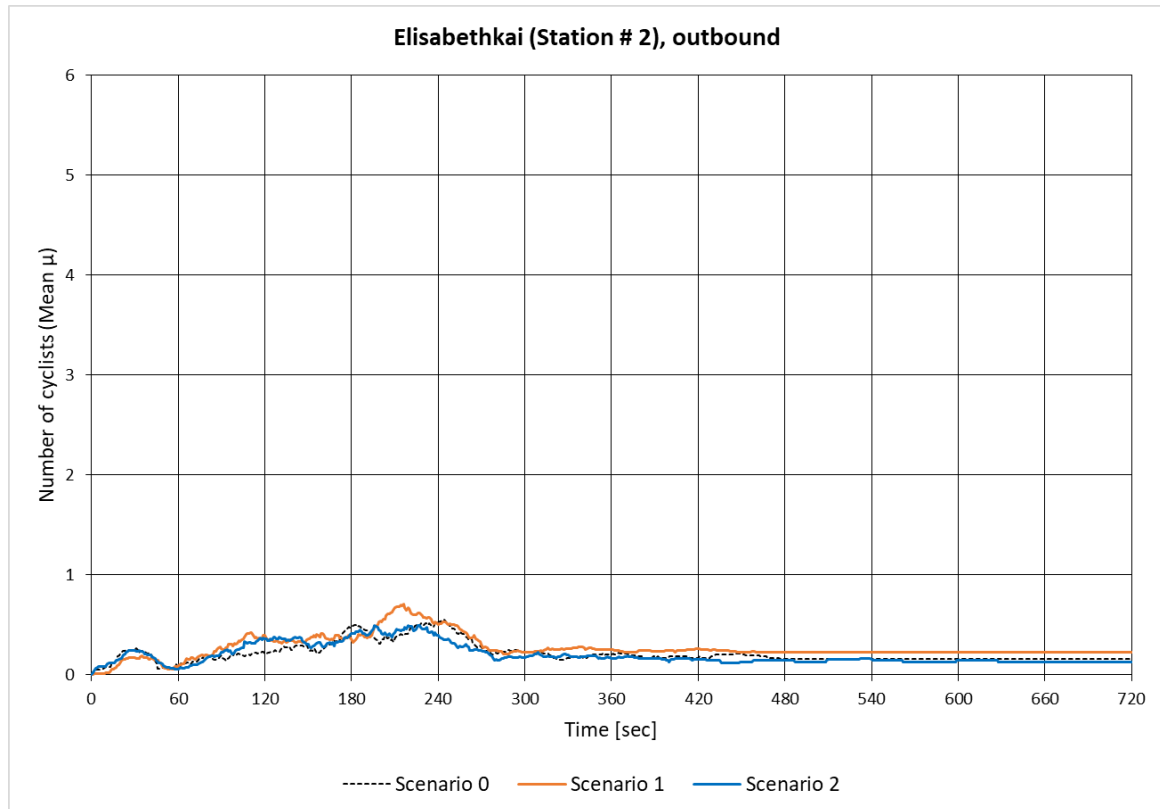


Fig. 3-7: Distribution of cyclists at CS 2 (Elisabethkai), outbound

The chart series for the three scenarios at the inbound 'Mozartsteg' counting station (Fig. 3-8) start with some turbulent activity, but then find their common lowest point around 330 seconds into the simulations. Interestingly, the part before this time mark exhibits a clearly visible alternation of scenario 1 and scenario 2 curves, while the time period afterwards appears almost equalised.

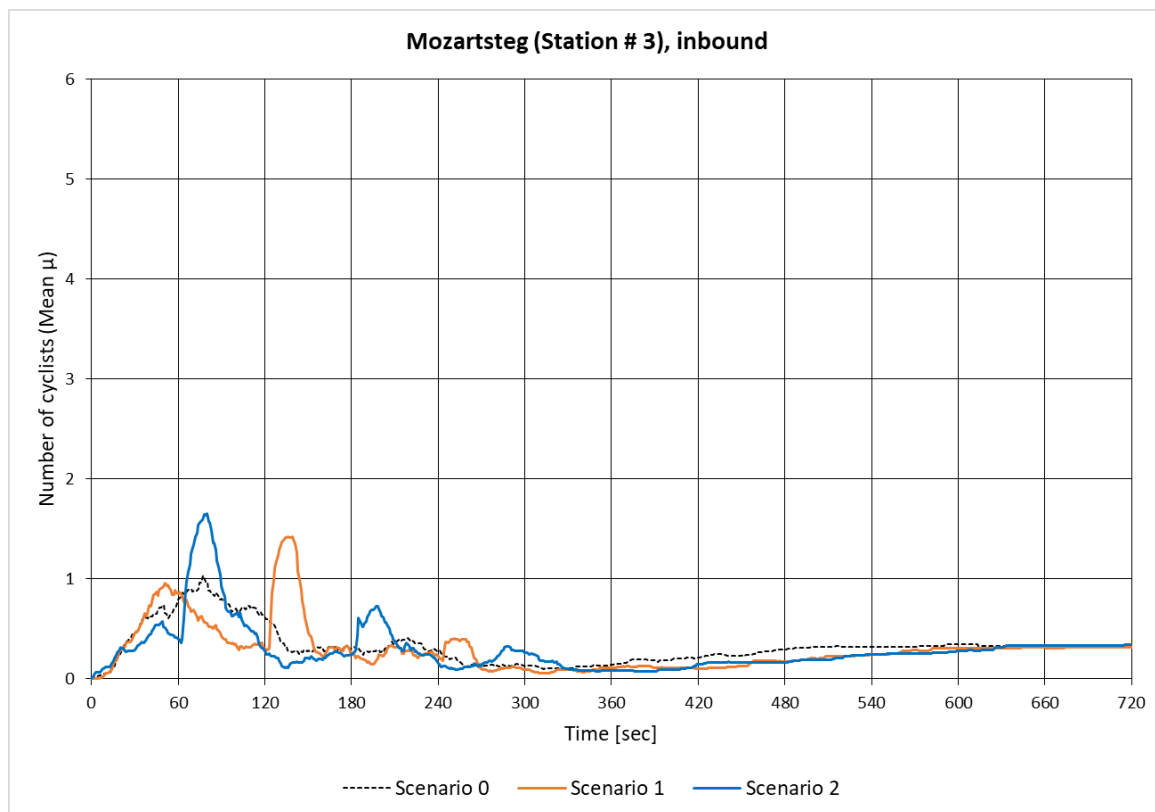


Fig. 3-8: Distribution of cyclists at CS 3 (Mozartsteg), inbound

The same counting station is very busy in the outbound direction (Fig. 3-9). While the curves for the scenarios 1 and 2 start and end at very similar levels as the reference curve of scenario 0, their levels increase much stronger between approx. 210 and 510 seconds. They also form another clear pattern: Both appear pulsating, but their peaks are shifted in time. The intersections of these two curves are delayed for approx. 10 seconds ( $\pm 2$  seconds) compared to the 60-second traffic light phase switches. This relatively constant delay means that the period also amounts to approx. 60 seconds.

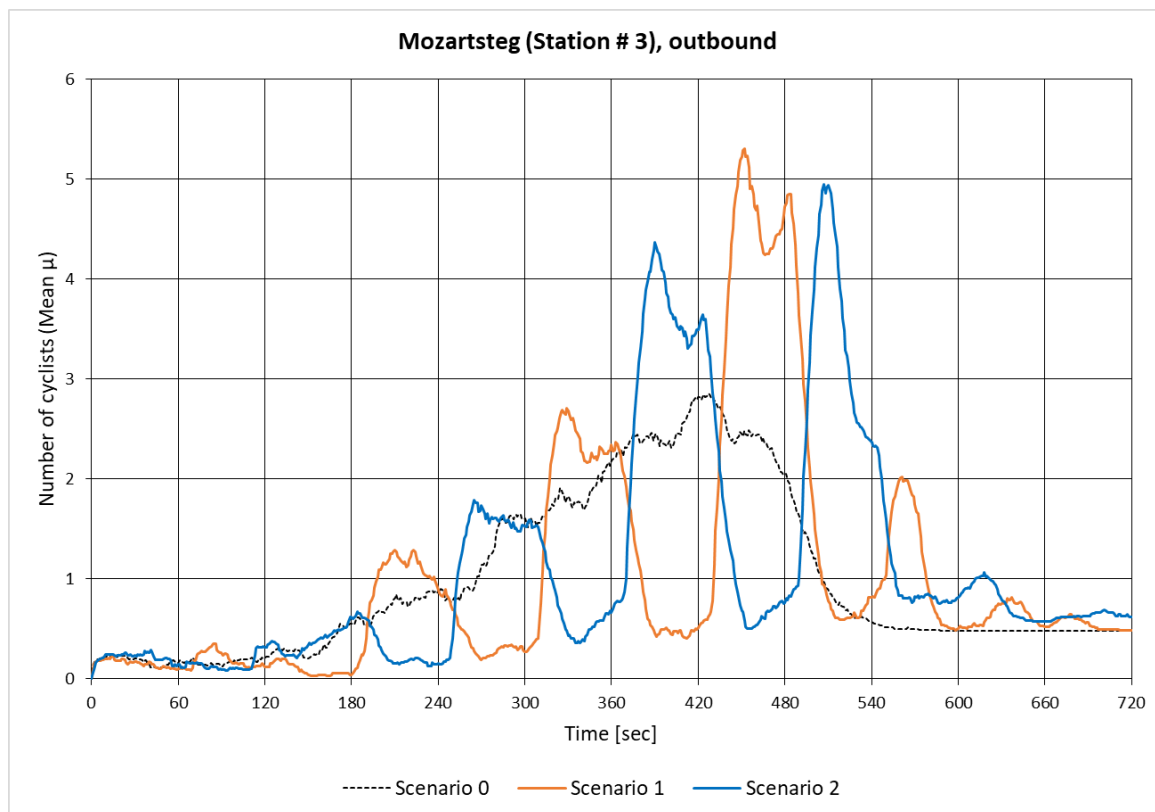


Fig. 3-9: Distribution of cyclists at CS 3 (Mozartsteg), outbound

The chart for the inbound 'Staatsbrücke' counting station (Fig. 3-10) shows some similarities with the 'Mozartsteg' station for the same direction (Fig. 3-8), as all curves start at higher (pulsating) levels and then even out after approx. 360 seconds. However, the peaks before the 360-second mark are much more pronounced than the ones for the 'Mozartsteg' station, while the ones after 360 seconds are lower and more leveled. This chart also shows a distinct (approx. 60 second-) shift between the peaks of the scenarios 1 and 2.

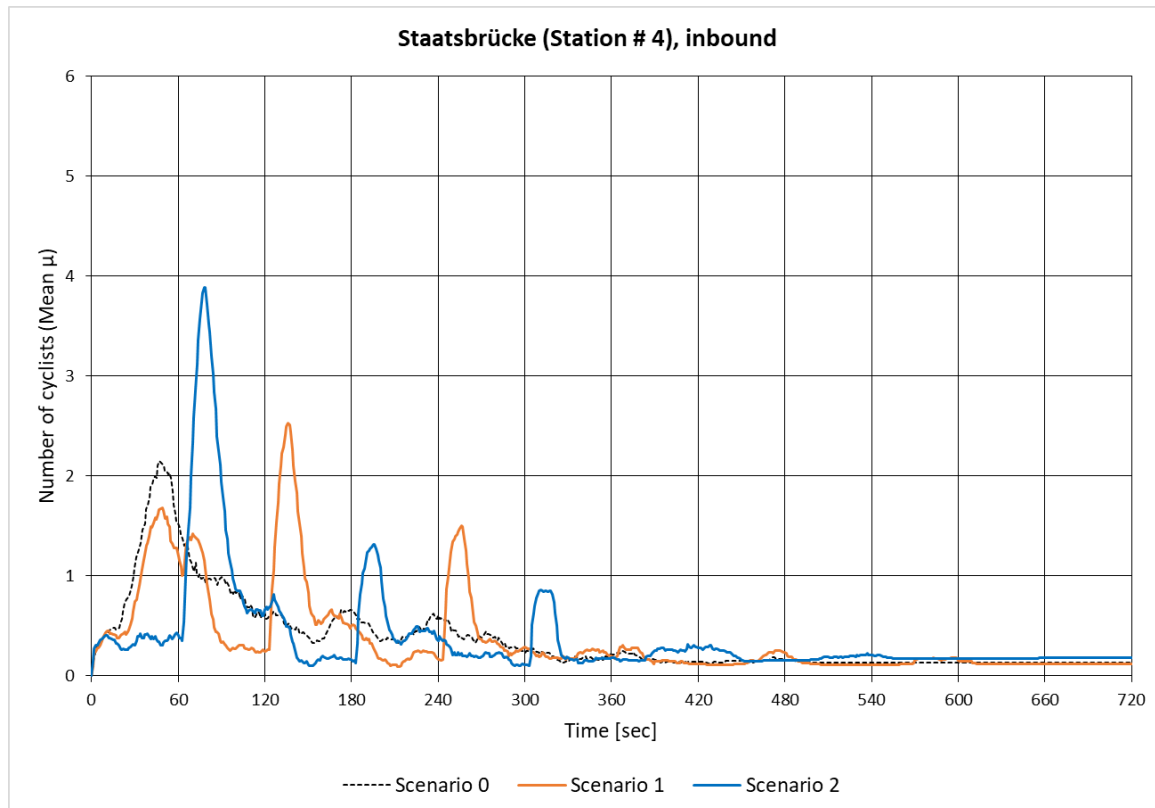


Fig. 3-10: Distribution of cyclists at CS 4 (Staatsbrücke), inbound

The three series for the 'Staatsbrücke' station in outbound direction (Fig. 3-11) start and end a bit irregular with regard to phase shifts, but the centre part between 240 and 480 seconds appears to follow the 60-second shift pattern that other counting stations already exhibited. The 'main' peaks again form an almost regular pattern of approx. 60-second phase shifts around the 360-second mark, as well as almost steadily increasing levels towards the highest value at approx. 380 seconds.

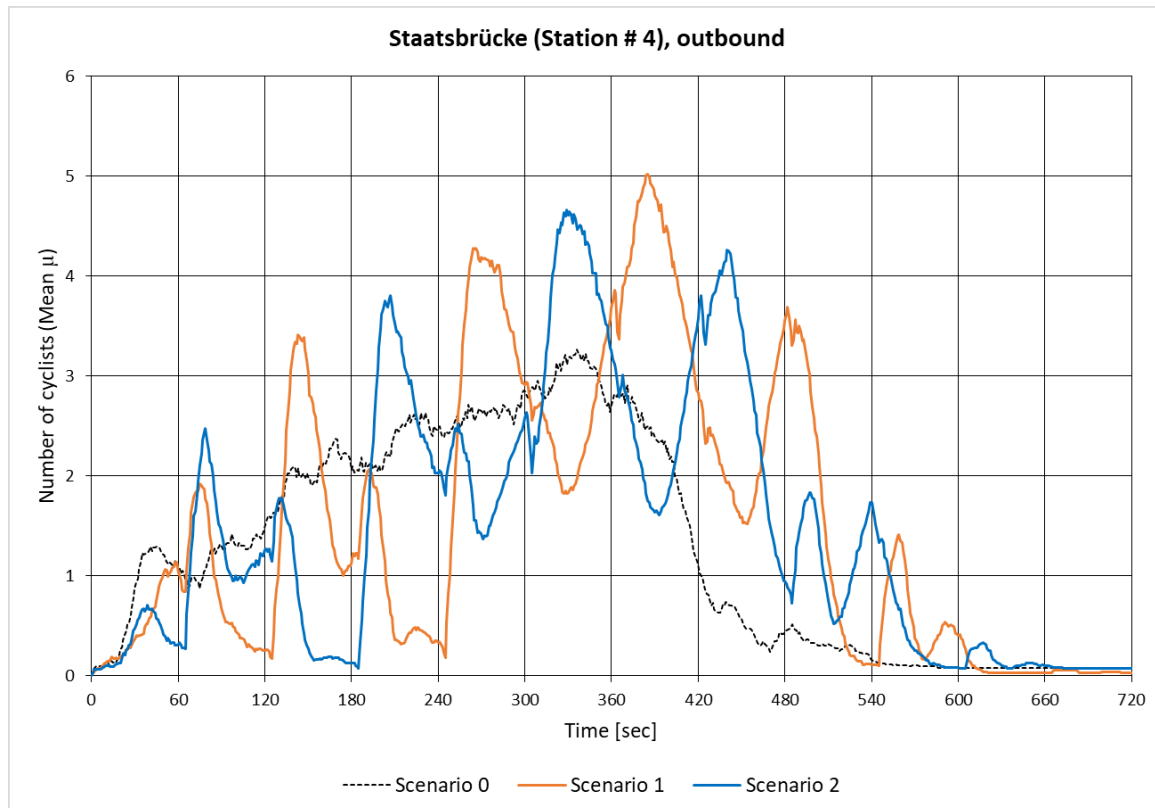


Fig. 3-11: Distribution of cyclists at CS 4 (Staatsbrücke), outbound



The chart in Fig. 3-12 appears somewhat unsettled. There seem to be two main 'waves' (around 60 seconds and around 210 seconds into the simulations) which are reflected in both, the reference scenario 0 and the two traffic light scenarios 1 and 2. Up to 300 seconds, the scenario 1 and 2 curves appear almost congruent, whilst they appear shifted (as in some of the other charts) between 300 and 480 seconds before they level out.

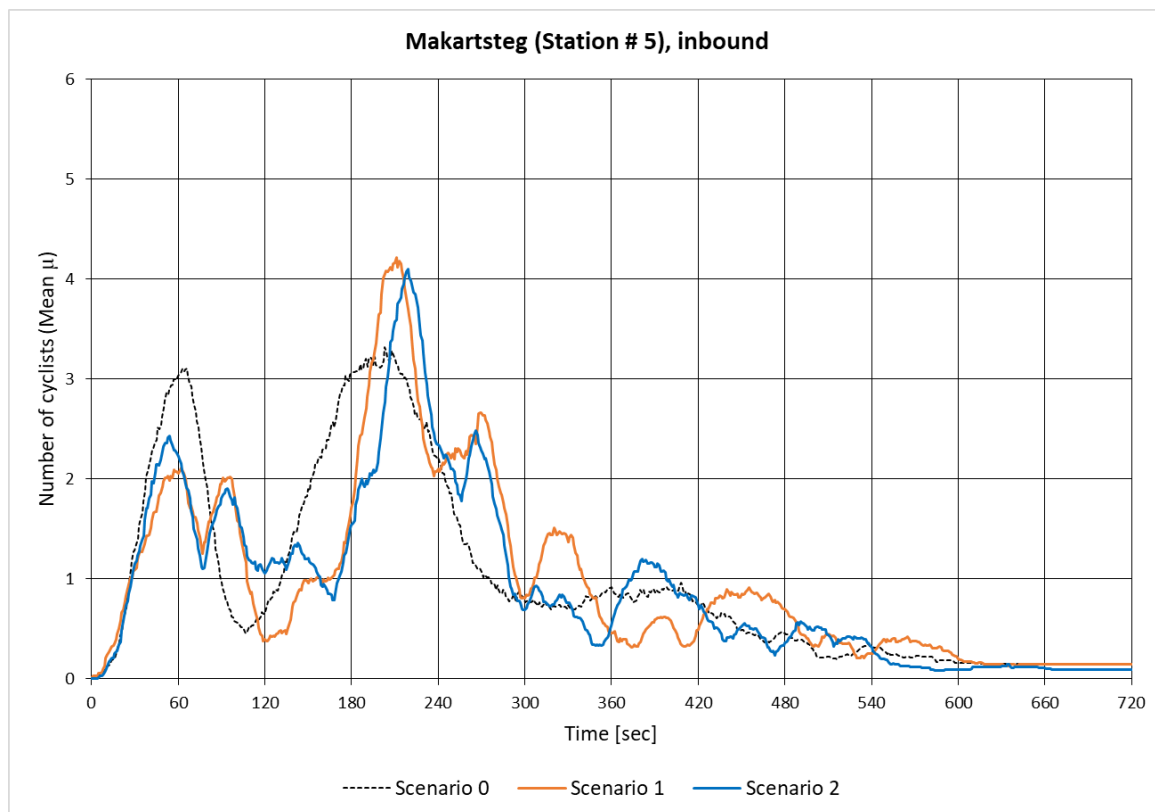


Fig. 3-12: Distribution of cyclists at CS 5 (Makartsteg), inbound

The congruency effect seen in Fig. 3-12 is even more pronounced in the second half of this chart (Fig. 3-13) for the outbound counting station on 'Makartsteg'. As in Fig. 3-12, the two traffic light series overall follow the shape of the scenario 0 curve with regard to the ascent and descent around the highest level at approx. 270 seconds. It is also noticeable in this chart that the traffic light scenario curves 1 and 2 still show quite some activity, in contrast to the curve for scenario 0.

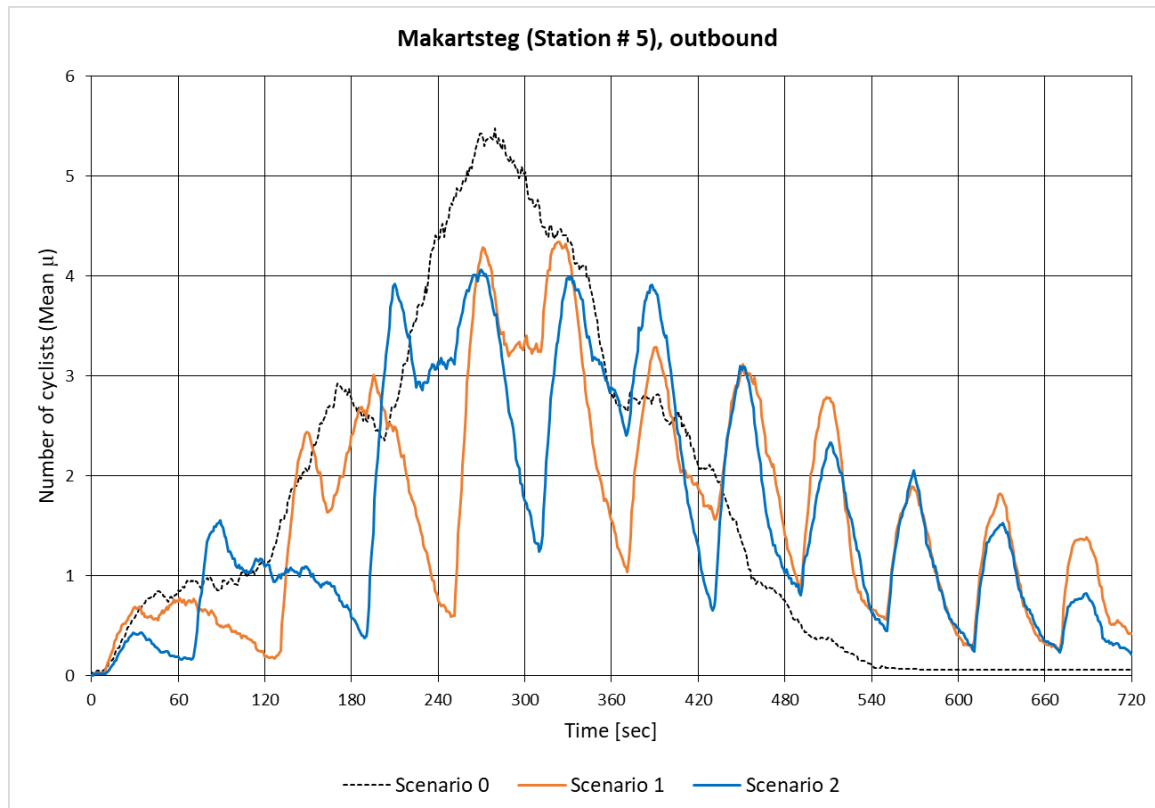


Fig. 3-13: Distribution of cyclists at CS 5 (Makartsteg), outbound

Again, as earlier in Fig. 3-12, there are many similarities between the three series up to the 210-second mark for the inbound 'Müllnersteg' station. Then the approx. 60-second shifts start to appear. As before, the overall shapes (in terms of where the curves have their highest levels) are also again very similar.

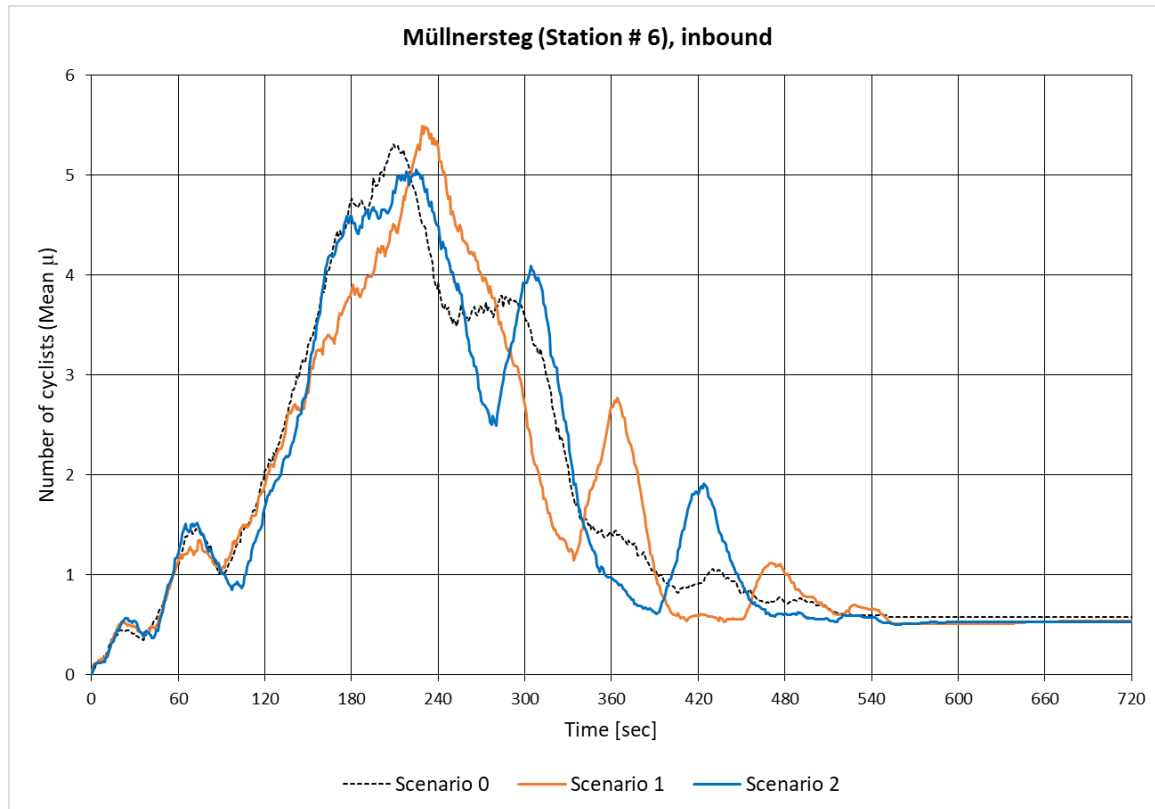


Fig. 3-14: Distribution of cyclists at CS 6 (Müllnersteg), inbound

The curve for scenario 0 in the outbound direction at the 'Müllnersteg' station series looks very similar to the curve for the inbound direction. While the patterns for the scenarios 1 and 2 are not so obvious until approx. 270 seconds into the simulations, they become very clear afterwards.

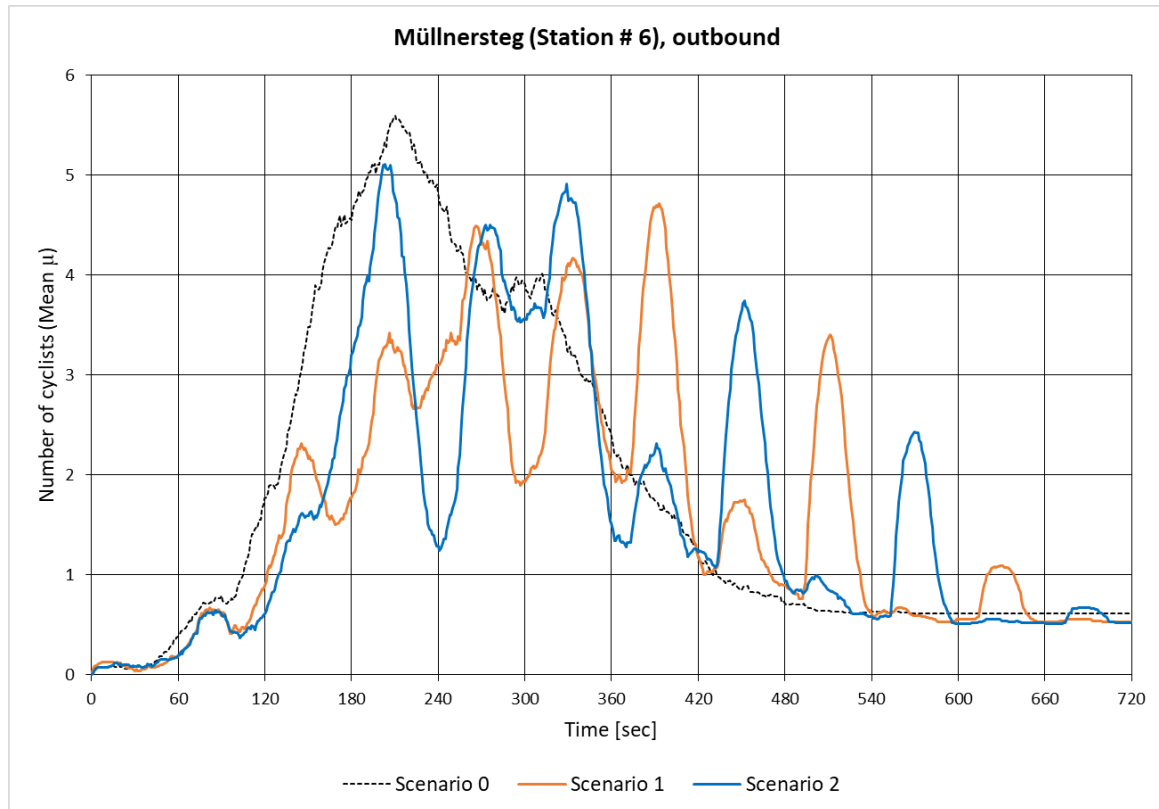


Fig. 3-15: Distribution of cyclists at CS 6 (Müllnersteg), outbound

## 4. Discussion

### 4.1. *Chart interpretation - general*

#### 4.1.1. Potential chart series inaccuracies

Caution should be applied in the result interpretation of the start and end phases of the chart series, especially with regard to the influence of traffic lights. Rather than basing it on the entire simulation duration of 720 seconds, it should probably focus on the time period around the half mark and spread out from there to earlier and later moments on the time axis (suggested range from observation of agent movements: approx. 60 - 660 seconds). This is due to the following issues:

##### 4.1.1.1. *Start cycles*

The cyclist agents start their trip in random locations within their 'homes' grid cells of 250 m x 250 m., i.e. the first segment in their trajectory leads from an origin off the road network towards their first target node on the network - from there, they travel along the edges of the road network. However, depending on the location of this first node relative to an agent's origin, some agents might arrive on a road with a counting station without passing a traffic light that would control their movement, while others might be affected by the traffic light. Insofar, the series for the scenarios 1 and 2 might not accurately reflect the numbers of cyclists at the beginning of the simulations.

##### 4.1.1.2. *End cycles*

The cycling agents are instructed to only complete one trip. The 'advanced\_driving' skill expects a node on the driving graph as the final location in an agent's trajectory – once the agent reaches this node, it is therefore removed from the graph to avoid that it blocks other agents which are still travelling. Since the trip start and end points are randomly selected to lead from a residential location to a node closest to a work place location or a university location, some trips could well be completed before the end of the simulation with 720 cycles. This means that the counts in the end phase of the simulation only reflect cyclists that haven't yet completed their trips, and their number might not be representative.

#### 4.1.2. Differences in chart series

The number of cyclists (Y-axis) is calculated as the mean  $\mu$  from 100 simulation results. The displayed differences between the chart series could lie within the tolerances of the individual simulation results, but they could also indicate a change in the spatial distribution of cyclists. Therefore, caution has to be exercised in the attempts to distinguish between the two. Some of the charts exhibit differences that are so strong that they can be attributed to the influence of traffic lights beyond any doubt, while others are not clear enough. The example in Fig. 4-1 shows very clear similarities between the three series in the first 60 seconds of the simulation (although they should probably be disregarded in the interpretation based on the restrictions in section 4.1.1). The three weak peaks at approx. 115 seconds (scenario 2), 170 seconds (scenario 1), and 225 seconds (scenario 2) could be related to phase timing shifts, the more since they almost fit the 60 second phase timing. Similarly, the offset between the three series between approx. 360 and 600 seconds could be due to phase timing shifts. However, this might also be a misinterpretation under the impression of the much more prominent phase timing patterns exhibited in some of the other charts.

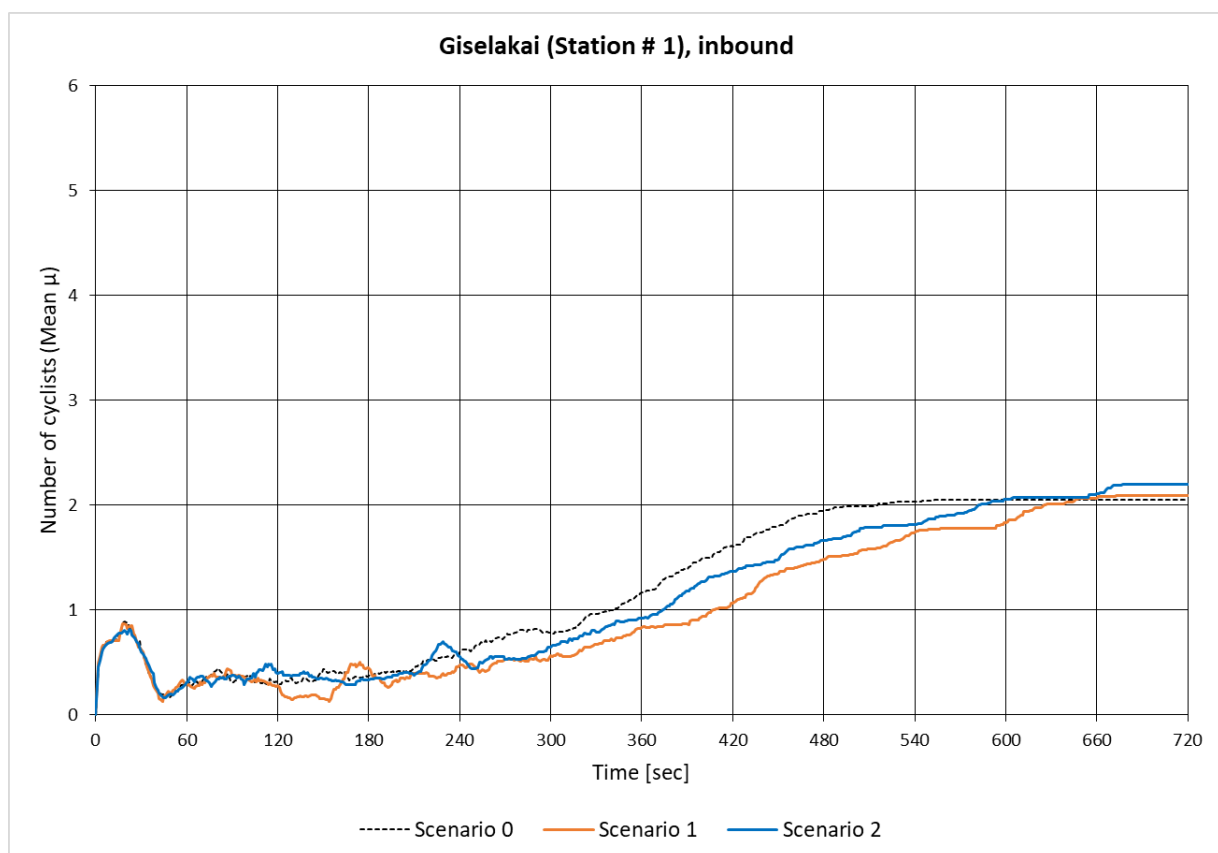


Fig. 4-1: Differences in chart series, example chart

### 4.1.3. Emerging patterns

The charts represent the traffic volume in both directions at the three original and the four added virtual counting stations. Table 4-1 provides an overview of the differences in the emerging patterns of the chart series.

Table 4-1: Overview of chart series pattern differences

<b>Counting station (original)</b>	<b>Difference between</b>		
<b>#, Name, Direction</b>	<b>Sc 0 – Sc 1</b>	<b>Sc 0 – Sc 2</b>	<b>Sc 1 – Sc 2</b>
CS 0, Rudolfskai, inbound	n/a	n/a	n/a
CS 0, Rudolfskai, outbound	n/a	↘	↘
CS 1, Giselakai, inbound	↘	↘	↘
CS 1, Giselakai, outbound	↗	↗	↗
CS 2, Elisabethkai, inbound	n/a	n/a	n/a
CS 2, Elisabethkai, outbound	n/a	n/a	n/a
<b>Counting station (additional)</b>	<b>Difference between</b>		
<b>#, Name, Direction</b>	<b>Sc 0 – Sc 1</b>	<b>Sc 0 – Sc 2</b>	<b>Sc 1 – Sc 2</b>
CS 3, Mozartsteg, inbound	↘	↘	↘
CS 3, Mozartsteg, outbound	↗	↗	↗
CS 4, Staatsbrücke, inbound	↗ ↘	↗ ↘	↗ ↘
CS 4, Staatsbrücke, outbound	↗	↗	↗
CS 5, Makartsteg, inbound	↗	↗	↘ ↗
CS 5, Makartsteg, outbound	↗	↗	↗ ↘
CS 6, Müllnersteg, inbound	↗	↘ ↗	↗
CS 6, Müllnersteg, outbound	↗	↗	↗
<b>Legend</b>			
Sc = Scenario			
↗ = strong			
↘ = weak			
n/a = not apparent			

With the exception of the outbound direction at the Giselakai station, the traffic at the three original counting stations (CS 1, CS 2, and CS 3) seems to be only minimally or not at all affected by traffic lights (Table 4-1). Their chart series largely appear to vary within the limits shown in chapter 2.7.1 ('Number of executed simulations'). Fig. 4-2 - Fig. 4-4 show reduced versions of the charts in section 3 ('Results') for direct comparison.

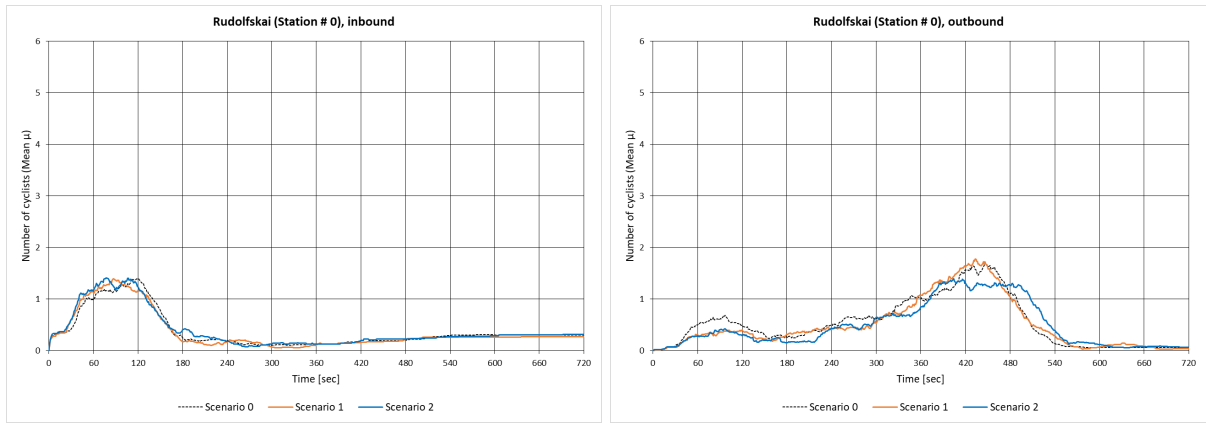


Fig. 4-2: CS 0 (Rudolfskai), inbound / outbound

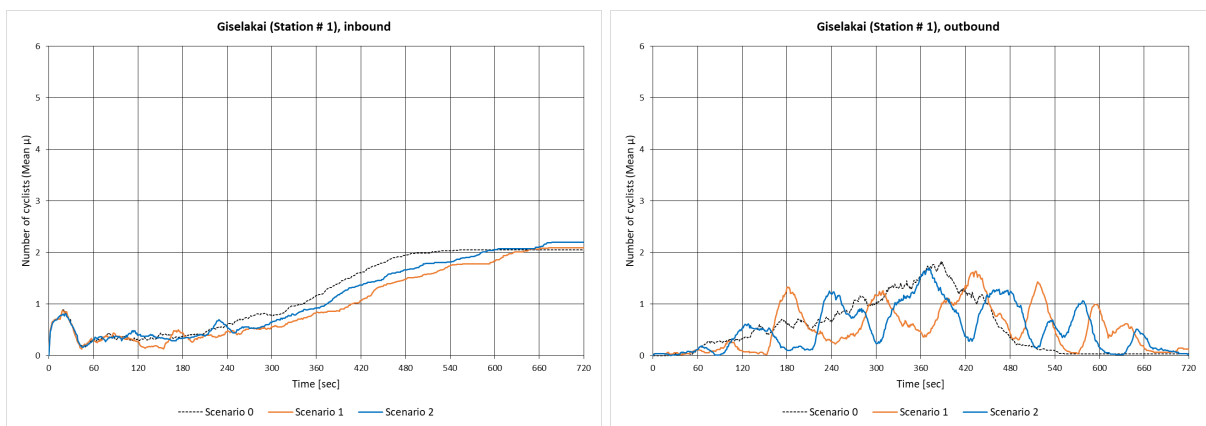


Fig. 4-3: CS 1 (Giselakai), inbound / outbound

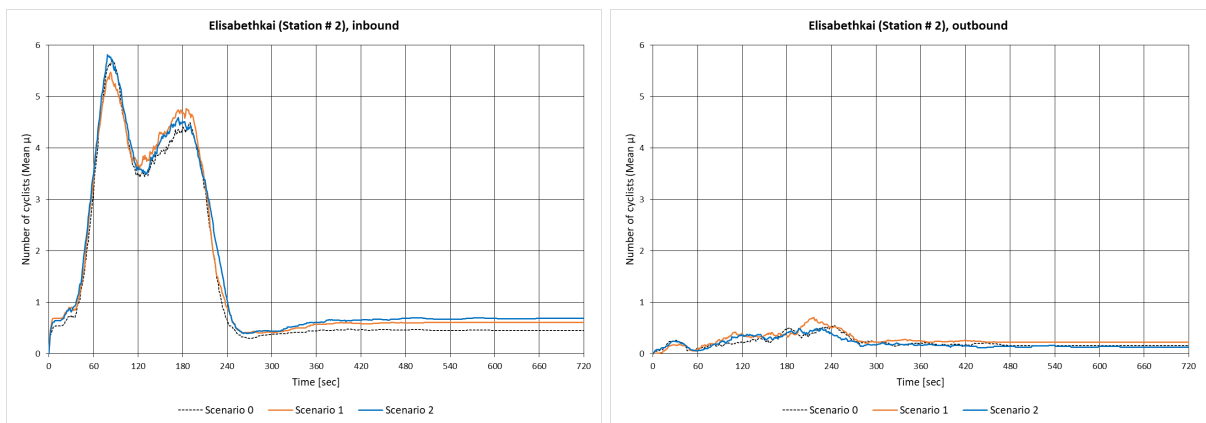


Fig. 4-4: CS 2 (Elisabethkai), inbound / outbound



The charts (reduced versions: Fig. 4-5 - Fig. 4-8) for the additional four virtual counting stations (CS 3 - CS 6) almost all show either strong or partially strong differences (two '↗ ↘' or '↘ ↗' symbols indicate situations where the series show the described differences only for a part of the simulations, but then change to become weaker or stronger for the rest).

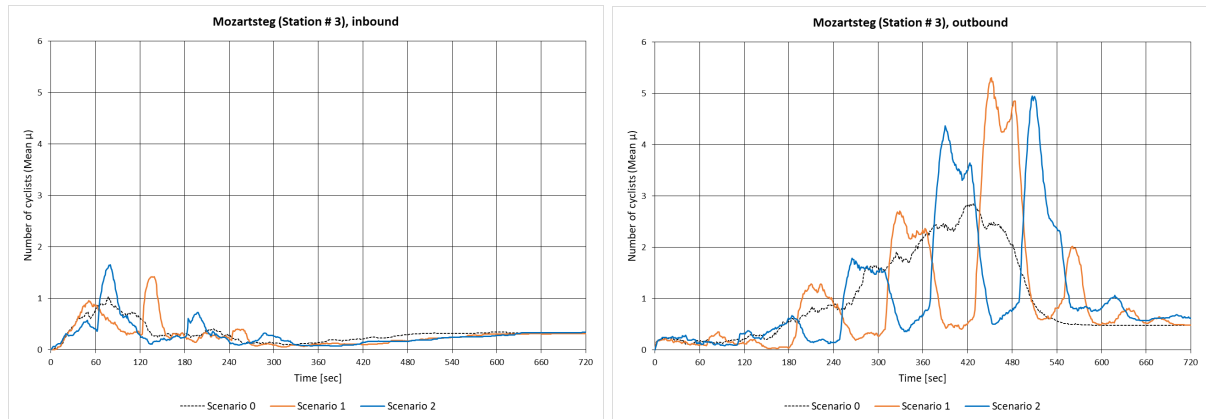


Fig. 4-5: CS 3 (Mozartsteg), inbound / outbound

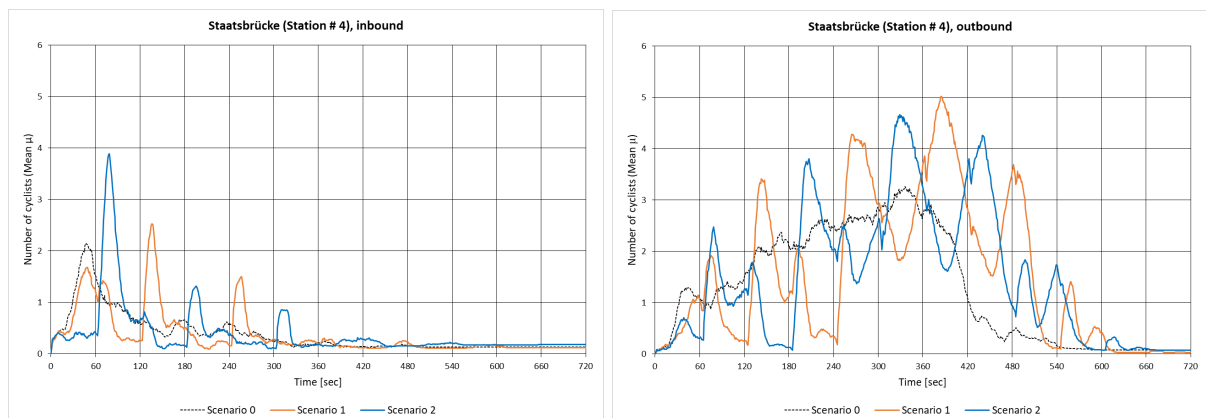


Fig. 4-6: CS 4 (Staatsbrücke), inbound / outbound

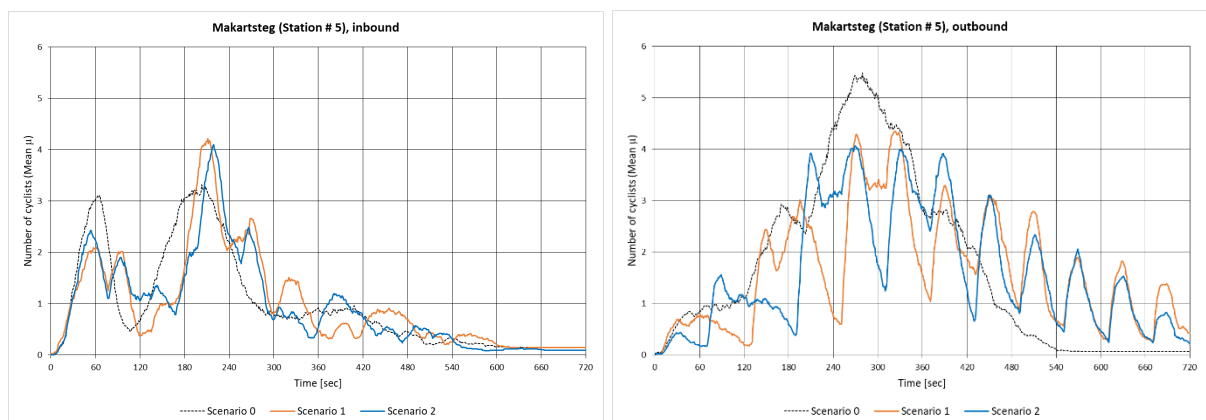


Fig. 4-7: CS 5 (Makartsteg), inbound / outbound

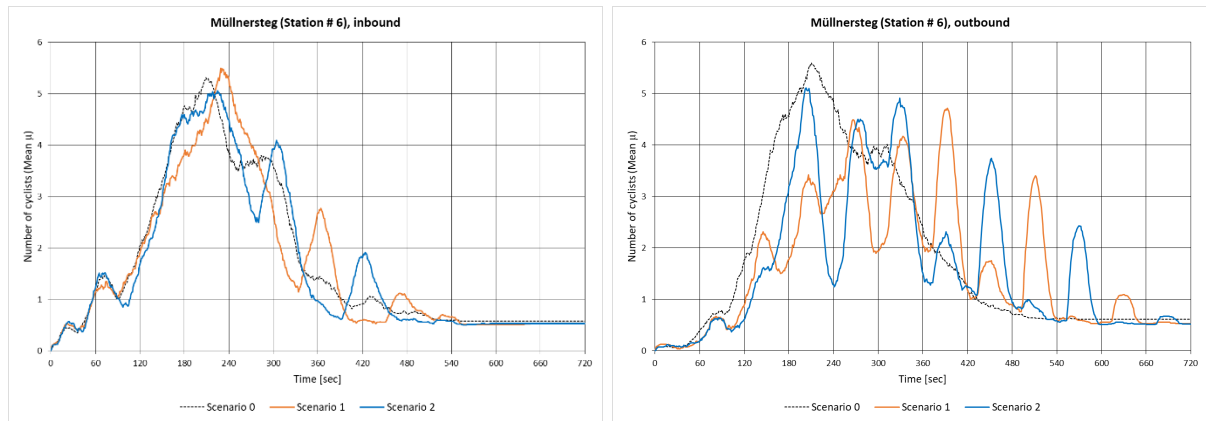


Fig. 4-8: CS 6 (Müllnersteg), inbound / outbound

#### 4.1.4. Categorisation of charts

The results can be generalised into two groups:

- (1) Charts with no apparent effect of traffic lights on the spatio-temporal distribution. This group contains the following counting stations:

Table 4-2: Overview of charts with no apparent effect of traffic lights

Counting station (original)	
#, Name, Direction	Chart
CS 0, Rudolfskai, inbound	Fig. 3-2 or Fig. 4-2 (left image)
CS 2, Elisabethkai, inbound	Fig. 3-6 or Fig. 4-4 (left image)
CS 2, Elisabethkai, outbound	Fig. 3-7 or Fig. 4-4 (right image)

- (2) Charts with visible effect of traffic lights on the spatio-temporal distribution. This group contains all other counting stations. However, the emerging chart series patterns in this group show different characteristics:

- (a) Distinctive phase shift between scenarios 1 and 2

The schematic diagram in Fig. 4-11 illustrates a distinctive shift between the two scenarios (red and blue): the cyclist number peaks at the same time in one scenario when it is at the lowest level in the other scenario.

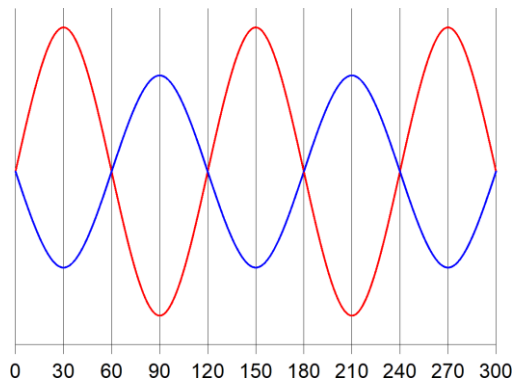


Fig. 4-9: Distinctive phase shift

The chart in Fig. 4-10 for the Mozartsteg counting station (CS 3, outbound) shows an example for this characteristic:

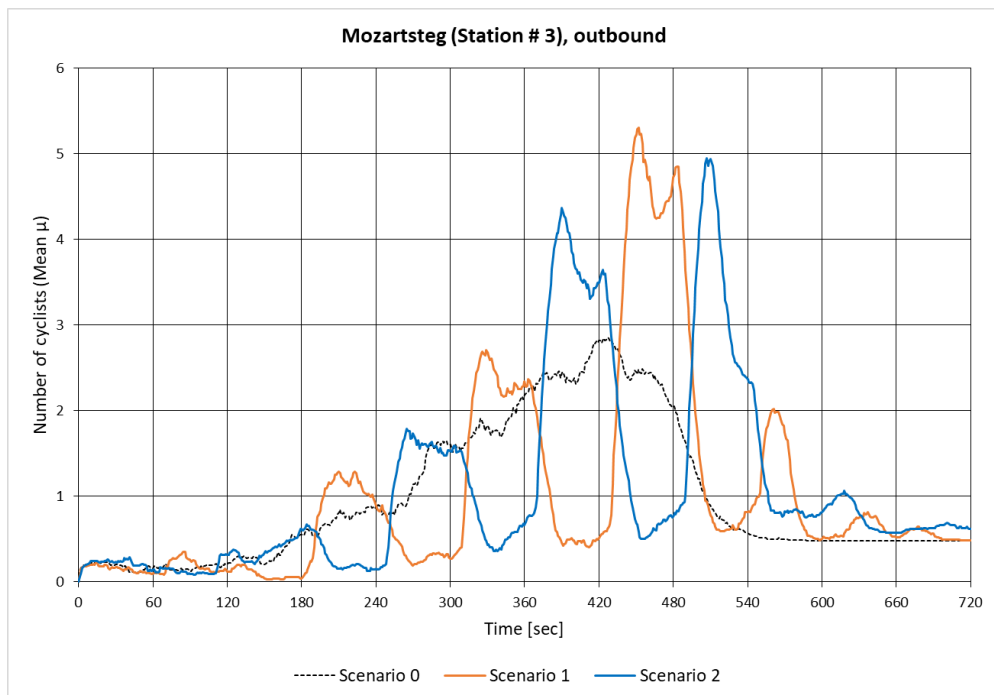


Fig. 4-10: CS 3 (Mozartsteg), outbound

- (b) Non-distinctive or no phase shift between scenarios 1 and 2

The peaks in the schematic diagram in Fig. 4-11 also alternate at their highest level, but the series also pass their low points at the same time, i.e. the two scenarios only differ through their levels. If the high levels would be lower and the low levels higher, the two scenario series in the example would be congruent.

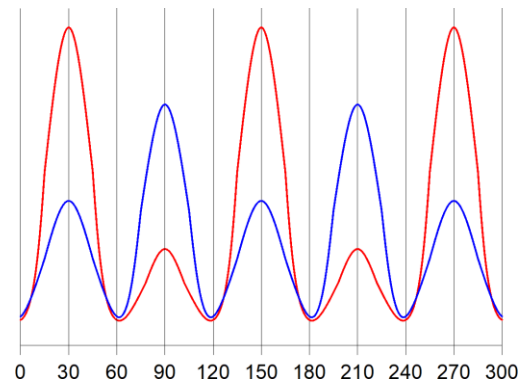


Fig. 4-11: Non-distinctive phase shift

The chart in Fig. 4-12 for the Müllnersteg counting station (CS 6, outbound) shows an example for this characteristic where the different levels make the peaks appear alternating. The chart for the Makartsteg counting station (CS 5, outbound) in Fig. 4-13 shows an example where the series for the two scenarios appear very similar in the second half of the simulation.

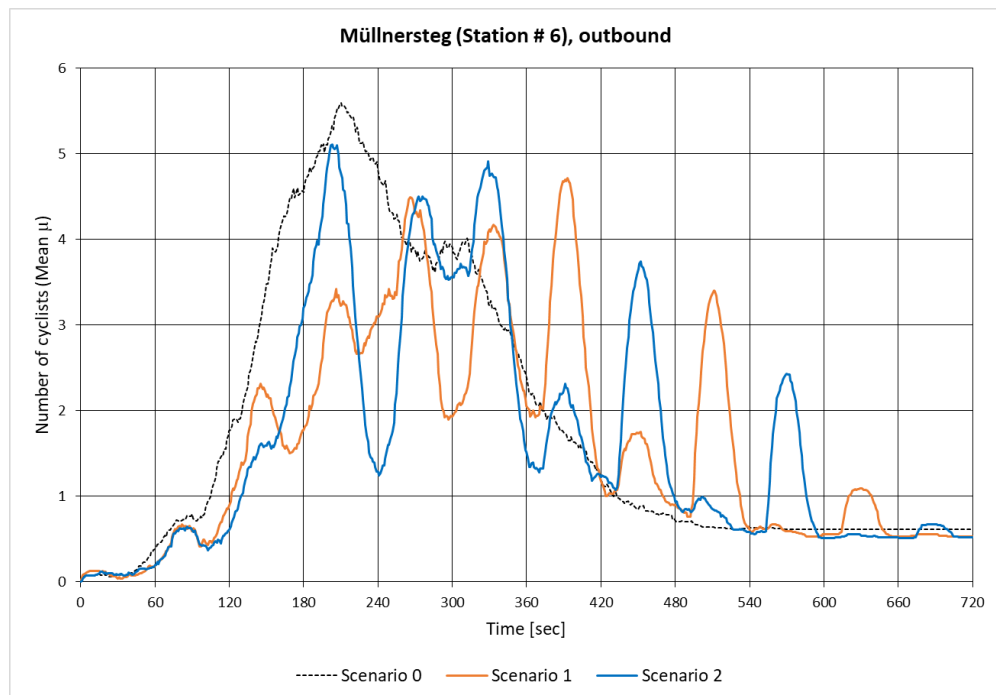


Fig. 4-12: CS 6 (Müllnersteg), outbound

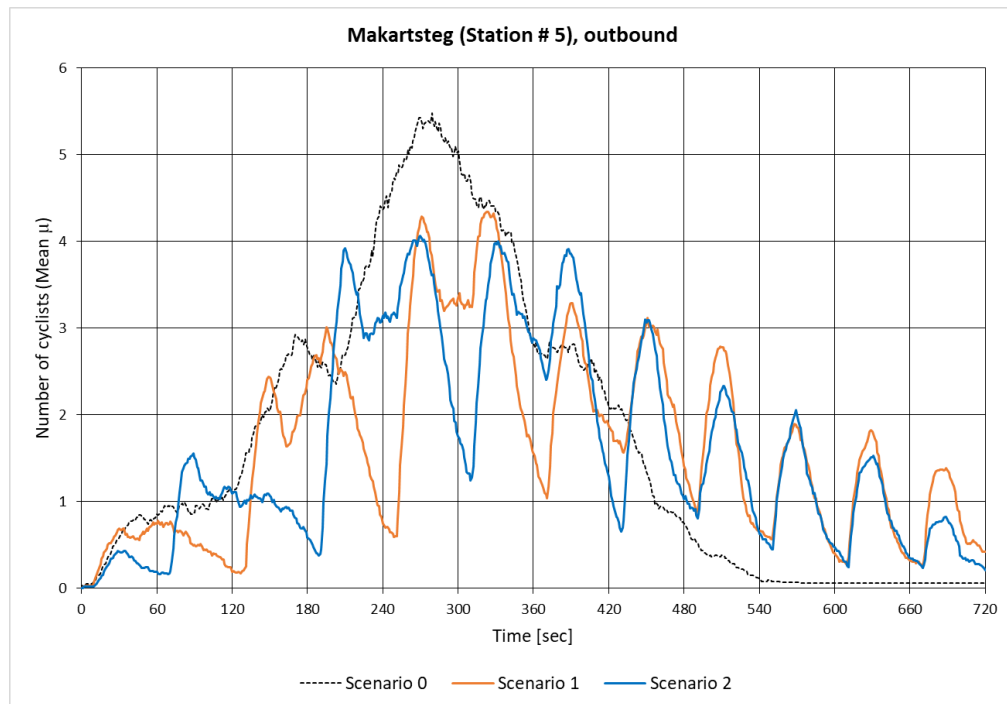


Fig. 4-13: CS 5 (Makartsteg), outbound

Although the peaks in the examples in group (b) are not alternating as clearly as in group (a), the emerging patterns also exhibit effects of the 60-second phase timing delay at the traffic lights.

#### 4.1.5. Observed errors in the results

During the interpretation of the results, a strange pattern exhibited in some of the charts was noticed, especially in the one for the inbound traffic at the 'Giselakai' station (CS 1). There was no explanation for the fact that the counting data at some stations remained steady at a certain level instead of decreasing towards the end of the simulations, as was to be expected and as they did in other charts. In the example of the 'Giselakai' station, this apparent steady stream of a high number of cyclists up to the end of the 12-minutes simulation couldn't be justified by the distribution of residencies that would have had to be located further out towards the study area boundary in order for the traffic to pass the station in the inbound direction so late in the simulations.

An investigation suggested that the count increases every time a cyclist agent is relocated from its final target node in order not to block the following traffic, as described as 'flashing points' in section 2.5 ('Traffic flow factors'). It seemed as if this phenomenon was (at least partially) triggered by cyclists travelling in the outbound direction. This outbound direction, however, is represented by a different road agent (inbound: 'road(2045)', outbound: 'road(1037)'). The number of cyclist agents on the road is determined with the 'count' operator that is applied to the list of agents on a specific road, as provided by the 'skill\_road' skill with the 'all\_agents' variable. It seems as if the removal of a cyclist agent from a node on a road triggers an increment of this variable value by '1' (which then affects the value of the calculated mean). It is not clear though whether this happens consistently or if it depends on additional factors. As with the issue of the dying agents described in section 2.5, no documentation was found that would have allowed for troubleshooting of this phenomenon.

However, with regard to the evaluation of the results in the charts, the effect of this malfunction on the chart series was deemed to be negligible insofar that it is recognisable as a level that remains steady after an increase. A higher number of cyclists would likely overwrite the variable value to a higher level again, so the level of error is suspected in the range between zero and the level that the series remain at. Furthermore, the main focus of this thesis is to identify obvious change in these levels through traffic light phase switches. Nevertheless, the identified problem sections in the charts will be pointed out in the following chart evaluation.

## 4.2. Chart interpretation - individual

### 4.2.1. Counting stations CS 0 to CS 2

#### 4.2.1.1. CS 2 ('Elisabethkai')

With the exception of the results for the outbound direction at the Giselakai station (CS 1), the charts for the three original counting stations exhibit very little or no activity that could be attributed to the existence of traffic lights (Table 4-1). However, when they are compared with each other, the chart for the inbound Elisabethkai station (CS 2) immediately stands out due to its significantly higher cyclist levels at the beginning of the simulations (Fig. 4-14, left). Referencing this to the residents distribution maps (Fig. 4-15 and Fig. 4-16) reveals that there are two factors responsible for this:

- The resident density is very high in the proximity of the counting station
- The counting station is located close to the northern limit of the study area

This means that there are many cyclists who start their trip at the same time in the same area, and that the vast majority of trip targets are located S of the counting station (i.e. in inbound direction). Furthermore, the three series appear very similar, since there aren't any traffic lights located N of the counting station. Most likely, the increasing and subsequently steady levels of cyclists around the 360-second mark have to be attributed to the malfunction in the counting as described in section 4.1.5 ('Observed errors in the results').

These findings for the inbound direction can be similarly applied to the results for the same counting station in outbound direction (Fig. 4-14, right):

- There is very little traffic in the beginning of the simulations, as only a few residents travel further N - but after these cyclists are dispersed, the levels drop to a minimum.

As mentioned in section 4.1.2 ('Differences in chart series'), the chart series are too similar to be certain that the slight differences are caused by traffic light influence. Since the charts series in this direction appear to remain fairly steady past the 480-second mark, the underlying data for this time period should also be assumed to have been generated in error.

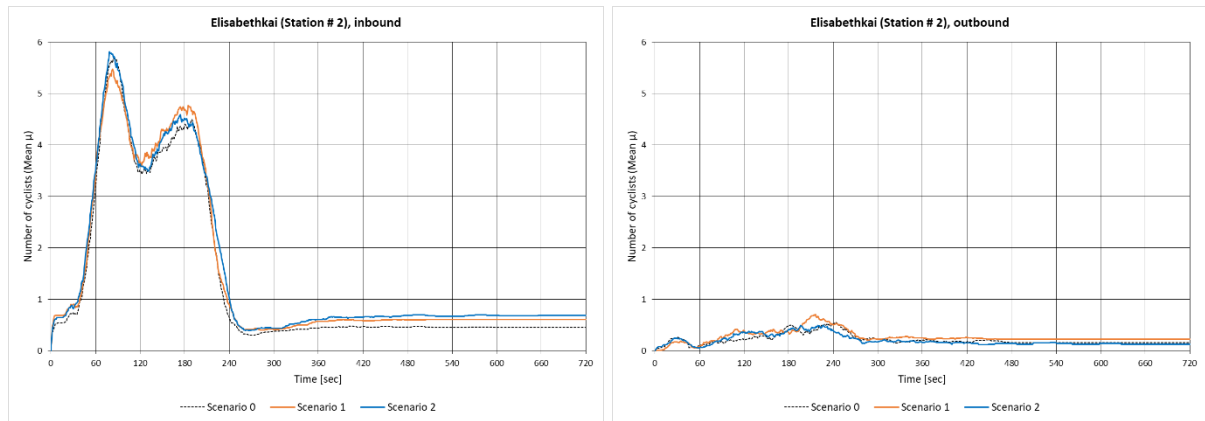


Fig. 4-14: CS 2 (Elisabethkai), inbound / outbound

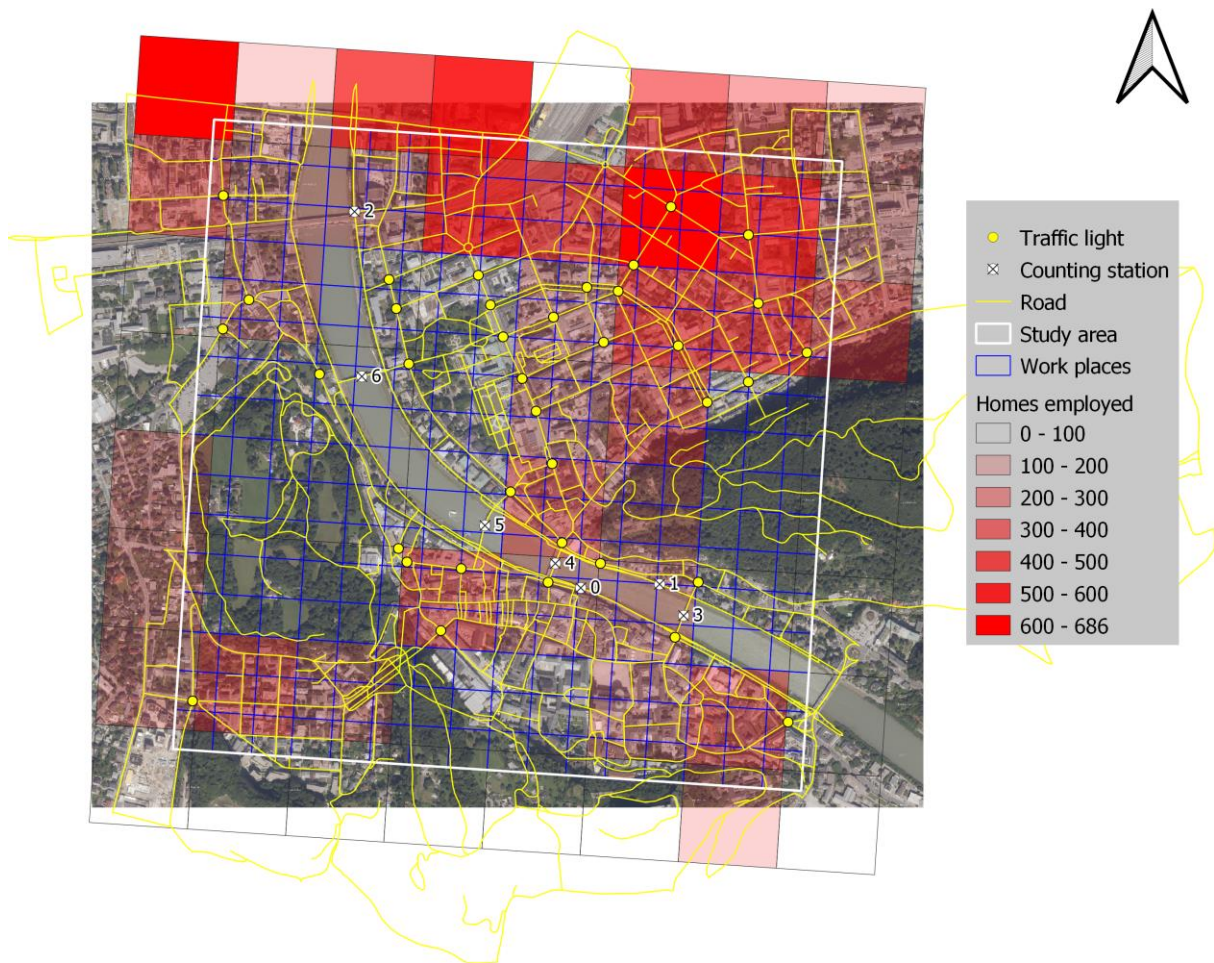


Fig. 4-15: Study area with distribution of employed residents



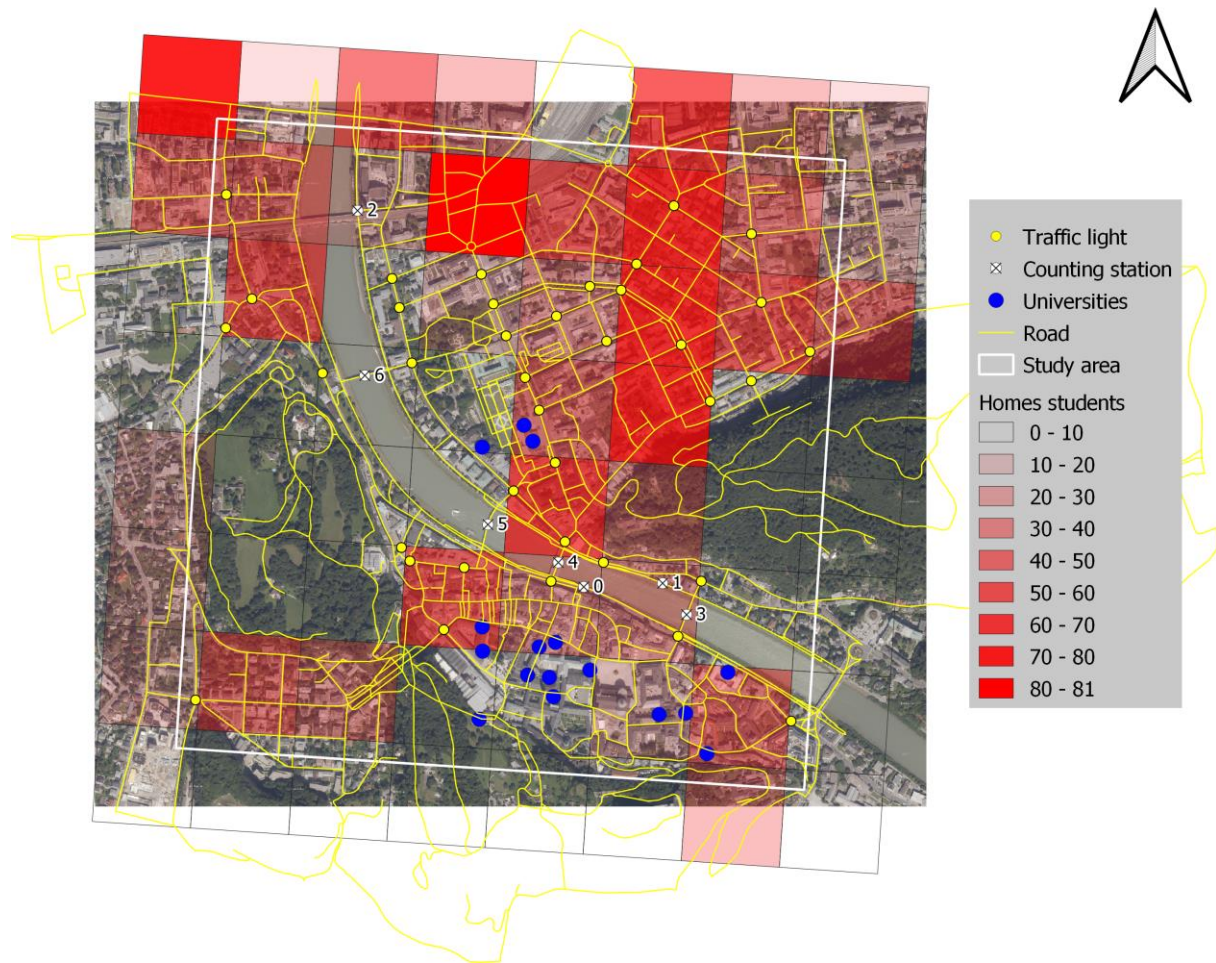


Fig. 4-16: Study area with distribution of universities

#### 4.2.1.2. CS 0 ('Rudolfskai')

The Rudolfskai station (CS 0) in inbound direction (Fig. 4-17, left) also shows its main activity in the beginning of the simulations, albeit shorter in duration than the discussed CS 2 (inbound). This is a bit surprising, since the station is located further towards the centre and away from the study area boundary. However, a cyclist with a speed of 20 km/h could travel 1000 m in 180 seconds (approx. the time when the activity dropped in the chart) - this would almost be enough to reach the station from the southeastern-most corner of the study area boundary, even when traveling along the 100 m x 100 m grid lines. As with the CS 2 station, once this traffic wave passed, the activity stays at a low level for the rest of the simulations. Starting at approx. 360 seconds, this continuation is suspected to be a result of the counting malfunction described earlier.

The outbound direction at this station sees its main activity much later in the simulations (Fig. 4-17, right). This could be due to cyclists with target locations in the SE of the study area just requiring more time to get there, but with the work places grid cells being distributed evenly

over the whole study area, it seems unlikely that the sudden traffic increase at this counting station is caused by 'worker' cyclists (who account for approx. 88% percent of the cyclists in this model setup). However, when linking this chart to the university locations in the SE of the study area (Fig. 4-16), the traffic pattern seems plausible.

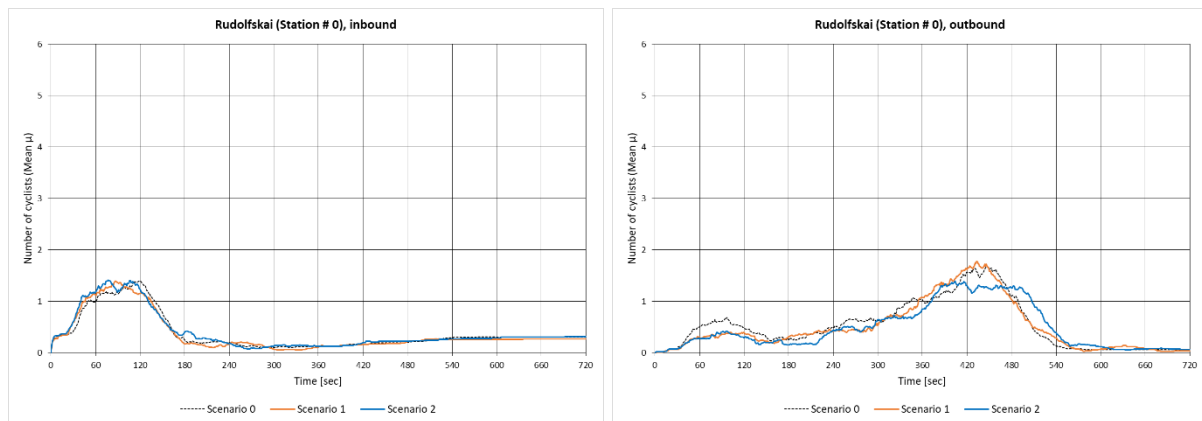


Fig. 4-17: CS 0 (Rudolfskai), inbound / outbound

The closest two traffic lights that could influence the traffic at the counting station CS 0 in outbound direction are #16 and #2081 (Fig. 4-18). However, the fact that the three chart series do not appear very different suggests that the cyclist traffic is barely affected by these traffic lights (which could be the case, for instance, if the main traffic flows along the shore of the Salzach river instead of through the traffic light intersections).

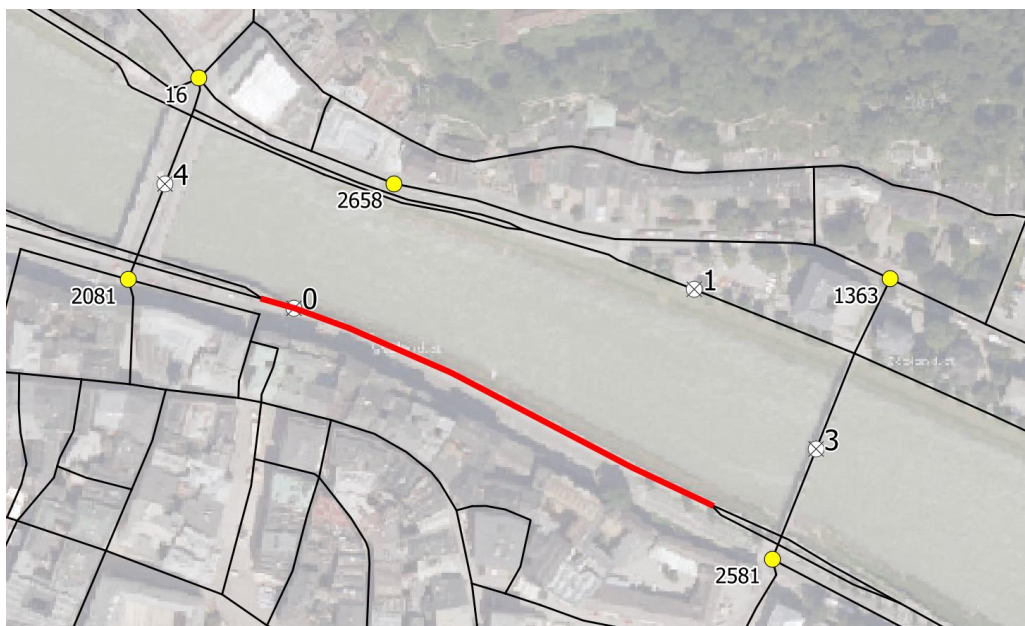


Fig. 4-18: CS 0 (Rudolfskai), with nearby traffic lights (Orthophoto: Geoland.at 2018)

#### 4.2.1.3. CS 1 ('Giselakai')

The series in the chart for the inbound traffic at the 'Giselakai' station (CS 1) seem somewhat 'unusual' (Fig. 4-19, left), compared to the other charts. The short peak period in the beginning of the simulations also appears in other charts (although in different forms) and suggests that some cyclists immediately entered the counting station road. However, the last quarter of the simulations shows a steady stream of cyclists, while the traffic in the other charts is winding down or already at a minimum in the same time period. There aren't very many residences further out in the southeastern part of the study area that could lead the traffic to pass this counting station on the shortest route to their destination and would require 12 minutes of travel time. Another potential explanation would be a cyclist agent blocking the road in such a way that the following agents remain on the counting stations road (and are counted repeatedly) until the end of the simulations. However, with the current setup (traffic light phase timing, number of cyclists, vehicle length, cyclist agent relocation at the end of their trip, etc.), such a situation should not occur. Further investigation led to the findings in section 4.1.5 ('Observed errors in the results') above, as this is the strongest example of this phenomenon. The affected time period in this chart probably starts around 300 seconds into the simulations.

The chart for the outbound direction at the Giselakai station (CS 1) is the only one in the group of original counting stations that shows obvious signs of the influence of traffic lights on the traffic flow (Fig. 4-19, right). By observing the vicinity of this station in the model's 'City display' map view during a simulation, it can be determined that this influence mainly comes from the traffic light #16 (Fig. 4-20), which controls much of the traffic between the areas N and S of the Salzach river and where at times line-ups of cyclists can be observed (which are then 'released' in batches when the traffic lights switch). The road with this counting station appears to be the shortest route for many cyclists coming from the northeastern part of the study area with a target location in the SE corner of the study area. Although the coarse shapes of the series for scenario 1 and 2 suggest that they are also influenced by cyclists that are not delayed by traffic lights, the overall rhythm of approx. 60 seconds between the peaks of the two series is clearly recognisable.

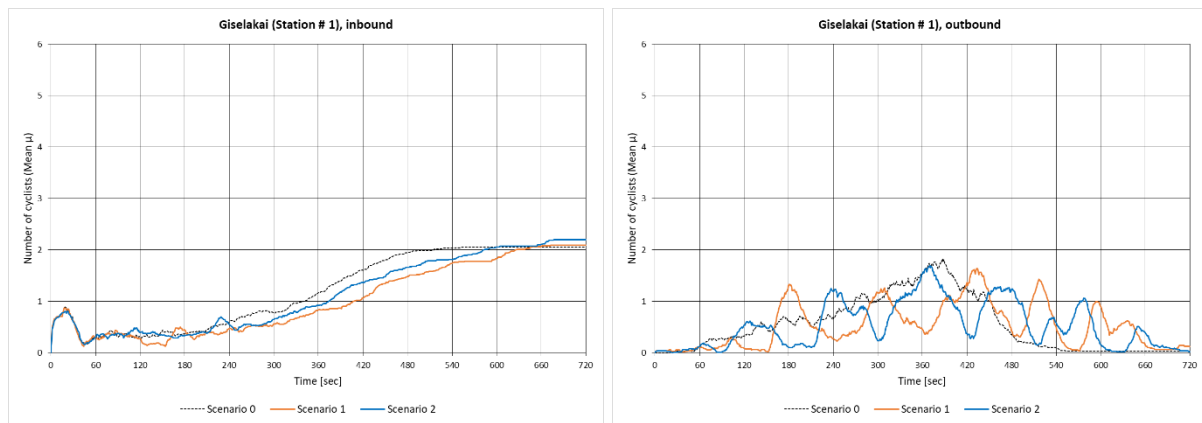


Fig. 4-19: CS 1 (Giselakai), inbound / outbound

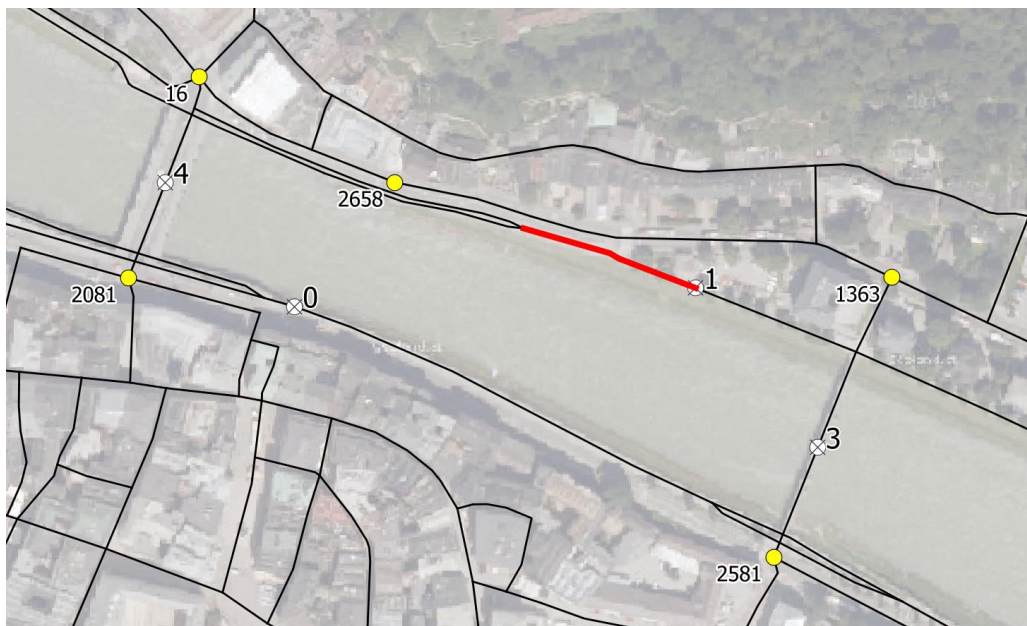


Fig. 4-20: CS 1 (Giselakai), with nearby traffic lights (Orthophoto: Geoland.at 2018)

#### 4.2.2. Counting stations CS 3 to CS 6

##### 4.2.2.1. CS 3 ('Mozartsteg')

What applies to the other counting stations with regard to their traffic volume related to their location in the study area also applies to the Mozartsteg counting station CS 3. The early inbound traffic shown by all three scenario series in Fig. 4-21 (left) can be attributed to those residents in the SE corner of the study area for whom the route across the Mozartsteg is the shortest connection to their target locations N of the Salzach river. This traffic doesn't last very long, but long enough to show a few clearly distinguishable peaks with an approx. 60-second shift in between in the series for the scenarios 1 and 2. The traffic light responsible for this is

#2581 in Fig. 4-22. There is only one more traffic light in this corner of the study area (Fig. 4-16), but this is too far away to have a visible effect, the more since there are hardly any residents living even further SE in the study area.

The chart for the outbound direction of the 'Mozartsteg' station (CS 3) shows a very clear pattern of peaks which are reaching high levels in the beginning of the second half of the simulations, and which are also alternating with a clear shift of approx. 60 seconds (Fig. 4-21, right). These peaks have to be seen in connection with the results for the outbound direction of the 'Giselakai' station (CS 1), since they are added in when the two traffic streams from the counting station CS 1 and the traffic light #1363 merge to travel southbound. This merging process can be well observed during simulations with the model's 'City display' map view. It is suspected that the 'double peaks' and the corresponding uneven low levels exhibited in the chart series for the scenarios 1 and 2 are a result of this (not perfectly synchronized) superimposed traffic flow. The steady level in the last quarter of the series for scenario 0 could well be related to the program malfunction mentioned earlier. The levels for the scenarios 1 and 2 could also be caused by ongoing traffic all the way to the end of the simulation.

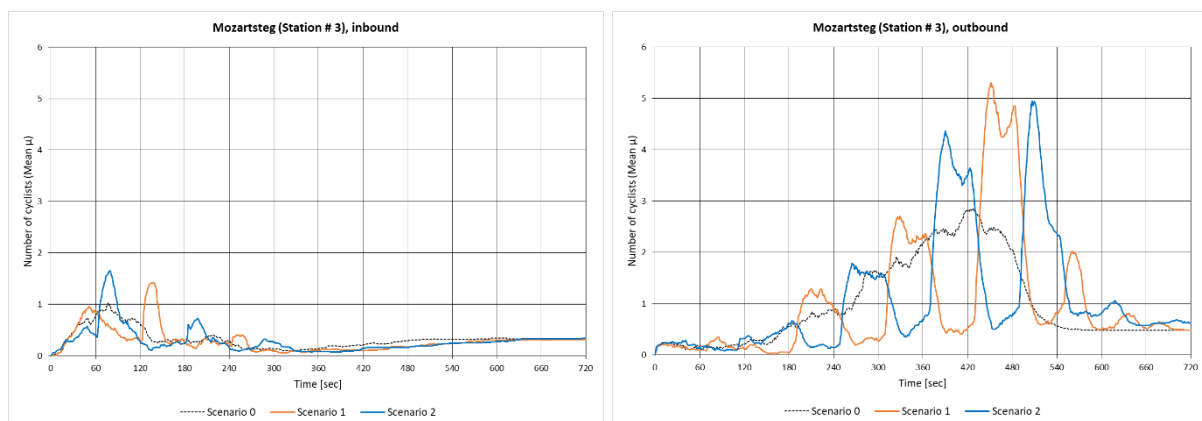


Fig. 4-21: CS 3 (Mozartsteg), inbound / outbound

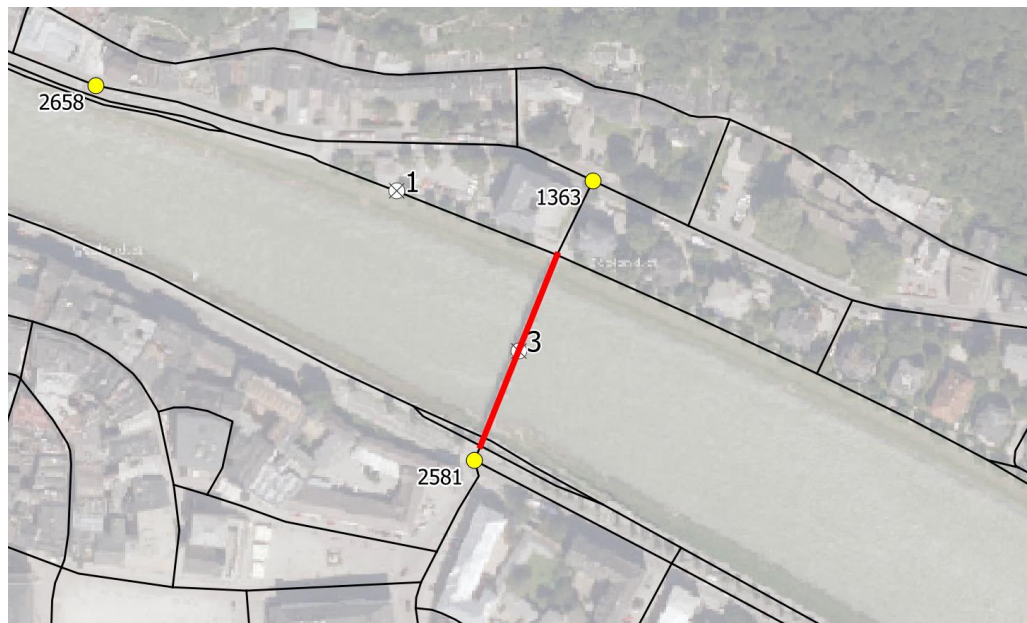


Fig. 4-22: CS 3 (Mozartsteg), with nearby traffic lights (Orthophoto: Geoland.at 2018)

#### 4.2.2.2. CS 4 ('Staatsbrücke')

As counting stations are located more centralized in the study area, the charts reflect a higher traffic volume. The comparison of the inbound traffic at the 'Staatsbrücke' station (CS 4) in Fig. 4-23 (left) with the inbound traffic at the 'Mozartsteg' station (CS 3) in the previous section (Fig. 4-21, left) demonstrates this difference. The area S of the Salzach river for which the 'Staatsbrücke' acts as the shortest connection with target locations N of the river is bigger than for the 'Mozartsteg', therefore the traffic flows longer and the numbers of cyclists are higher. The inbound traffic across the 'Staatsbrücke' is clearly affected by the traffic light #2081 (Fig. 4-24), the only traffic light within a radius of 200 m on this side of the river. Since this traffic light and its pendant S of the 'Mozartsteg' (Fig. 4-22, #2581) are very similarly located and both 'red' during the same phases in the scenarios 1 and 2, the emerging patterns are also very similar: both start with their highest peak being recorded during simulations with scenario 2 and at almost exactly the same time in the simulation, and both subsequently maintain the same 60-second rhythm. However, also the last third of the series in Fig. 4-23 might be subject to the influence of the model malfunction mentioned above.

The outbound traffic at the 'Staatsbrücke' station (CS 4) also leads to clear phase shift patterns around the centre mark of the simulations (Fig. 4-23, right), although not as 'picture-perfect' as in some of the other charts. The main influence is definitely coming from the traffic light #16 again, but this intersection is a merging point for four major roads (in terms of the directions which they come from), and three of these roads are controlled by other traffic lights

within a radius of approx. 200 m. It is suspected that this multitude of 'feeder' roads and traffic lights is the reason why the major peaks in the series for the scenarios 1 and 2 show some additional activity in their flanks, and why the smaller peaks in the beginning and the end phases of the simulations appear less clear structured and partially overlapping.

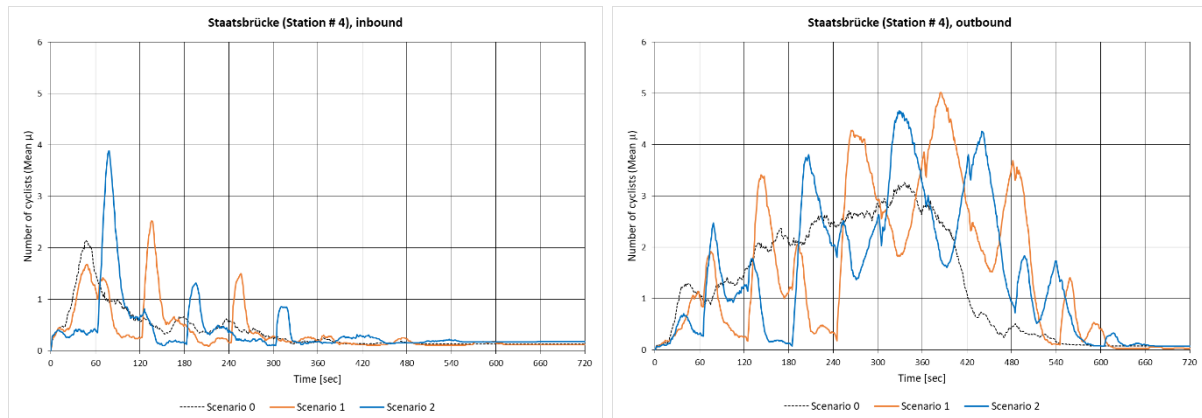


Fig. 4-23: CS 4 (Staatsbrücke), inbound / outbound

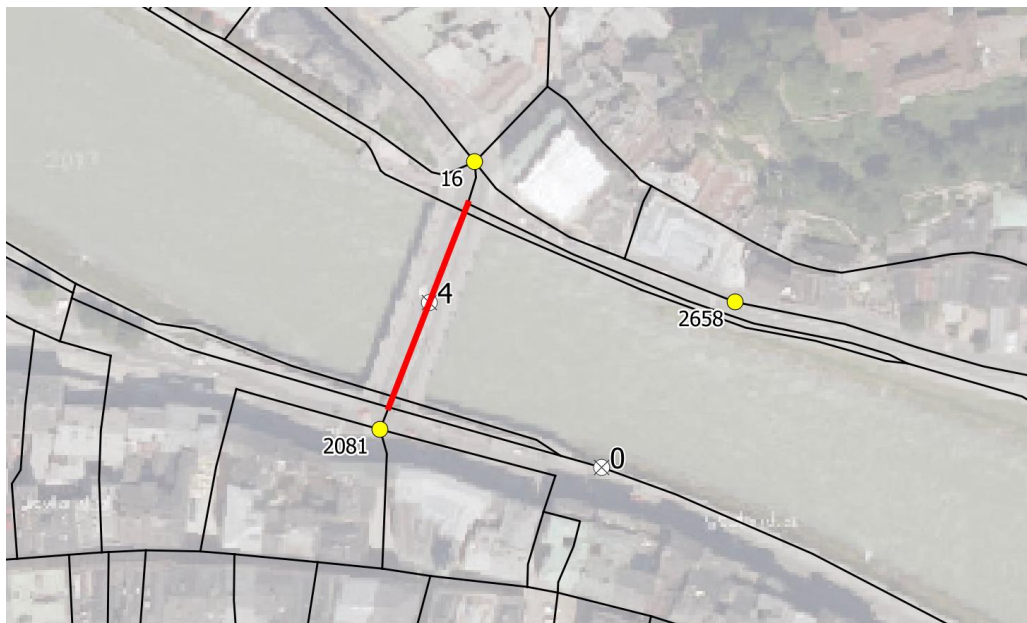


Fig. 4-24: CS 4 (Staatsbrücke), with nearby traffic lights (Orthophoto: Geoland.at 2018)

#### 4.2.2.3. CS 5 ('Makartsteg')

The 'Makartsteg' station (CS 5) counting data for the inbound direction results in the probably most 'chaotic' of the chart series (Fig. 4-25, left). The closest traffic light (and hence the one that has the most influence on the resulting patterns) is #2147 (Fig. 4-26). However, although the charts series show some of this influence (especially in the peaks in the first half of the simulations), there is an underlying wave form that is also visible in the reference series for

scenario 0. This could be attributed to the distribution of the homes of both, the employed population and the student population. Both overview maps with the population grid cells (Fig. 2-20 and Fig. 2-21) show a higher density in the 250 m x 250 m grid cell immediately SW of the Makartsteg and in the two adjacent grid cells in the SW corner of the study area. The time difference between the two 'waves' (around 60 seconds and 210 seconds into the simulation) is approx. 150 seconds. With a speed of 20 km/h, a cyclist agent could travel approx. 830 m within that time period. Even considering that there are two traffic lights along the route that is most likely the shortest connection between the SW corner of the study area and the Makartsteg, this time difference seems very plausible with regard to the approx. distance between these areas.

The two traffic lights are approx. 200 m (or approx. 40 seconds) apart from each other, but both in the 'red' phase at the same time within the same traffic light scenario. However, the stochastic deployment of cyclist agents and the relatively coarse simulation results that led to the minimal phase shift between the scenarios 1 and 2 in the chart do not justify any statement about how these factors are related. It is also unclear whether the last 60 seconds in the simulations are related to the malfunction in the cyclist relocation or to legitimate traffic.

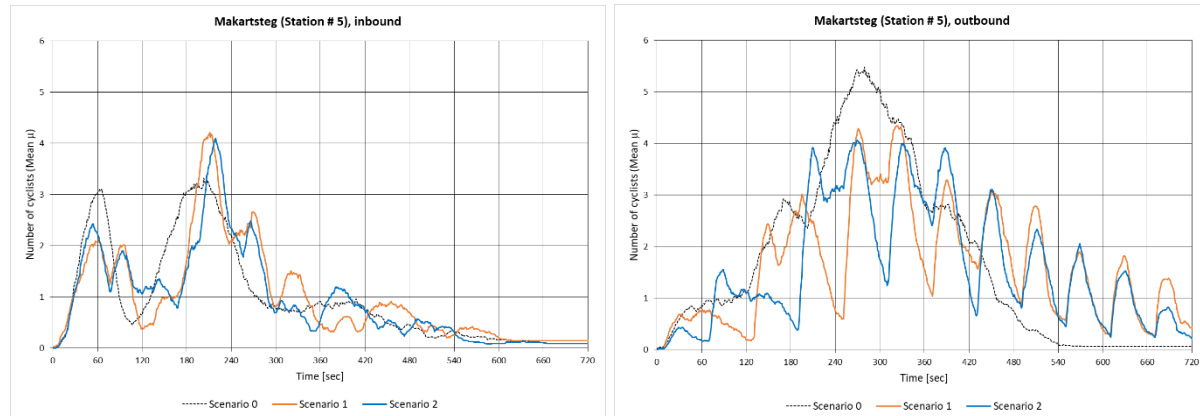


Fig. 4-25: CS 5 (Makartsteg), inbound / outbound

The almost congruent peaks between the traffic light scenario series in parts of the inbound chart also appear in the chart of the outbound direction for the 'Makartsteg' station (Fig. 4-25, right). Although still turbulent, the series show a much more orderly overall picture. The dominant peak around the 270-seconds mark in the series for scenario 0 suggests that there is a group of cyclist agents building up over time on the way to the 'Makartsteg'. The observation of a test simulation revealed that there are many cyclists from the densely populated northern residence areas (Fig. 2-20 and Fig. 2-21) travelling southbound parallel to the Salzach river



until they cross the river on the shortest route to their target locations S of the river. They turn right at the intersection with the traffic light #1442 in Fig. 4-26, but since there is no traffic light functionality applied in scenario 0, they only have to yield to the other traffic during the turn. The time delay is simply due to the long way along the river to reach this turning point.

The explanation for the phenomenon that the series for the scenarios 1 and 2 show some effect of the 60-second phase shift in the beginning of the simulation, but then change to increasingly congruent patterns at approx. the same time (270 seconds) is more difficult, since the simulations for the two scenarios can only be observed individually in the model's 'City display' map view. The misleading part when doing so is that it is not correct to assume that agents passing a traffic light at a specific time in a specific direction would just stand still at that same traffic light and at the same time in the other scenario – they might not be there in the other scenario, since the roads they are coming from are also controlled differently by traffic lights. In both scenarios, once the simulation has been running for enough time (i.e. approx. 270 seconds), there are multiple cyclists waiting at that one traffic light to be 'released' when the light switches to 'green', but they are not waiting on the same road. In the example of the traffic light #1442, they are waiting after coming from the NW in one scenario, but coming from the NE in the other scenario - they just can never be observed together when watching only one scenario in a simulation. The charts represent that situation that would occur when they would be together, because the scenario series are superimposed. This is why the series appear almost congruent.

The decreasing levels towards the end of the simulations are due to the fact that less and less cyclists are still travelling (basically the ones who are on a trip across the city) – the ones with shorter trajectories already reached their final destinations. The same applies to the cyclists represented in the series for scenario 0: since they were not held up by traffic lights, they finished their trips – the steady level in the last quarter of the simulation is likely again a result of the aforementioned program malfunction.



Fig. 4-26: CS 5 (Makartsteg), with nearby traffic lights (Orthophoto: Geoland.at 2018)

#### 4.2.2.4. CS 6 ('Müllnersteg')

The counting station on the 'Müllnersteg' (CS 6) also sees high levels of traffic in the inbound direction (Fig. 4-27, left). Since the residence density SW of it is very low (Fig. 4-15 and Fig. 4-16), and since the residences in the SW corner of the study area have shorter connections available to cross the Salzach river to the N side, it can be assumed that this traffic originates mainly from the residence areas in the NW corner of the study area. The observation of simulations in the model's 'City display' map view confirm this. This traffic arrives on two roads at the 'Müllnersteg': on the road directly next to and parallel to the Salzach river, and on the road further W that is controlled by traffic light #2097 (Fig. 4-28). The series in the chart can therefore be understood as the added results from the two traffic flows, where the small peaks represent the influence of the traffic light. As in the other charts, the alternating peaks of the scenarios 1 and 2 are shifted for almost exactly 60 seconds. As before, it also can be assumed that the steady level at the end of the simulations with all three scenarios is caused by erroneous counting in connection with the relocation method for cyclist agents that reached their final target location.

The series for scenario 0 in the chart (Fig. 4-27, right) for the outbound direction at the 'Müllnersteg' station (CS 6) looks very similar to the one for the inbound direction. The situation is also very similar: the traffic volume is built from cyclist agents coming from the densely populated residence areas in the N and NE of the study area (Fig. 4-15 and Fig. 4-16). Although the area NE of the Müllnersteg is bigger and more populated than the one referenced on the W

side of the Salzach river for the inbound traffic, the peak level of the series for scenario 0 is almost the same. The reason for this is that not every cyclist wants to cross the river at the 'Müllnersteg' in outbound direction, they also travel to other crossings. However, the ones that cross at the 'Müllnersteg' are influenced by the traffic light #1373 (Fig. 4-28). The ones that have to stop at the traffic light in the simulations with the scenarios 1 and 2 reduce the duration of the traffic flow at the counting station to the narrower peaks in the chart. Since they don't all are 'released' at the same time at the traffic light, they come in waves. Once more, the waves exhibit the 60-second rhythm from the traffic light phase timing scenarios. As with the inbound direction, the series for the three scenarios end with the increased level caused by the issue with the cyclist agent relocation.

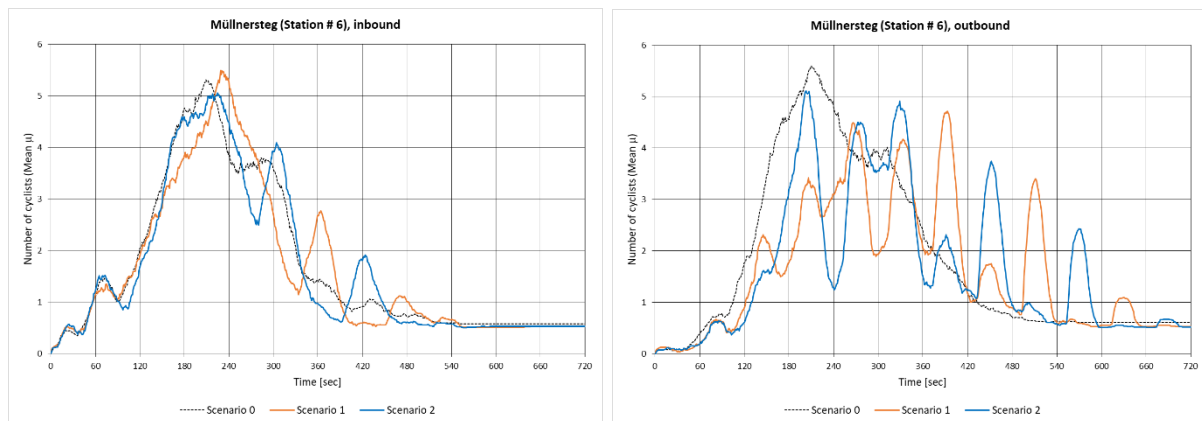


Fig. 4-27: CS 6 (Müllnersteg), inbound / outbound

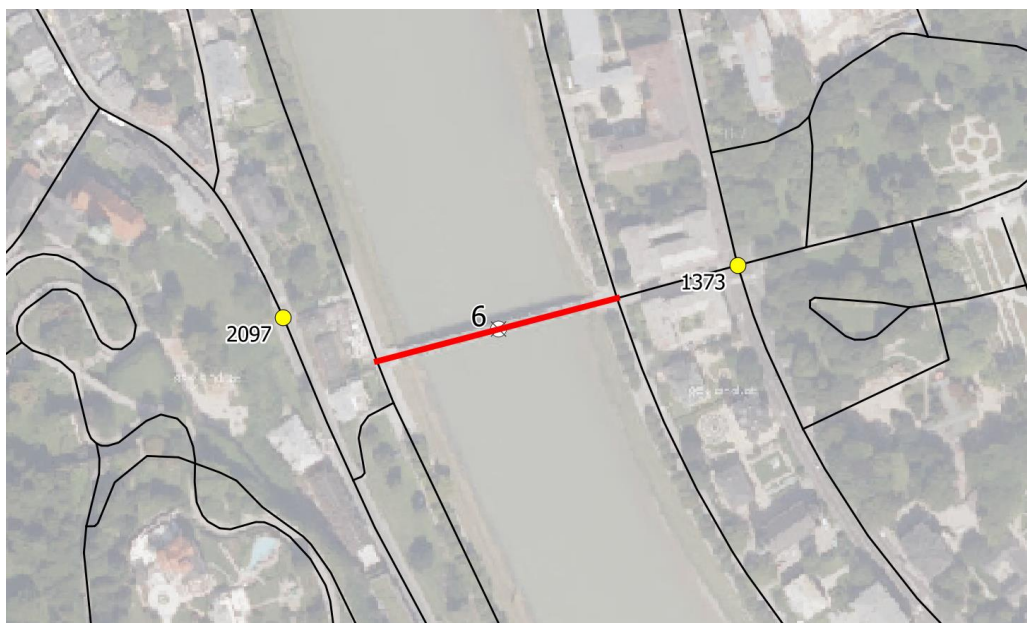


Fig. 4-28: CS 6 (Müllnersteg), with nearby traffic lights (Orthophoto: Geoland.at 2018)

### 4.3. Discussion summary

#### 4.3.1. Model detail level

The situations which the model was set up to simulate were based on:

- A generic road network
  - without additional weights to differentiate between route types (e.g. safest route)
  - without bicycle-specific infrastructure (e.g. cycle paths) or restrictions (e.g. pedestrian zones)
  - with one lane per direction
  - with one setting for maximum speed (20 km/h)
  - without other traffic
- Simplified traffic light functionality
  - with only 'red' or 'not red' states
  - with basic turning rules
- Three scenarios
  - One reference scenario without influence of traffic lights
  - Two scenarios with traffic light influence, with identical (but shifted) phase timing periods (60 seconds, alternating)
- Two types of cyclists
  - Employed cyclists, travelling to work places (blue agents)
  - Students, travelling to universities (green agents)
  - Identical behaviour, the distinction was made to influence the trip trajectories with regard to target locations
- Agent properties / Cyclist behaviour
  - The properties of the road, node, and cyclist agents were set to reflect cyclist behaviour (where feasible, based on available information)
- Simple trips
  - All cyclists were deployed at the same time and for a single trip
  - They all traveled along the shortest route
  - They were removed once they reached their destination
- Two types of departure / destination locations
  - Departure locations: Polygon grid cells with a population density
  - Destination locations: Polygon grid cells and point locations

#### 4.3.2. Model category

This combination of different levels of modeled detail (e.g. fairly explicit cyclist reactions to traffic and traffic lights at intersections which themselves are modeled very generalised and located on an even more generalised road network) makes it difficult to fit this model into a category – however, a classification at the microscopic level still seems most appropriate.

#### 4.3.3. Processing effort

Although these modeled situations might be perceived as not realistic enough, the simplicity of the model proved to be crucial for the ability to execute the number of simulations needed to obtain meaningful results, based on the stochastic nature of the cyclists' trips. Additional traffic light phase timing scenarios or alternative model parameters (e.g. different route settings) would have multiplied the number of required simulations (and the resulting 72000 counting data values per scenario, counting station, and direction). More variety (e.g. cyclist types with specific behaviours, traffic lights with special functionalities, etc.) would have led to results that would have been more complex and difficult to interpret with regard to what caused which type of traffic light influence on the temporal distribution of the bicycle traffic.

Due to the computational effort for the thesis model, the manageable number of deployed cyclists was significantly smaller than reported by Taillandier (2014) in reference to an application example for the 'advanced\_driving' skill. Although this example model was also set up with a temporal resolution of one second (which was appropriate to detect the traffic light effects in the thesis model), this increased effort was most likely due to two factors:

- the stop list content was updated (based on list access) during every simulation cycle
- the counting data was written out into CSV-files with the same frequency

This does not include the effort to generate the stop indicator arrows in the 'City display' map view (which was deactivated during the final simulation executions).

Please note that the last GAMA version used for the model development was 1.8.0 RC2, since it was suggested that this version would speed up the processing of large numbers of agents. Unfortunately, additional potential improvements since version 1.7.0 RC2 could not be considered in this thesis.

#### 4.3.4. Confirmation of traffic light influence

The review of the charts and their comparison with maps and repeated simulations in the model's 'City display' map view revealed that the effect of traffic lights on the spatio-temporal distribution of bicycle traffic can be observed in two ways with this model:

- (1) The traffic lights lead to a delay with regard to the time that elapses until the cyclists in scenario 0 (without traffic lights) and the scenarios 1 and 2 (with traffic lights) complete their trips. This can be well observed in Fig. 4-29, where the chart series for the scenarios 1 and 2 continue to show activity while the activity with scenario 0 ended 180 seconds earlier. Fig. 4-30 confirms this as a cross-check: the plotted charts series for the three scenarios are almost congruent due to a lack of traffic lights on the route before the counting station.

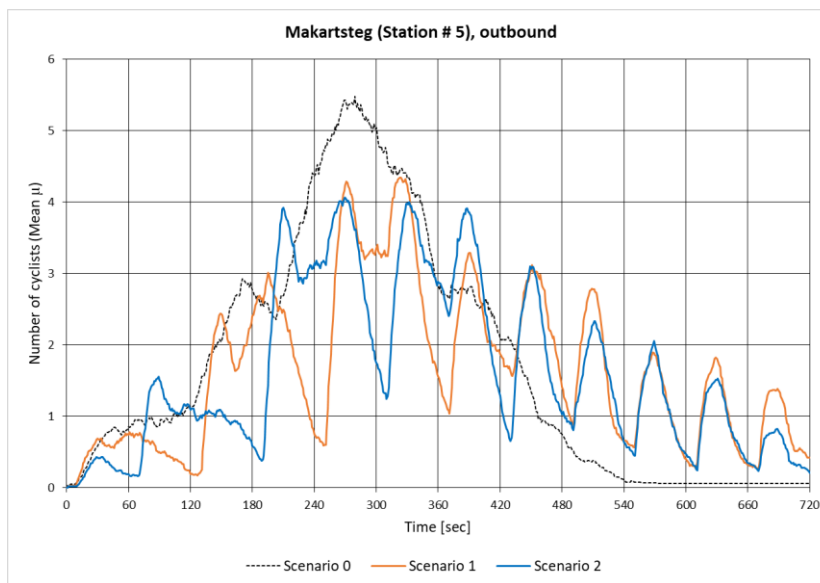


Fig. 4-29: Distribution of cyclists at CS 5 (Makartsteg), outbound

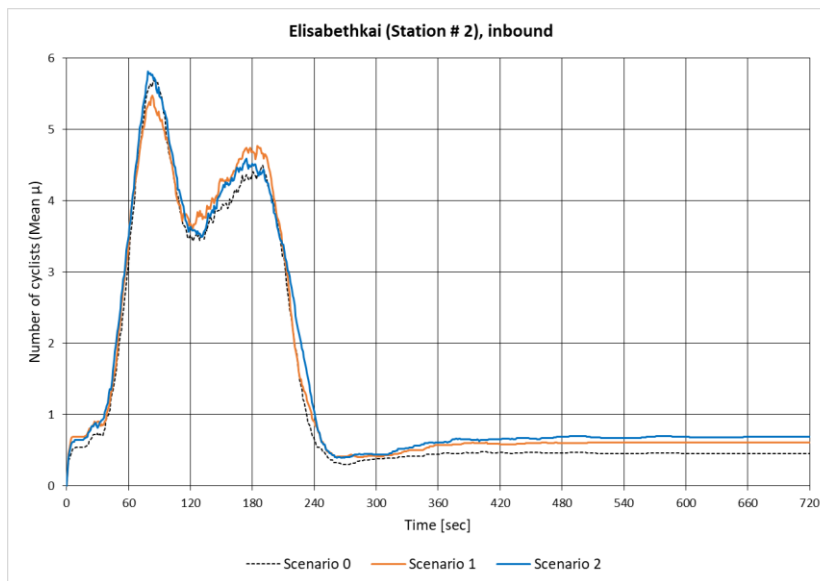


Fig. 4-30: Distribution of cyclists at CS 2 (Elisabethkai), inbound

- (2) The 60-second phase shift between the scenarios 1 and 2 is clearly recognisable in charts such as Fig. 4-31 (described as 'distinctive phase shift'). Although there are situations where the superimposed chart series appear almost congruent (Fig. 4-29, described as 'non-distinctive phase shift'), they still show a 60-second rhythm nevertheless.

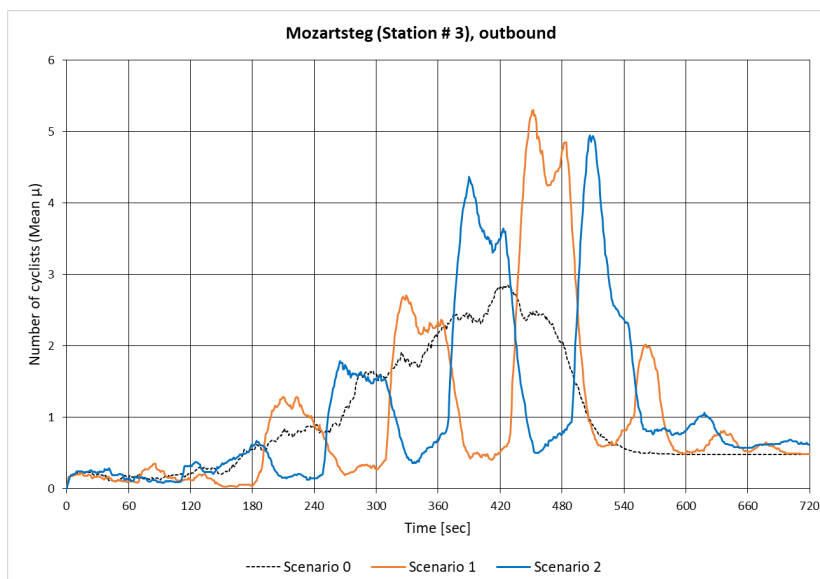


Fig. 4-31: Distribution of cyclists at CS 3 (Mozartsteg), outbound

The oscillations in the chart series are caused by increasing and decreasing numbers of cyclists on the monitored roads closest to the counting stations during the course of the simulations. Theoretically, such changes in the bicycle traffic volume could also be caused by other phenomena without the influence of traffic lights (for instance by constructive

interference of coincidentally occurring traffic from multiple roads, as partially exhibited in Fig. 4-31), but the shifts with the 60 seconds base timing that can be observed in the majority of the charts are too orderly and accurate to be the product of random effects - they can clearly be attributed to the influence of the traffic lights.

As the amplitudes of the oscillations (i.e. the number of cyclists) depend on many factors (e.g. the rate of cyclist accumulation at traffic lights as a function of the routes chosen by the cyclists), they could not have been foreseen to the extent at which they occurred. It appears reasonable though that the highest levels in the two traffic light scenario series were recorded approx. during the same time period as the highest level in the series for the scenario without traffic lights (Fig. 4-29), but also that the traffic light series levels didn't decrease at the same overall rate afterwards.

It has to be noted though that the counting data are collected from the counting station roads (not the actual point locations of the stations), therefore the lengths of these road segments are also a factor. The monitored counting station road segments vary in length between 82.1 m and 246.7 m (Table 4-3). Longer road segments could theoretically count more agents at the same time (leading to higher amplitudes) and individual agents could be recorded for a longer period of time (i.e. the oscillations themselves might be wider).

Table 4-3: Overview of monitored counting station road segments with their lengths

Counting station	Direction	Road	Length [m]
CS 0 (Rudolfskai)	inbound	0893	246.77
CS 0 (Rudolfskai)	outbound	1916	246.77
CS 1 (Giselakai)	inbound	2045	91.10
CS 1 (Giselakai)	outbound	1037	91.10
CS 2 (Elisabethkai)	inbound	2058	143.57
CS 2 (Elisabethkai)	outbound	1051	143.57
CS 3 (Mozartsteg)	inbound	1078	102.76
CS 3 (Mozartsteg)	outbound	2084	102.76
CS 4 (Staatsbrücke)	inbound	2114	82.07
CS 4 (Staatsbrücke)	outbound	1110	82.07
CS 5 (Makartsteg)	inbound	2124	121.45
CS 5 (Makartsteg)	outbound	1121	121.45
CS 6 (Müllnersteg)	inbound	2119	123.95
CS 6 (Müllnersteg)	outbound	1116	123.95

This doesn't mean that the counts for longer roads always have to be higher though (e.g., the monitored road for counting station CS 0 is approx. 100 m longer than the one for station CS 2, but the situations around them are very different). It means that the levels of the amplitudes and the oscillation widths might not be directly comparable, but this only concerns



the comparison between different counting stations. The two linked roads (inbound/outbound directions) for the same counting station have the same length and the counts are therefore comparable. The same applies to the comparison of different scenarios for every individual counting station. Based on these considerations, the characters of the chart series with regard to the cyclist numbers are still considered representative as one of the influences of traffic lights on the spatio-temporal distribution of the bicycle traffic.

However, the time component (as the main focus of the research question) of the results exceeds the expectations. The shifts between the oscillations of the traffic light scenario series resemble the anticipated emerging patterns very closely – individually, and for the superimposed scenario series. The accuracy with which the 60-second rhythm of the traffic light phases reappears in the chart series was not anticipated though. The biggest factor is likely that all cyclist agents travel with approx. the same speed (with minor variations, as permitted by the speed coefficient set in the 'advanced driving' skill). The other factor is the balanced combination of this speed with the distances between traffic light intersections and the traffic light phase durations as set in the scenarios 1 and 2. As mentioned above, the shortest of the seven counting station road segments is 82.1 m long. This segment is part of a 107.1 m long road between the closest two traffic light intersections. With a speed of 20 km/h, a cyclist agent needs approx. 19 seconds (not considering acceleration and deceleration) to travel this distance. This is approx. 1/3 of the 60-second traffic light phase durations. With this combination (as can be observed in the model's 'City display' map view during simulations), the traffic lights are green long enough to allow all lined-up agents to pass them, and they are red short enough to not cause extensive line-ups that could affect the flow of traffic somewhere else.

#### 4.3.5. Positioning of counting stations

Even within a distance of a few blocks, this traffic light effect can still be observed at the counting stations. However, due to influences from other connected roads, it might be more difficult to detect with increasing distance between the two locations. The counting stations CS 3 and CS 1 in outbound direction are a good example of how one result can be understood by observing another result and putting the two counting stations spatially into relation (see section 4.2.2.1, 'CS 3 ('Mozartsteg)'). Similarly, in the case of the counting station CS 5 in outbound direction (section 4.2.2.3, 'CS 5 ('Makartsteg)'), one or two additional stations on the roads N of and parallel to the Salzach river would have made it easier to understand the emerging chart series patterns.

#### 4.3.6. Transferability to other locations

These results clearly demonstrate that the adaptive behaviour by cyclists as a consequence of the influence of traffic lights in a setting like the inner city of Salzburg can be visualised. Due to the generic nature of the used datasets, the same applies to any other similar location.

#### 4.3.7. Model as a reference

The model (and the parameters applied within) provides a reference from which conclusions can be drawn with regard to the magnitude of the observed results in relation to the input data and how the model uses these input data. For instance, if it can be observed (with the presented charts) over 100 simulations when 100% of 1140 cyclists (who all start their trip at the same time and travel from randomly selected locations to randomly selected locations) stop at red traffic lights, how would it manifest itself if 10% of these cyclists occasionally decided to disobey a traffic light or to U-turn to take a different route? Hence, this model might be helpful in feasibility considerations for future studies in the area of agent-based modeling of adaptive behaviour in active transportation.

## 5. Conclusion

As demonstrated in this thesis, the visualisation of emerging patterns in the spatio-temporal distribution of bicycle traffic from adaptive cyclist behaviour with an agent-based model is possible. There are many factors that can cause cyclists to adjust their behaviour. The level of detail applied in the thesis model was sufficient to detect one of them: the influence of traffic lights. The challenge in the delimitation of the modeled environment was not only a question of spatial extent, but also of functional level (with one affecting the other). The literature review revealed that there are hardly any comparable conditions – it seems as if almost every situation (e.g. intersections and the cyclists passing through them) is unique. This inevitably leads to generalisation. The modeling approach for this thesis was to create comparable situations to be able to highlight the differences in the outcome by already limiting them to the necessary minimum at the input (e.g. all agents starting their trips at the same time, two traffic light scenarios of equal phase timing and without overlap). Nevertheless, it quickly became apparent that the more factors are incorporated into such a model at the same time, the more difficult it will be to relate the results to the causes. As the model shows, this can be compensated to a certain degree with monitoring infrastructure in appropriate locations. The 'driving' plug-in (and its associated skills) provided with the agent-based modeling platform GAMA promises to be a very potent ally in future attempts to model adaptive behaviour in bicycle traffic with a spatial component – however, as shortcomings in the model code might reveal (and contrary to the assurances in the GAMA documentation), the complexity of the platform makes it challenging for non-professional programmers.

## 6. References

- Alvarez Lopez, P., Behrisch, M., Bieker-Walz, L., Erdmann, J., Flötteröd, Y.-P., Hilbrich, R., Lücken, L., Rummel, J., Wagner, P., and Wießner, E., 2018. Microscopic Traffic Simulation using SUMO. In: *The 21st IEEE International Conference on Intelligent Transportation Systems*. Maui, USA: IEEE.
- Bazzan, A.L.C. and Klügl, F., 2014. A review on agent-based technology for traffic and transportation. *The Knowledge Engineering Review*, 29 (03), 375–403.
- Bonneson, J., Sunkari, S., and Pratt, M., 2009. *Traffic Signal Operations Handbook*. College Station, Texas: Texas Transportation Institute, No. FHWA/TX-09/0-5629-P1.
- Dora, C. and Phillips, M., 2000. *Transport, environment and health*. Copenhagen, Denmark: World Health Organization Regional Office for Europe.
- Damant-Sirois, G., Grimsrud, M., and El-Geneidy, A.M., 2014. What's your type: a multidimensional cyclist typology. *Transportation*, 41 (6), 1153–1169.
- ESRI, 1998. *ESRI Shapefile Technical Description: An ESRI White Paper*. ESRI. <http://www.esri.com/library/whitepapers/pdfs/shapefile.pdf>.
- gama-platform, 2016a. Regular Species [online]. *Github*. Available from: <https://github.com/gama-platform/gama/wiki/RegularSpecies>.
- gama-platform, 2016b. Road Traffic [online]. *Github*. Available from: <https://github.com/gama-platform/gama/wiki/RoadTrafficModel>.
- gama-platform, 2018. Built-in Skills [online]. *Github*. Available from: <https://github.com/gama-platform/gama/wiki/BuiltInSkills>.
- Geller, R., 2006. *Four Types of Cyclists*. Portland Office of Transportation.
- Geoland.at, 2018. Orthofoto TileCache of Austria [online]. *data.gv.at - Offene Daten Österreichs*. Available from: <https://www.data.gv.at/katalog/dataset/orthofoto> [Accessed 1 Dec 2018].
- Geoland.at, 2019. Orthofoto TileCache of Austria [online]. *data.gv.at - Offene Daten Österreichs*. Available from: <https://www.data.gv.at/katalog/dataset/orthofoto> [Accessed 19 Jan 2019].
- Grignard, A., Taillandier, P., Gaudou, B., Vo, D.A., Huynh, N.Q., and Drogoul, A., 2013. GAMA 1.6: Advancing the Art of Complex Agent-Based Modeling and Simulation. In: G. Boella, E. Elkind, B.T.R. Savarimuthu, F. Dignum, and M.K. Purvis, eds. *PRIMA 2013: Principles and Practice of Multi-Agent Systems*. Berlin, Heidelberg: Springer Berlin Heidelberg, 117–131.
- Grimm, V., Berger, U., Bastiansen, F., Eliassen, S., Ginot, V., Giske, J., Goss-Custard, J., Grand, T., Heinz, S.K., Huse, G., Huth, A., Jepsen, J.U., Jørgensen, C., Mooij, W.M., Müller, B., Pe'er, G., Piou, C., Railsback, S.F., Robbins, A.M., Robbins, M.M., Rossmanith, E., Rüger, N., Strand, E., Souissi, S., Stillman, R.A., Vabø, R., Visser, U., and DeAngelis, D.L., 2006. A standard protocol for describing individual-based and agent-based models. *Ecological Modelling*, 198 (1), 115–126.
- Grimm, V., Berger, U., DeAngelis, D.L., Polhill, J.G., Giske, J., and Railsback, S.F., 2010. The ODD protocol: A review and first update. *Ecological Modelling*, 221 (23), 2760–2768.
- HEI Panel on the Health Effects of Traffic-Related Air Pollution, 2010. *Traffic-Related Air Pollution: A Critical Review of the Literature on Emissions, Exposure, and Health Effects*. Boston, MA: Health Effects Institute, Special Report No. 17.
- Kazyieva, D., Wallentin, G., and Loidl, M., 2019. *Bicycle model (Version 1.0.0)*. CoMSES Computational Model Library.
- Kazyieva, D., Wallentin, G., Loidl, M., Mohr, S., and Neuwirth, C., 2018. Reviewing Software for Agent-based Bicycle Flow Models. *GI\_Forum*, 1, 291–296.

- Loidl, M. and Zagel, B., 2010. Wie sicher ist sicher?-Innovatives Kostenmodell zur Ermittlung des Gefährdungspotenzials auf Radwegen. *Angewandte Geoinformatik 2010*.
- Macal, C. and North, M., 2014. Introductory tutorial: Agent-based modeling and simulation. *In: Proceedings of the Winter Simulation Conference 2014*. Presented at the Proceedings of the Winter Simulation Conference 2014, 6–20.
- Morvan, G., 2012. Multi-level agent-based modeling - Bibliography. *CoRR*, abs/1205.0561.
- Pai, C.-W. and Jou, R.-C., 2014. Cyclists' red-light running behaviours: An examination of risk-taking, opportunistic, and law-obeying behaviours. *Accident Analysis & Prevention*, 62, 191–198.
- QGIS Development Team, 2018. *QGIS Geographic Information System*. Open Source Geospatial Foundation Project. <http://qgis.osgeo.org/>.
- Richardson, M. and Caulfield, B., 2015. Investigating traffic light violations by cyclists in Dublin City Centre. *Accident Analysis & Prevention*, 84, 65–73.
- Schmiedbauer, T., 2016. Max-Ott-Platz [online]. *Salzburgwiki*. Available from: <https://www.sn.at/wiki/Datei:Max-Ott-Platz.jpg>.
- Soares, G., Kokkinogenis, Z., Macedo, J., and Rossetti, R., 2014. Agent-Based Traffic Simulation Using SUMO and JADE: An Integrated Platform for Artificial Transportation Systems. 44–61.
- SUMO, 2017. Simulation/Bicycles [online]. *SUMO*. Available from: <http://sumo.sourceforge.net/userdoc/Simulation/Bicycles.html> [Accessed 4 Feb 2019].
- Taillandier, P., 2014. Traffic simulation with the GAMA platform. *In: International Workshop on Agents in Traffic and Transportation*. France, 8 p. HAL Id: hal – 01055567.
- The World Bank, 2018. Urban population [online]. *The World Bank*. Available from: <https://data.worldbank.org/indicator/SP.URB.TOTL> [Accessed 1 Dec 2018].
- Wallentin, G., 2016. *Salzburg Bicycle model (Version 1.0.0)*. CoMSES Computational Model Library.
- Wallentin, G. and Loidl, M., 2015. Agent-based Bicycle Traffic Model for Salzburg City. *GI\_Forum*, 1, 558–566.
- Wilensky, U., 1999. *NetLogo*. <http://ccl.northwestern.edu/netlogo/>. Center for Connected Learning and Computer-Based Modeling, Northwestern University, Evanston, IL.
- Wu, C., Yao, L., and Zhang, K., 2012. The red-light running behavior of electric bike riders and cyclists at urban intersections in China: An observational study. *Accident Analysis & Prevention*, 49, 186–192.
- Ziemke, D., Metzler, S., and Nagel, K., 2017. Modeling bicycle traffic in an agent-based transport simulation. *Procedia Computer Science*, 109, 923–928.

### 6.1. Data sources

- [1] Magistrat Salzburg, 2017. Counting data. [online] Available through: Eco counter <<https://www.eco-visio.net/Ecovisio>> [Accessed 3 April 2018].
- [2] Statistics Austria, 2013. Abgestimmte Erwerbsstatistik 2013. [online] Available through: Statistics Austria <<http://www.statistik.at>> [Accessed 17 December 2015].
- [3] Stadt Salzburg. [Received 02 March 2017].
- [4] OpenStreetMap contributors, 2017. Planet dump. [online] Available through: Geofabrik <<https://www.geofabrik.de>> [Accessed 20 April 2015].
- [5] Graph Integration Platform GIP, 2015. Intermodal Transport Reference System Of Austria. Available through: Graph Integration Platform GIP <<http://www.gip.gv.at>> [Accessed 31 March 2015].
- [6] OpenStreetMap contributors, 2017. Planet dump. [online] Available through: Geofabrik <<https://www.geofabrik.de>> [Accessed 27 April 2017].
- [7] Stadt Salzburg, 2017. Stadt Salzburg Web Feature Service OGD. [online] Available through: Stadt Salzburg <<https://data.stadt-salzburg.at>> [Accessed 2 August 2017].
- [8] Statistics Austria, 2011. Registerzählung 2011. [online] Available through: Statistics Austria <<http://www.statistik.at>> [Accessed 19 August 2014].
- [9] Created by thesis author

### 6.2. Link to model file and associated data files

[https://github.com/prgis/SBM\\_PR\\_MSC\\_Thesis-model/invitations](https://github.com/prgis/SBM_PR_MSC_Thesis-model/invitations)

*This repository can be accessed by registered GitHub users upon invitation.*